Development of a Simulation Method for Urban-Scale Residential Time-Series Electricity Demand and Evaluation of the Effects of Renewable Energy Introduction

王, 恒煊

出版情報：Kyushu University, 2024, 博士（工学）, 課程博士
バージョン：
権利関係：

Doctoral Thesis

博　士　論　文

Development of a Simulation Method for Urban-Scale Residential Time-Series Electricity Demand and Evaluation of the Effects of Renewable Energy Introduction

都市規模での住宅の時系列電力需要シミュレーション手法の開発と再生可能エネルギー普及効果の評価

2024 年

Hengxuan Wang

王　恒煊

Table of Content

Chapter-1
Introduction

1.1 Background

1.1.1 National decarbonization

To address climate change, most countries in the world adopted the Paris Agreement [1]. The agreement came into effect within a year and aims to significantly reduce global greenhouse gas emissions, limiting the global temperature increase within this century to well below 2℃ while striving to further restrict it to 1.5℃. Each contracting country declared their respective carbon neutrality goals. Among them, Japan aims to achieve carbon neutrality by the year 2050, as per its newly formulated long-term strategy. Additionally, Japan commits to making efforts to reduce greenhouse gas emissions by 46% from the 2013 levels by the year 2030. Furthermore, there is a persistent commitment to challenging even higher goals, striving towards a more ambitious target of reducing emissions by 50% [2].

1.1.2 Regional decarbonization

To achieve the carbon neutrality, collaborative efforts and co-creation between the national and local levels are indispensable. Hence, National and Regional Decarbonization Conference has been established, aiming for the realization of regional decarbonization with local communities taking a leading role. Additionally, focusing on initiatives and policies to be concentrated on by 2030, a "Regional Decarbonization Roadmap" has been formulated, outlining the steps, timelines, and specific measures [3]. It was proposed that regional decarbonization initiatives would be vigorously implemented over a concentrated period of five years until 2025. The aim is to create a " Domino Effect" where regional decarbonization spreads from regions with high motivation and feasibility (leading regions) to other regions. As of 2024, the Decarbonization Leading Region Evaluation Committee has selected 74 regions as leading regions through four rounds of evaluation across Japan [4]. Each region has one or more areas that can be classified to 4 classifications include residential area,

Table 1.1 Definition of each classification

Classification	Definition
Residential area	• Mainly detached houses • Mainly apartment houses
Business area	• Central urban areas of small local municipalities (town/village offices, shopping streets, etc.) • Urban areas in the center of large cities (shopping streets/commercial facilities, office districts/business buildings) • Specific sites such as university campuses
Natural area	• Rural villages (areas where agriculture and forestry are carried out, including farmland and forests) • Fishing village (area where fishing is carried out, including fishing operation areas and fishing ports) • Remote island • Tourist area / National park (Zero Carbon Park)
Public facilities	• A group of facilities where it is reasonable to centralize energy management

business area, natural area and public facilities group as shown in Table 1.1. For example, in the case of Yusuhara town, solar power systems and storage batteries have been installed on private houses in residential area and public facilities in business area, facilitated by Power Purchase Agreements (PPA). These installations are strategically positioned to link the town center with facilities in tourist destinations through dedicated private lines, with energy management overseen by regional energy companies. In addition to providing waste heat through wood biomass power generation, they plan to expand wood pellet factories and undertake initiatives to create local employment, promote the revitalization of agriculture and forestry which belong to natural area, and achieve overall regional economic stimulation. Therefore, region Yusuhara town has three areas are classified as residential area, business area and natural area. In the case of Ishikari city with only one area which is classified as public facilities group, through the introduction of solar power and a specific power transmission and distribution project that utilizes woody biomass power generation, renewable energy will be provided to data centers and other facilities that are expected to cluster in the target area. Appendix A shows the detailed classifications of these 74 leading regions and the total number of each classification are shown in Figure 1.1. By comparing the four rounds of evaluation, it can be observed in the initial round, the numbers of the four classifications were essentially equal, as the evaluation process advances, the counts of natural area and facility groups decrease. The probable reason is that decarbonization targets are more attainable in these two classifications. (Natural area feature a higher presence of renewable energy and lower energy demand. Public facilities benefit from centralized energy management.) As the stocks of classifications with high motivation and feasibility for achieving decarbonization decrease, future decarbonization efforts are anticipated to be more concentrated in urban residential and business areas. These areas exhibit higher energy demand, limited renewable energy resources, and pose challenges in achieving decarbonization.

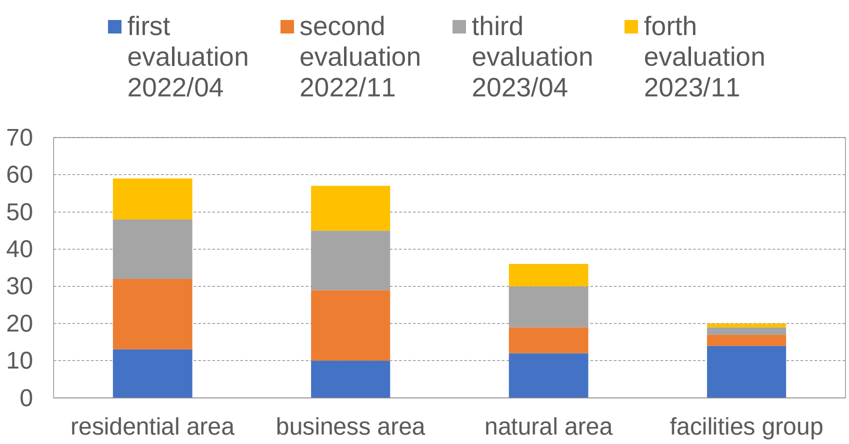

Figure 1.1 Number of each classification in 4 rounds evaluation

1.1.3 Measures of regional decarbonization and related issues

Carbon neutrality cannot be realized by ordinary efforts, it is important to accelerate efforts toward structural changes in energy and industrial sectors. Given this context, the Ministry of Economy, Trade and Industry, in collaboration with other ministries and agencies, developed the "Green Growth Strategy through Achieving Carbon Neutrality in 2050."[5]. The strategy outlines 14 promising fields poised for growth and furnishes them with action plans, encompassing perspectives from both industrial and energy policies as shown in Table 1.2. The field corresponding to urban residential and business areas is sector 12 (part of Housing/ Building) and explained as:

- Considering the introduction of further measures to improve the compliance rate with energy efficiency standards for housing.

In various urban business areas, time-series energy demand exhibits relatively consistent patterns. This consistency is primarily due to the energy demand of dominant non-residential buildings being determined by fixed work schedules of users. However, in various urban residential areas, the patterns of time-series energy demand show greater variations, stemming from the greater diversity exhibited by residents of residential buildings compared to non-residential buildings. This diversity arises from the varied composition of households across different urban areas. Specifically, the diversity in household composition leads to different daily behavior patterns, resulting in varied electricity demand patterns. At the same time, the type (apartment, detached) and the thermal insulation performance of residential building in different urban areas are also significant factors that cannot be overlooked in influencing electricity demand. Therefore, it could be expected the implementation of related energy policies to promote houses with high energy efficiency would complicate the time-series energy demand of residentional area (e.g., as residential energy-efficiency standards are continually enhanced and strengthened, driven by the number of retrofits houses with high-standard, the energy demands for exiting houses are expected to decrease compared to current levels.).

Table 1.2 14 growth sectors

Energy related industries	Transport/manufacturing industries	Home / Office related industries
01_Offshore wind power Solar, heat energy	05_Automobilie, Storage batteries	12_Housing/Building, Next generation, electric power management
02_Hydrogen, Fuel Ammonia	06_ Semiconductors Info/Com	13_Resource circulation
03_Next generation, heat energy	07_Shipping	14_Lifestyle related
04_Nuclear power	08_Logistics, people flow, Civil eng.	
	09_Food, Agri. Fishery, forestry.	
	10_Aircraft	
	11_Carbon Recycling, Materials	

Additionally, the Japanese government aims to achieve a renewable energy share of 22-24% in the power composition by 2030. To expedite the adoption of renewable energy, in urban areas where available space and resources are limited, distributed renewable energy solutions, such as installing photovoltaic (PV) systems on building rooftops, have become the primary choice. These PV systems scattered in different areas of the urban have the following characteristics:

- The power generated fluctuates from tens of seconds to minutes, depending on the weather conditions.
- Regarding the supply side of PV, the demand of buildings is also dynamic. The peaks and troughs of both are interlinked, potentially causing issues such as surplus power generation, which may lead to damage to the grid.

Considering the efforts of improving residential energy efficiency, the widespread introduction of distributed energy will contribute to increasingly complex electricity supply and demand challenges as shown in Figure 1.2.

Since the electricity demand of houses mainly comes from appliances, lighting, ventilation, and air conditioning. The electricity consumption of these devices depends on their operation timing and duration, which in turn depends on the behavior of occupants (e.g., starting the IH cooker before meal). The behavior of occupants is also related to household composition. Also, the electricity consumption of air-conditioning is related to house type (apartment or detached house) and housing insulation performance, which in turn related to construction year of houses as shwon in Figure 1.3. (The earlier a house was built, the poorer its thermal performance tends to be). Furthermore, the types of housing, construction periods, and household compositions vary significantly across different urban areas. As a result, the differences in residential electricity demand between these areas are substantial. The implementation of the same energy-saving policy will have different effects in these regions, necessitating separate evaluations.

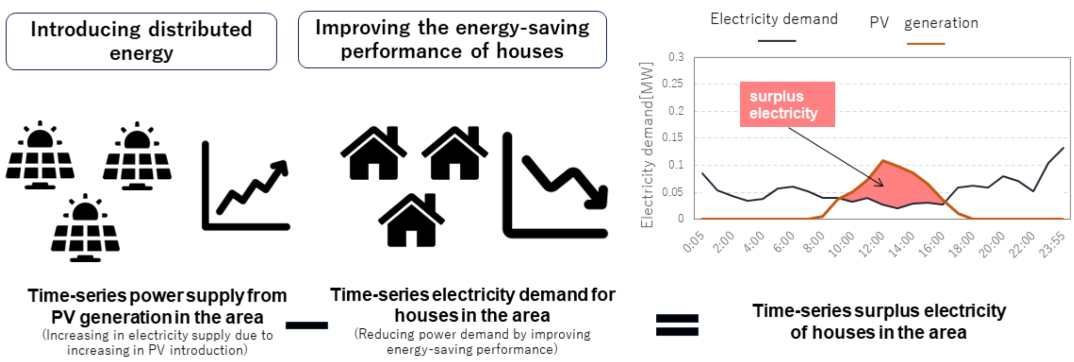

Figure 1.2 Changes in local electricity demand and supply due to different energy policies

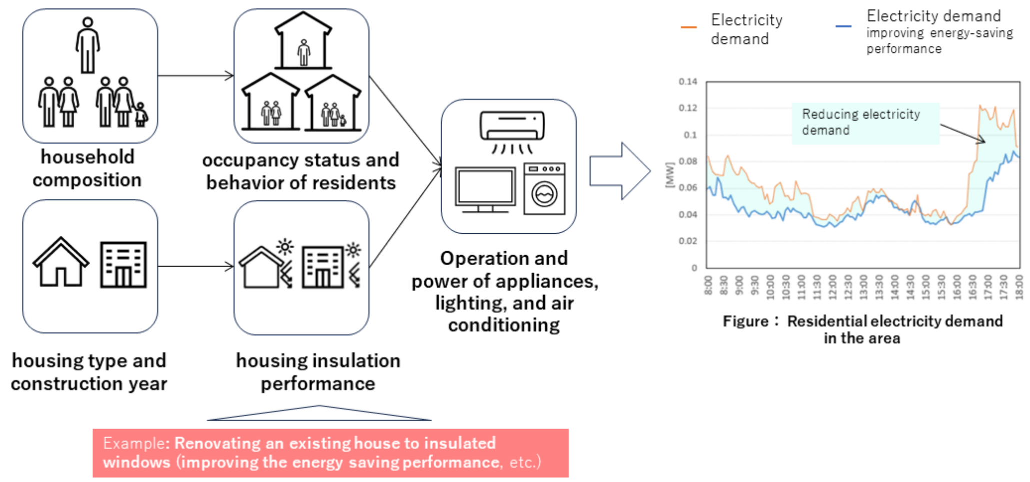

Figure 1.3 Factors influencing regional residential electricity demand reduction

1.1.4 Shortcomings of established solution

Dealing with this issue, transitioning to a next-generation grid like smart grid [7] would indeed be an excellent choice. As mentioned in sector 12 (part of Next generation, electric power management) [4], detailed efforts include:

- Promoting aggregation business using distributed energy through digital control and market trading.
- Building a next-generation grid that utilizes digital technology and markets to relieve congestion in the power grid caused by massive introduction of renewable energy.
- Promoting local energy production for local consumption, enhancement of resilience and regional revitalization through microgrids.

Through various operational and energy measures, such as advanced metering infrastructure and smart distribution boards integrated with home control and demand response, smart grids enable the power industry to observe and control specific parts of the system at higher resolution in time and space, addressing the imbalance in power supply and demand mentioned above. [8] For example, in special residential area, turning off air-conditioners during short-term spikes in electricity demand or charging electric vehicle (EV) during peak solar generation period. However, next-generation grid represented by smart grid is facing many issues currently as follow:

- **Investment and cost**

  Construction and upgrade of smart grids require substantial investments. the initial costs can pose challenges especially in suburban and sural areas. [9]
- **Technology integration**

  Integrating smart grid technologies (e.g., communication, real-time data processing, remote monitoring and control) into existing power infrastructure is a complex and time-consuming process. [10]
- **Cybersecurity and privacy issues**

  Smart grid involves the collection and analysis of a substantial amount of user data, and the digitization aspect increases the cybersecurity risk. [8]

1.1.5 Bottom-up simulation model

Given that the large-scale construction and implementation of next-generation power grids is unrealistic currently or in the near future, urban energy simulation methods remain the only means to obtain urban information of energy supply and demand and to assess the effect in different urban areas of various energy policies. Swan and Ugursal [11] classified the existing methods of building operational energy estimation into two key types of methods: top-down models and bottom-up models as shown in Figure 1.4. Top-down models don not focus on specific end-use energy consumption but treat urban as a user. It uses historical energy data along with relevant demographic and economic data to understand and predict the overall supply and demand of urban energy. Instead, bottom-up models evaluate energy use of individula units (i.e., individual building or collective set of buildings) with extensive data (i.e., building structure, lifestyle of occupants), and extended the evaluation results to the larger scale (region or urban). This characteristic makes it suitable for assessing the impacts of various urban energy policies (i.e., the residential energy-saving renovations, the integration of PV) on energy supply and demand of individual buildings, as well as the different regions and the whole city.

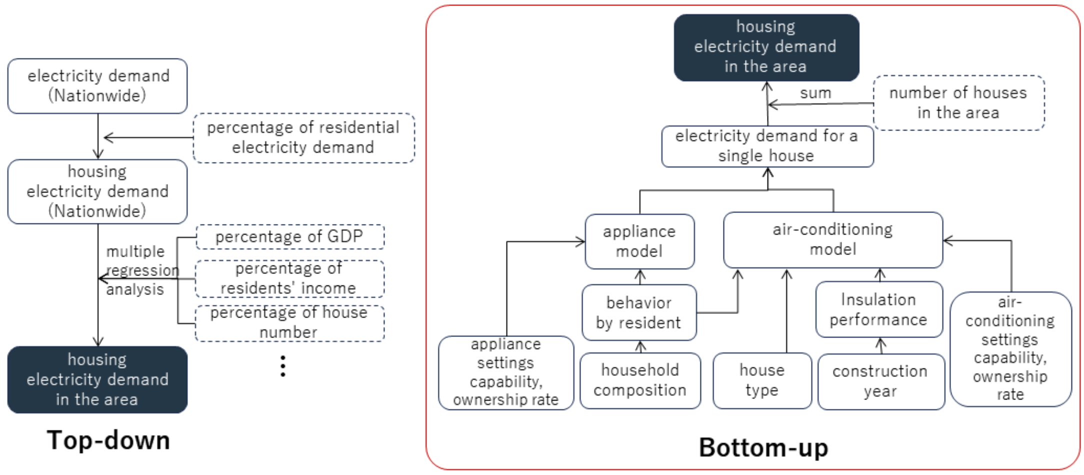

Figure 1.4 Top-down and Bottom-up model

1.2 Research purpose

To achieve decarbonization, urban areas will implement various energy policies as mentioned before. Due to differences in types, numbers of buildings and demographic compositions among different urban areas, these energy policies will inevitably have different effects. To evaluate these effects and assist decision-makers in implementing the most suitable energy policies in different areas, this study aims to develop a time-series bottom-up electricity simulation method of residential buildings tailored to urban scales, to evaluate the effects of various energy policies across different urban areas. Through the model developed in this study, the time-series residential electricity supply and demand results for various regions of any city in Japan will be clarified. Additionally, the effects of various energy policies on local or overall electricity supply and demand in urban areas will be understand. Furthermore, the results of this research can assist in evaluating the decarbonization potential in different regions, thereby contributing to the formulation of decarbonization roadmaps and regional decarbonization efforts.

1.3 Simulation configuration

For urban-scale simulations, acquiring information about residential buildings in diverse urban areas is crucial. Consequently, this study integrates Geographic Information Systems (GIS) to obtain both the location and attribute information of each residential building. However, GIS does not include information about the household residing in residential buildings, which is crucial for simulating residential electricity demand. Therefore, in addition to GIS data, this study also collected National Census Data, National Lifetime Use Survey, National Land and Houses Survey.

The research focusing on the following three tasks:

① Occupants behavior model

The time-series electricity demand of houses is influenced by the operation of appliances and air conditioners, which, in turn, is determined by the behavior of household members. Drawing on statistics data of National lifetime Use Survey, a model has been developed to generate a substantial number of daily behavior schedules representing urban occupants based on the occupant type and day. Furthermore, the generated schedules for individual household member are filtered and combined into combination of households, considering the correlation between household members.

② Residential electricity demand simulation model in urban scale

With the behavior schedules of occupants, a residential electricity simulation model has been proposed to accommodate a diverse range of subjects, taking into consideration household composition, housing type, floor area, and thermal insulation performance. With this model, the 5-minute interval electricity demand for residential buildings in each street-level area of Fukuoka (the target city) over the course of one year can be simulated.

③ Evaluation of scenarios involving houses retrofitting and EVs introduction

By incorporating the electricity demand results with the calculated PV electricity generation, surplus electricity is determined for each area. Furthermore, the influence of house retrofitting on surplus electricity and the minimum EV introduction rate necessary to maximize the utilization of surplus electricity in each area are explored.

1.4 Previous research

Concerning the bottom-up electricity demand simulation and optimization of energy supply for residential areas, numerous prior studies have been conducted and published in Japan. Shimoda et al. [12] developed an energy consumption model for houses known as TREES (Total Residential End-use Energy Simulation). This model considers factors such as weather conditions, lifestyle, occupant behavior, housing specifications, and equipment specifications. It enables a comprehensive understanding of the structure of energy consumption in houses. With this model, they also evaluated the potential contribution of residential cogeneration systems to energy conservation and global warming mitigation on a city scale in [13]. Takamura et al. [14] predicted electricity demand of several districts includes residential district considering PV generation and future energy saving technology.

Fujimoto et al. [15] assessed the impact of energy demand management on mitigating the deterioration of voltage quality in power distribution resulting from the widespread adoption of residential PV systems. Taniguchi et al. [16] evaluated the contribution of the residential sector to summer peak demand reduction with several behavioral measures. Tanimoto et al. [17] also developed a bottom-up model to simulate utility loads, including electricity for multi-dwellings, using Monte Carlo methods to determine the ON/OFF state of HVAC systems. Ueno et al. [18] developed electricity demand simulation model for the specified housing group with several hundreds to thousands of households in a particular area, the accuracy was verified and corrected with smart meter data.

In addition, many previous studies have been conducted overseas as well. Fischer et al. [19] evaluated impact of refurbishment, efficiency increase in devices on the electricity load profile of residential areas by stochastic bottom-up simulation approach. Zahiri et al. [20] evaluated council housing building performance and occupants' energy use behaviour by exploring the correlations between occupancy and energy consumption patterns with bottom-up building simulation model. Davila et al. [21] developed a citywide urban building energy model based on official GIS datasets and a custom-building archetype library, one energy management policy based on one urban PV scenario had been evaluated by the proposed model.

Utilizing a similar bottom-up residential energy simulation model for urban-level energy supply and demand assessment, this study offers several advancements compared to previous research.

- **Constructing bottom-up simulation model**

In previous studies [12], insulation performance classification of houses was based on thermal performance statistics data at the city level. This study estimates the houses construction year based on the population mobility statistics data at street-level (machi in Japanese) and classify insulation performance accordingly. Considering the probabilities of appliances operation based on occupants' behavior, previous study had set them accoring to period of day, while this study calculated the probabilities based on measured data.

- **Simualtion target**

In previous studies, it is common to conduct simulations for all households in representative regions, or to conduct sampling simulations for houses in cities or nationwide. In this study, simulations are conducted for all households within the target city.

- **Consideration of regional differences**

In previous studies, it is common to develop bottom-up models of urban residential demand. These studies typically focused on entire cities or representative regions, analyzing the impact of specific energy-saving measures or renewable energy sources on the electricity supply and demand of buildings. This study target wider urban areas and consider differences in occupant lifestyles and residential thermal insulation performance. The study aims to reflect the differences in electricity demand and supply that arise from variations in occupants and housing thermal insulation performance across regions.

Based on these three points, it can be asserted that there is considerable academic progress. Since the simulation model developed in this study relies solely on accessible public statistic data, it can be applied in any city or rural area in Japan. It is expected to facilitate the formulating renewable energy introduction plans for various regions.

1.5 Thesis structure

Chapter 1 Introduction

Chapter 1 outlines the background, purpose, and structure of this thesis. It provides a summary of previous research and positions the current study within the context of related research.

Chapter 2 Simulation model & results of occupants' behavior schedules

Chapter 2 develops a model for simulating occupants' behavior schedules in urban scale using only public stochastic data. By the proposed model, 1000 behavior schedules for 5 types of occupants have been generated and combined based on household members' behavior interactions.

Chapter 3 Simulation model & results of residential buildings' electricity demand

Chapter 3 develops a model for simulating electricity demand of urban houses using the behavior schedules results in chapter 2. By the proposed model, the results of target city are simulated with three scenarios in 2020, 2025 and 2025 considering houses retrofitting.

Chapter 4 Simulation model & results of surplus electricity from PV generation and EV charging

Chapter 4 develops models for simulating residential photovoltaic (PV) generation and electrical vehicle (EV) charging in urban scale. Based on the proposed models, surplus electricity (the difference between PV generation and electricity demand as simulated in Chapter 3) and the minimum introduction rates of EVs (EV ownership rate of households) required to fully utilize this surplus electricity have been calculated and evaluated separately with characteristic of residential buildings in each urban area, considering three scenarios in Chapter 3.

Chapter 5 Summary and discussion

Chapter 5 summaries the results in this thesis and discuss the drawbacks as well as work in the future.

Reference

[1] United Nations Climate Change, Paris Agreement, 2015

[2] Ministry of the Environment, Cabinet decision on “Global Warming Countermeasures Plan”, 2016

[3] National/Local Decarbonization Realization Council, Regional decarbonization roadmap, June 2021

[4] Decarbonization leading region evaluation committee, Decarbonization leading region selection results, November 2023

[5] Ministry of Economy, Trade and Industry, Green Growth Strategy Through Achieving Carbon Neutrality in 2050, June 2021

[6] Ministry of Economy, Trade and Industry, Housing and building (housing and building industry, next generation power management industry), June 2021

[7] Federal Energy Regulatory Commission, Assessment of demand response and advanced metering, staff report, Washington, D.C.: Federal Energy Regulatory Commission, 2008.

[8] A. V. Meier, Electrical Engineer 137A: Electric Power Systems. Lecture 2: Introduction to Electric Power Systems, pp.33,2013

[9] R. Aalbers, V. Kocsis and V. Shestalova, Optimal regulation under unknown supply of distributed generation, CPB Netherlands Bureau for Economic Policy Analysis, 2011.

[10] I. Colak, S. Sagiroglu, G. Fulli, M. Yseilbudak and C. Covrig, A survey on the critical issues in smart grid technologies, Renewable and Sustainable Energy Reviews, 54, pp.396-405, 2016.

[11] L G. Swan, V I. Ugursal, Modeling of end-use energy consumption in the residential sector: a review of modeling techniques, Renewable and Sustainable Energy Reviews, vol.13, pp.1819–1835, 2009

[12] T. Ueno, K. Takahashi and D. Sumiyoshi, Estimation for energy demand fluctuation in commercial and business area by Monte Carlo simulation, Journal of Environmental Engineering, vol.84, no.757, pp.291-301, 2019.

[13] Y. Shimoda, A. Taniguchi-Matsuoka, T. Inoue, M. Otsuki and Y. Yamaguchi, Residential energy end-use model as evaluation tool for residential micro-generation, Applied Thermal Engineering, vol.114, pp. 1433-1442, 2017.

[14] S. Takamura, Y. Yamaguchi, H. Habara and Y. Shimoda, District electricity demand prediction under large diffusion of photovoltaics and energy saving technology, Journal of Environmental Engineering, vol.77, no.680, pp.805-811, 2012.

[15] T. Fujimoto, Y. Yamaguchi, K. Kusakiyo, H. Sugihara and Y. Shimoda, Evaluation of effect of residential energy demand management to mitigate voltage increase in high-voltage distribution line to large-scale diffusion of PV, Transactions on Electronics, Information and System, vol.133, no.10, pp.1873-1883, 2013.

[16] A. Taniguchi, T. Inoue, M. Otsuki, Y. Yamaguchi, Y. Shimoda, A. Takami and K. Hanaoka, Estimation of the contribution of the residential sector to summer peak demand reduction in Japan using an energy end-use simulation model, vol.112, no.15, pp.80-92. 2016.

[17] J. Tanimoto and A. Hagishima, Total utility demand prediction considering variation of occupants' behavior schedules applied to multi dwellings, Journal of Environmental Engineering, vol.76, no.660, pp.141-149, 2011.

[18] T. Ueno and Y. Sinohara, Construction and verification of a model for estimating electricity consumption of residential buildings in a region for the development of an area energy demand simulation tool, Transactions on Power and Energy, vol.142, no.8, pp.366-375, 2022.

[19] D. Fischer, A. Surmann and K. B. Lindberg, Impact of emerging technologies on the electricity load profile of residential areas, Energy and Building, vol.208, 109614, 2020.

[20] S. Zahiri, H. Elsharkawy, Towards energy-efficient retrofit of council housing in London: Assessing the impact of occupancy and energy-use patterns on building performance. Energy and buildings, vol.174, pp.672-681, 2018.

[21] C C. Davila, C F. Reinhart, J L. Bemis, Modeling Boston: A workflow for the efficient generation and maintenance of urban building energy models from existing geospatial datasets, Energy, vol.117, pp.237-250, 2016.

Appendix A 74 leading decarbonization regions through four rounds of evaluation

Table A.1 leading regions in first evaluation

Name	level	Classifications			
		residential	business	natural	facilities group
Ishikari	city				●
Kamishihoro	machi	●	●		
Shikaoi	machi			●	●
Higashimatsushima	city	●	●		
Akita	city				●
Ogata	village	●	●		
Saitama	city	●	●		●
Yokohama	city	●	●		
Kawasaki	city				●
Sado	city			●	●
Matsumoto	city	●	●	●	
Shizuoka	city	●	●		
Nagoya	city				●
Maibara	city			●	
Sakai	city	●	●		
Himeji	city		●	●	
Amagasaki	city			●	
Awaji	city	●		●	
Yonago	city				●
Onan	machi	●	●	●	
Maniwa	city			●	●
Nishiawakura	village				●
Yusuhara	machi	●		●	●
Kitakyushu	city				●
Kuma	village	●		●	●
China	machi	●		●	●

Table A.2 leading regions in second evaluation

Name	level	Classifications			
		residential	business	natural	facilities group
Sapporo	city	●	●		●
Okushiri	machi	●		●	●
Miyako	city	●	●		
Kuji	city	●	●	●	
Utsunomiya	city	●	●		
Nasushiobara	city	●	●	●	
Ueno	village	●	●	●	
Chiba	city	●	●		
Odawara	city		●		
Sekikawa	village	●	●	●	
Tsuruga	city	●	●		
Iida	city	●	●		
Okazaki	city	●	●		
Konan	city	●	●	●	
Kyoto	city	●	●	●	
Kasai	city	●	●		
Misato	machi	●	●		
Yamaguchi	city	●	●		
Nobeoka	city	●	●		
Yonabaru	machi	●	●		●

Table A.3 leading regions in third evaluation

Name	level	Classifications			
		residential	**business**	**natural**	**facilities group**
Sai	village	●	●	●	
Shiwa	machi	●	●	●	
Aizuwakamatsu	city	●	●		●
Nikko	city	●	●	●	
Kai	city	●	●	●	
Komoro	city	●	●		
Ikusaka	village	●	●	●	
Ikoma	city	●	●		
Tottori	city	●	●		
Matsue	city	●	●	●	
Setouchi	city	●	●	●	
Susaki	city	●	●	●	
Kitagawa	village	●	●	●	
Kuroshio	machi	●	●	●	
Asagiri	machi	●	●	●	
Hioki	city	●	●		●

Table A.4 leading regions in forth evaluation

Name	level	Classifications			
		residential	**business**	**natural**	**facilities group**
Tomakomai	city	●	●		
Sendai	city	●	●		
Tsukuba	city	●	●		
Sosa	city	●	●	●	
Takaoka	city	●	●		
Ueda	city	●	●		●
Takayama	city	●	●	●	
Osaka	city	●	●		
Ukiha	city	●	●	●	
Nagasaki	city	●	●	●	
Kumamoto	prefecture		●	●	
Miyakojima	city	●	●	●	

Chapter-2

Simulation model & results of occupants' behavior schedules

2.1 Introduction

2.1.1 Purpose of model

As mentioned before, the electricity demand of residential building is decided by appliances' operation, which is influenced by the behavior of the occupants with significantly personal characteristics. In previous studies about energy demand estimation for residential buildings, the behavior schedules of occupants had been set to several cases. This assumption would significantly affect the accuracy of results. The reason is that even the same type occupants in urban scale would have numerous kind behaviors at the same time, but there are only a few cases in these few schedules that would overlay the peak or trough energy demand amount. Thereby, the demand results and the amount of renewable energy devices need to be introduced would be a departure from reality. Thus, a model to simulate the occupants' behavior schedules is the premise of understanding the electricity demand of residential buildings in urban scale.

2.1.2 Previous research

There is much previous research about the occupants' behavior model in urban scale [1]. The models could be divided into two types based on whether to use dataset called Time Use Data (*TUD*), which describe occupants' behavior by time.

For the first type without *TUD*, Tanimoto et al. [2] developed a model using only public stochastic data of *TUD* include mean and standard deviation of behaviors' duration time in a day and percentages of occupants adopt the behavior at special moments by 15-minutes interval of a day. They firstly selected the behaviors according to probabilities and arranged their total duration time into 24 hours. Next, they placed the first behavior into the slot in timeline according to random number and placed the next behavior into the end of previous behavior one by one. As one merit, this method could generate the occupants' behavior schedules with only public stochastic data. But the accuracy of the simulation results was greatly influenced by the randomly decided slot for the first behavior, which was inserted. Additionally, the results had not been validated.

For the type of models using *TUD*, Richardson et al. [3] developed a model using the Markov Chain, which is a stochastic model to determine the transition of behavior from another only depend on the condition at the previous time step. They collected the *TUD* from a great number of households and analysis the transition probability between behaviors. But the behavior items were limited in at room or not.

Widén et al. [4] proposed a Markov Chain model and expanded analysis of the number of behavior items. They simulated the household's members independently. These Markov Chain models considered and simulated the transitions probability between the behaviors precisely, but the accuracy of behavior duration time was dependent on the timing and number of behavior transitions. This could be a weakness for simulating the occupants' behavior schedules. Yamaguchi et al. [5] developed a occupants' behavior model dealing with above problems. They divided behaviors into routine and non-routine and considered them separately. The behaviors' duration time and transition probabilities between them were acquired by analyzing the *TUD* from the national time-use survey conducted by Statistics Japan in 2006 and been utilized for placing the behaviors into the timeline. They firstly placed the routine behaviors (including sleeping, commuting to work & school, dining and bathing) into timeline, then selected the non-routine behaviors according to the probabilities and placed them in the gap between the routine behaviors until all gaps had been filled. They improved the model in [6] considering the interaction among household members (e.g., household members always have dining together at one time and bathing one by one) and time-dependent characteristics of the specific behaviors (e.g., for a single person, bathing often happens immediately after waking up or breakfast, but it's not shown in *TUD* because it was originated from a wide range of people.). In [7], they explored several machine learning methods to pre-process the *TUD* to improve the accuracy of behavior model. Although the duration time and transition probabilities of behaviors were detailed considered in their model, predetermining the number of behavior occurrences with a subjective assumption was made. For example, three meals over a day, one sleeping at night with long period were considered in their model. But according to the public stochastic data, there are also sleeping at the daytime for many type people), this might be a weakness of their model for ignoring these specific cases. On the other hand, raw *TUD* are required to make this kind of model while only public stochastic data are available in many countries.

As mentioned above, until now there are many developed occupants' behavior models in urban scale with own strengths and weaknesses. But there is still no precise occupants' behavior model that considering the interaction among household members, without prior analysis of large amount of raw *TUD*, pre-classification of behaviors according to routinely or not and predetermined number of occurrences with subjective assumption.

2.1.3 Procedures of model

Therefore, a new occupants' behavior model considering above issues has been proposed and verified. Utilizing the developed model, the behavior schedules of working men, working women, housewives, elder, children, middle school students, and college students were simulated with large quantities. Then, these individual schedules were combined to form combinations of households' members' behavior schedules.

The steps of proposed model are introduced as follow:

① Public data called National Lifetime Use Survey by Japan Broadcasting Corporation (NHK) had been corrected and analyzed.

② A model was developed to generated a large number of daily behavior schedules including many behaviors (e.g., sleeping, eating, bath) with 5-minute intervals based on the type of occupants and day. Using an evolutionary algorithm, following a specific number of iterations, the input parameters for generating those behavioral schedules were continuously refined and optimized to ensure the statistical values of the generated outcomes align with those obtained from public data.

③ Based on the mutual influence of behaviors among members of the same household, combinations of household members' behavior schedules were amalgamated from the optimized schedules of various occupant types in the previous step.

By employing this approach, behavior schedules for a diverse range of households were acquired and prepared for integration into urban-scale simulations of residential electricity demand.

2.2 National Lifetime Use Survey

2.2.1 Overview

The National Lifetime Use Survey [8] is a survey designed to provide insights into Japanese people's daily lives and lifestyles over time. Conducted by NHK, this survey takes the form of a questionnaire administered every five years, allowing individuals to gain a comprehensive understanding of their daily lives and lifestyle. In detail, the survey targets 7,200 people over the age of 10 nationwide. It focuses on capturing information about the daily behaviors and home status of the participants, organized by 15-minute intervals on target day. After compiling summary statistics, the survey data is further presented in the form of 4 types of stochastic data include:

- probabilities of adopting given behavior by 15-minutes interval (***PM***)
  (***PM*** would be processed into 5-minutes interval by liner interpolation in the process of model)
- probabilities of adopting given behavior over a day (***PA***)
- average duration time of adopting given behavior (***MTB***)
- standard deviation of duration time of given behavior (***SDTB***)

and is classified by 5 methods include:

- by all people
- by gender/age
- by occupation
- by school attendance
- by region

Some samples of this data are shown in Table 2.1, which is available for free download in [8] and was used in the proposed model.

Table 2.1 Samples of public data of several behaviors of work-male in resting day

Occupant/Day	work-male/resting day			
Behavior	sleeping	eating	wash up	work
PA	99.5%	97.3%	98.9%	86.5%
MTB	7'25"	1'27"	1'14"	9'14"
SDTB	1'14"	0'46"	0'58"	3'53"
Time	***PM***			
0:00	66.7%	1.1%	4.3%	2.3%
0:15	67.2%	0.9%	4%	2.2%
⋮	⋮	⋮	⋮	⋮
23:30	57.6%	0.8%	1%	6.4%
23:45	59.7%	1%	0.2%	6.2%

2.2.2 Classification of behaviors

The categories of behaviors in the survey are presented in Table 2.2. Since residential electricity consumption, stemming from the usage of home appliances or lighting, air conditioners, relies on the specific behaviors (such as watching TV) and presence status of occupants, it is essential to reclassify the behaviors on minor classification. Based on the usage of home appliances and occupants' presence status, the reclassified behaviors are simplified into 24 types and presented in Table.2.3.

Table 2.2 Categories of behaviors in the survey

Major classification	Minor classification	Example
necessary behavior	sleep	sleeping or napping for more than 30 minutes
	eating	breakfast, lunch, dinner, midnight snack,
	wash up	washing face, toilet, bathing
	medical treatment/relaxation	treatment, being hospitalized
restraint behavior	work	actions to earn income.
	work relationship	farewell parties
	classes and campus activities	classes (including online classes)
	learning outside	learning at home
	cooking, cleaning, laundry	meal preparation
	shopping	shopping for food
	caring for children	child's partner
	household chores	organizing and tidying up
	commuting	round trip between home and workplace
	social participation	ceremonial occasions, volunteer activities
free behavior	conversation/interaction	chatting, phone, mail
	sports	gymnastics, playing ball
	excursions/walking	go to recreational areas and downtown areas
	hobbies/entertainment/culture (without internet)	appreciating, watching, playing games
	hobbies/entertainment/culture (Internet, excluding videos)	using the Internet and SNS as a hobby/entertainment
	internet video	watch videos from the internet
	TV	watch TV
	recorded programs/DVDs	watch DVDs
	radio	listen to radio
	newspaper	read newspaper
	magazines/manga/books	read magazines
	music	listen to music
	rest	breaks, snacks, tea,
others	others	others
	unknown	

Table 2.3 Categories of behaviors in the thesis

Interior Behavior (lighting & air conditioners used)		**Exterior Behavior**
Appliance used	**Non-appliance used**	
eating	children care	shopping
wash up	leisure	conversation, personal relationships
sleep	newspaper	work
hobbies, entertainment and culture (with Internet)	magazines comics	leisure and exercise
hobbies, entertainment and culture (without Internet)		class and lecture
cooking, cleaning, laundry		commuting
radio		sporting
household chores		

2.3 Structure of proposed behavior model

2.3.1 Process of generating behavior schedules

During the process of simulation, a blank timeline with 288 time slots (time of a day with 5-minutes interval) is generated firstly and prepares for filling up with behaviors separately as shown in Figure 2.1. The given behavior's occurrences will span corresponding time slots in the timeline depend on its duration time length. Figure 2.2 shows the detail steps and are explained as:

1) Iterates over all given behaviors in order of the ***PA***'s values and determines whether to adopt based on its ***PA***.

2) Once the given behavior has been adopted, the duration time (***DT***) is determined according to the Gaussian Distribution defined by ***MTB*** and ***SDTB***. (An example of behavior eating of work-male in resting day is shown in Figure 2.3).

3) To insert these given behaviors with into the timeline, it is critical to decide several parameters' solutions of the given behavior.

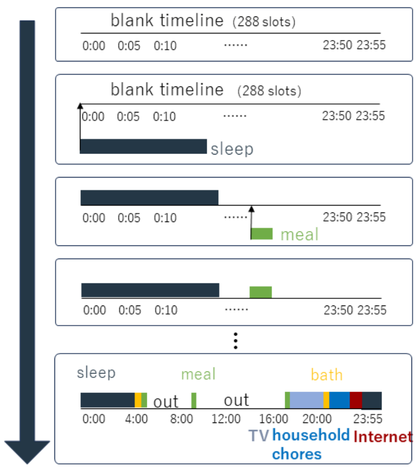

Figure 2.1 Image of behavior schedules' generation

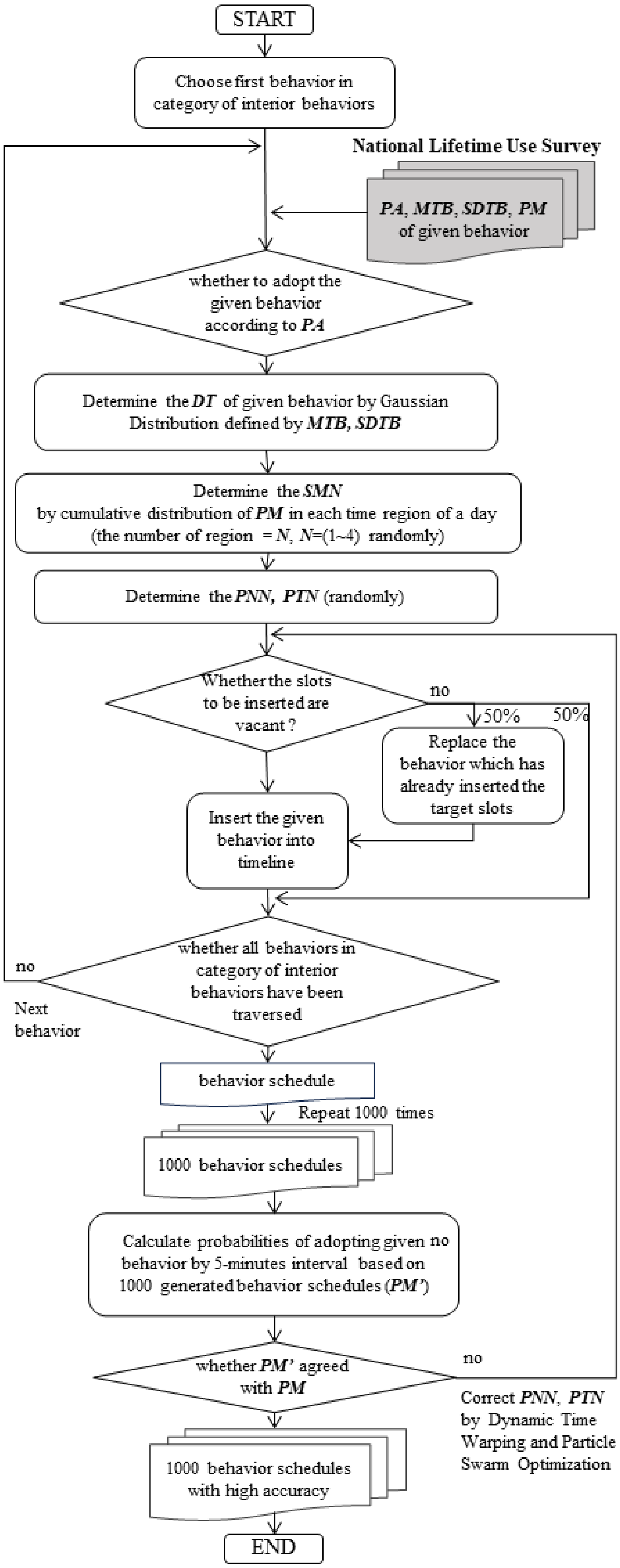

Figure 2.2 Calculation process of proposed model

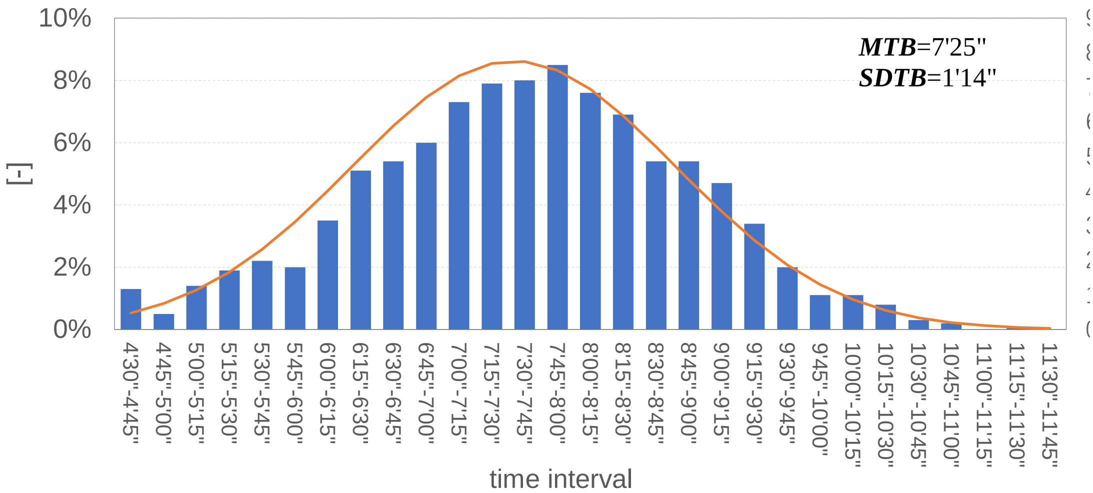

Figure 2.3 Percentages of *DT* of eating for work-male based on the Gaussian Distribution defined by *MTB* and *SDTB*

a) ***n***: number of behavior occurrence

b) ***sm***: start moment of each behavior occurrence.

smn: [sm_1, sm_2, …, sm_n]

The method determining ***smn*** is shown in Figure 2.4. In detail, one day is divided into ***N*** time regions which have the same sum of ***PM***. The start moment of splitting time region is generated randomly (e.g., 6:30). It is assumed that object behavior occurs once in each time region. Based on that assumption, the cumulative distribution function of ***PM*** in each time region has been calculated to determine the ***sm*** of each occurrence.

c) *pt*: each occurrence's duration time as percentage of ***DT.***

ptn: [pt_1, pt_2, …, pt_n]

For one behavior schedule, ***n*** and ***ptn*** could be randomly generated, however in the context of large-scale generation of schedules, randomly generating these two parameters would result in significant errors compared with public data. Hence, it is necessary to introduce new parameters ***PNN*** and ***PTN*** to regulate the generation of ***n*** and ***ptn***.

d) ***PNN***: [PN_1, PN_2, PN_3,…, PN_n]

PN*:* probability of each number of behavior occurrences in numerous schedules

(*e.g.,* PN_2: probability of behavior occurring twice in numerous schedules)

e) ***PTN***: [PT_1, PT_2, PT_3,…, PT_n]

PT: probability of each occurrence's duration time as percentage of ***DT*** in numerous schedules.

(e.g., Figure 2.5 shows the difference between PTN_1: $[\frac{1}{3}, \frac{1}{3}, \frac{1}{3}]$ and PTN_2: $[\frac{1}{2}, \frac{1}{3}, \frac{1}{6}]$

4) Once all the essential parameters for the given behavior have been established, insert it into the timeline at the appropriate location. If this position has been already occupied by other behaviors, there is a 50% probability of either overwriting the original behavior or abandoning the insertion.

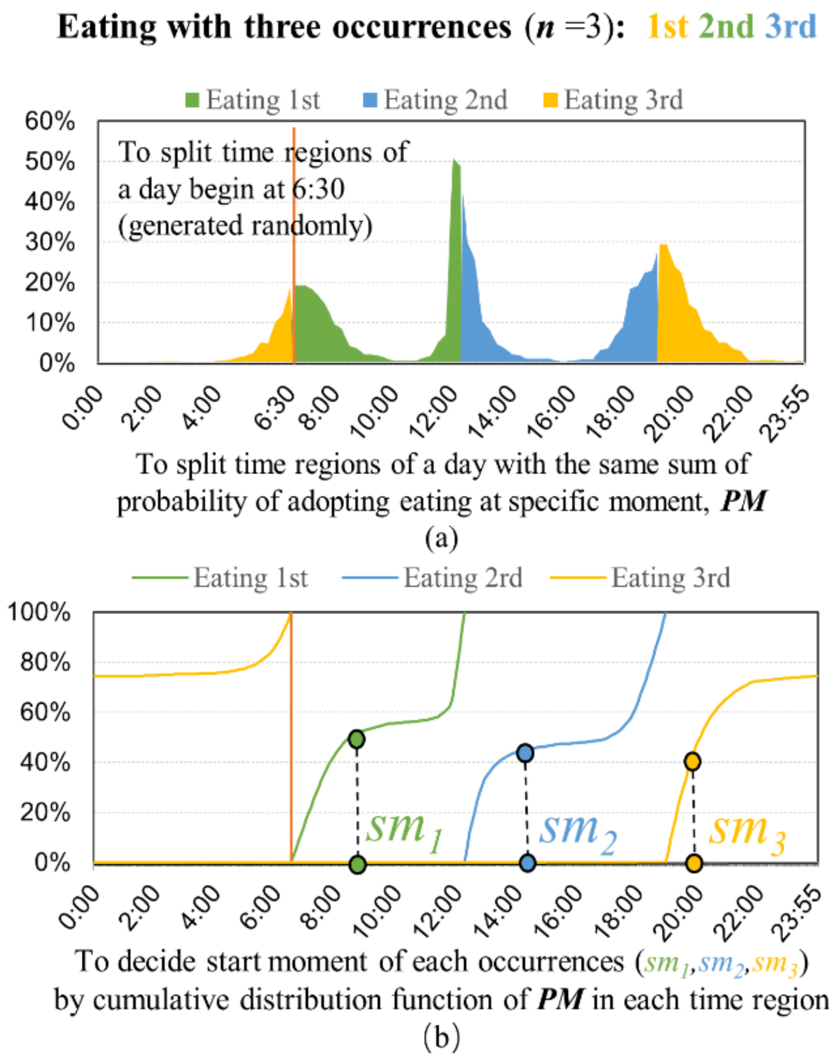

Figure 2.4 Processes of determining *SMN*

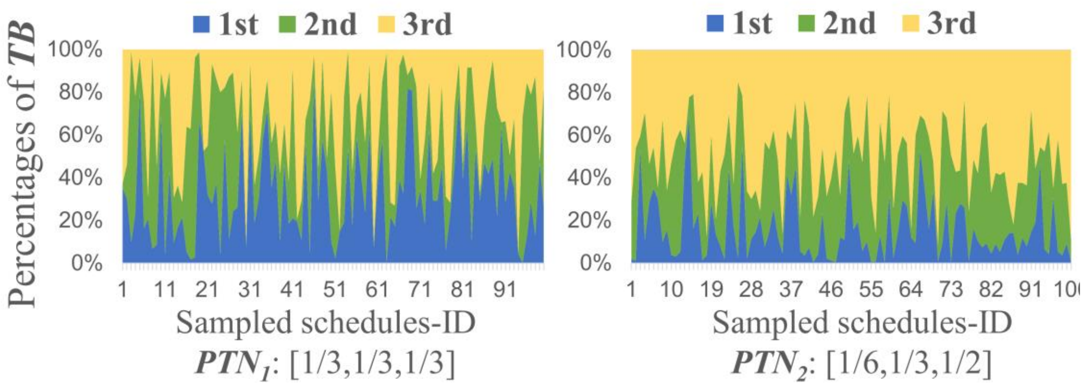

Figure 2.5 Percentages of each occurrence's duration time to *DT* in sampled schedules

5) After traversing all interior behaviors, the behavior schedule is successfully generated. Empty slots in the behavior schedule, where behaviors are not inserted, are considered as engaging in other behaviors unrelated to residential electricity consumption and are not included in the proposed model's scope.

6) Through the proposed method, 1000 behavior schedules have been generated. Then, probabilities of adopting each behavior by 5-minutes interval in these schedules (***PM'***) are compared with ***PM*** in public data.

7) Correct ***PTN*** and ***PNN*** to generate new set of schedules with ***PM'*** close to ***PM***.

2.3.2 Process of correcting model

Without effective methods, the correction of parameters in step *7)* requires continuous attempts, which is a blind and cumbersome process. Therefore, it is necessary to introduce new methods for controlling the correction process, ensuring that it progresses in the right direction, aiming for reduction of error between ***PM'*** and ***PM***.

Dynamic Time Warping

PM and ***PM'*** are both time series data set, the magnitude of the difference at the same time may not precisely reflect the similarity between the two sets of data. For example, if there is minimal difference between ***PM*** and ***PM'*** at different but closely spaced times, and they exhibit the same trend, it can be considered to have met the accuracy requirement. However, even if ***PM'*** is identical to ***PM*** at some times but shows an opposite trend, accuracy cannot be guaranteed. Therefore, a method is necessary to determine how to match two sets of data for comparison. Dynamic Time Warping (*DTW*) introduced in [9] is used to combine the ***PM'*** and ***PM*** and the differences between the ordinary matching method is shown in Figure 2.6.

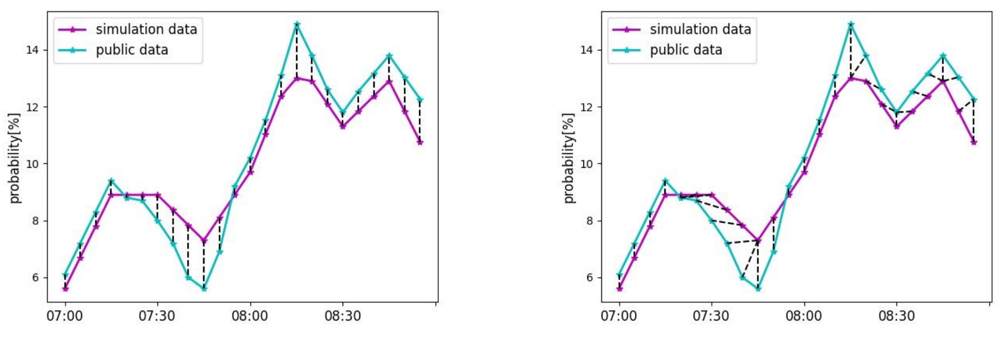

match at the same time　　　　　　　　match by *DTW*

Figure 2.6 Difference between two sets of matching methods.

DTW of ***PM*** and ***PM'*** is calculated by Eq. (2-1):

$$DTW\,(\boldsymbol{PM}, \boldsymbol{PM'}) = \min\sqrt{\sum\left(x_i - y_j\right)^2} \tag{2-1}$$

$$\boldsymbol{PM} = [x_1, x_2, \ldots, x_{287}]$$

$$\boldsymbol{PM'} = [y_1, y_2, \ldots, y_{287}]$$

The list of index pairs $[l_1, l_2, \ldots, l_{287}]$ shows the matching pairs of the elements of ***PM*** and ***PM'*** (e.g., $l_k = (i_k, j_k)$ shows the x_{i_k} and y_{j_k} would be matched) that satisfies the following properties are shown in Eqs. (2-2, 2-3, 2-4):

$$0 \leq i_k, j_k \leq 287 \tag{2-2}$$

$$l_0 = (0, 0),\ l_{287} = (287, 287) \tag{2-3}$$

$$l = (i_k - 1, j_k) \text{ or } (i_k, j_k - 1) \text{ or } (i_k - 1, j_k - 1) \tag{2-4}$$

Different from the traditional matching method which would match ***PM*** and ***PM'*** at the same index pairs $((x_1, y_1), (x_2, y_2), \ldots, (x_{287}, y_{287}))$. In *DTW*, based on the above properties, there is a large number of possible matching solutions as candidates, which is shown in Eq. (2-5):

$$[l_0, l_1, l_2, \ldots, l_{287}] = \begin{bmatrix} (x_0, y_0) & (x_1, y_0) & (x_1, y_1) & (x_2, y_1) & \cdots & (x_{287}, y_{287}) \\ \vdots & \vdots & \vdots & \vdots & \ddots & \vdots \\ (x_0, y_0) & (x_0, y_1) & (x_0, y_2) & (x_1, y_2) & \cdots & (x_{287}, y_{287}) \end{bmatrix} \tag{2-5}$$

all matching solutions' distances between ***PM*** and ***PM'*** would be compared and the smallest one would be chosen as matching method. The distance between ***PM*** and ***PM'*** by this method was used as objective function to evaluate ***PNN&PTN*** candidate solutions, the most suitable ***PNN&PTN*** solution would be decided with the minimal distances (function value).

Particle Swarm Optimization

The preceding section outlines the matching of ***PM*** and ***PM'*** using *DTW* and utilizes their distance as the objective function for evaluating the fitness of ***PNN&PTN***. To enhance the fitness of ***PNN&PTN*** by minimizing the value of the objective function, this section introduces the Particle Swarm Optimization (*PSO*) [10] to search the minimal function value. *PSO* is an evolutionary algorithm that could optimize a problem by iteratively trying to improve a candidate parameters' solution to get the better position in a D-dimensional space (D is the number of parameters).

In the process of the *PSO* algorithm, firstly, a large number of particles have been generated and each particle is a candidate solution of ***PNN&PTN*** with different function values. At 1st iteration, particle' initial position (p_1) and velocity (v_1) are randomly generated. p_1 means solution of ***PNN&PTN*** and v_1

means the distance between p_1 and p_2 (position at 2nd iteration) as showed in Eq. (2-6). These particles make up a cloud that covers the entire space, then the function values of all particles are calculated to decide their fitness. Based on fitness values, the globally best particle position (pg_1) and locally best particle position (pl_1) are determined. As showed in Eq. (2-7), according to pg_1, pl_1 and p_1, v_1 would be updated to v_2, which would continue to update p_2 to p_3.

$$p_{k+1} = p_k + v_k \tag{2-6}$$

$$V_{k+1} = wv_k + m_1(pg_k - p_k) + m_2(pl_k - p_k) \tag{2-7}$$

k:	k^{th} iteration	pl_k:	locally best particle's position at k^{th} iteration
w:	inertia weight	m_1, m_2:	$m_1 = c_1r_1,\ m_2=c_2r_2$
v_k:	particle's velocity at k^{th} iteration	r_1, r_2:	random numbers in the range [0,1]
p_k:	particle's position at k^{th} iteration	c_1, c_2:	$c_1= c_2=2$
pg_k:	globally best particle's position at k^{th} iteration		

With the iteration advancing, the cloud contracts gradually and performs the exploration for best ***PNN&PTN*** solution with minimal function value.

Correction of schedule generation process

In the process of applying the *PSO* algorithm to find the optimal solution for ***PNN&PTN***, two significant errors persist in behavior sleep and eating that cannot be rectified by increasing the number of *PSO* iterations. The example of sleep and eating of work-male in resting day are shown in Figure 2.7 and Figure 2.8. The causes and dealt methods of above errors would be explained as follows:

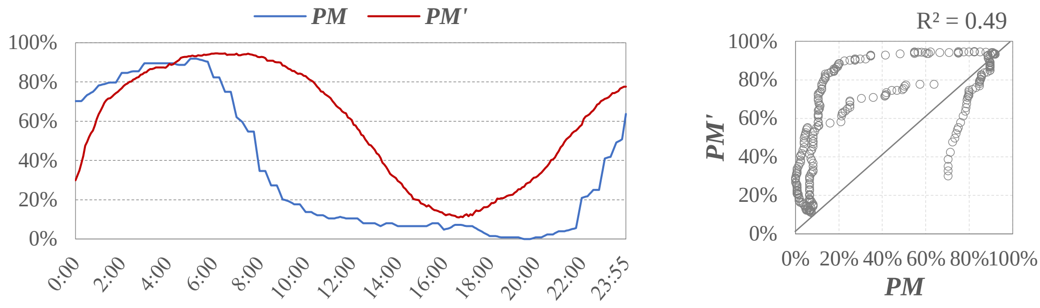

Figure 2.7 Comparation of *PM'* and *PM* (sleeping)

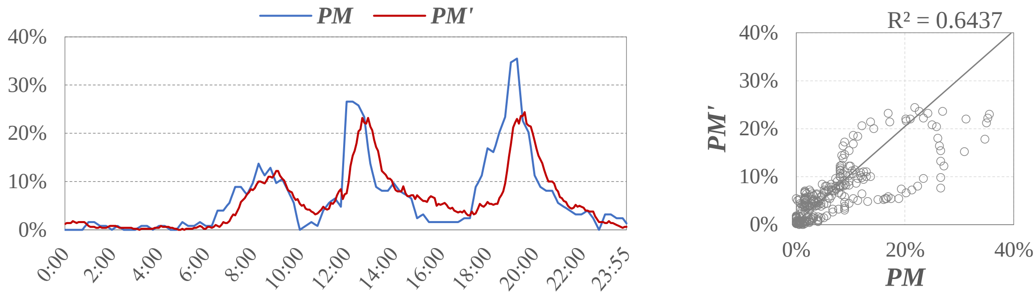

Figure 2.8 Comparation of *PM'* and *PM* (eating)

In Figure 2.7, the error of behavior sleep can be attributed to the inaccurate determination of start moments of sleeping. Different from other behaviors, people always have a long period sleeping in the evening and add a short period sleeping during the daytime. For this type of behavior with a clear temporal characteristic, the method deciding behavior start moments based on sum of ***PM*** is not suitable any longer. To solve this problem, the model has been revised to simulate sleeping behavior in the following process:

a) The number of sleeping occurrence (***n***) is set to 1~2. If sleeping occurs once, it occurs at night; if sleep occurs twice, the first and longer sleeping occurs in the evening and second one occurs at daytime.

b) For sleeping in the evening, people wake up at a more concentrated time than when they fall asleep. Therefore, we use the moments of waking up (ending of sleeping) to decide the position of sleeping in timeline where being inserted into.

c) The range of end moments of first sleeping in the evening is set as 0:00-12:00, the range of start moments of second sleep is set as 12:00-18:00. The specific moments in the range are searched by *PSO* method too.

To sum up, the parameters of sleeping for *PSO* method are reset showed as Eq. (2-8):

$$\boldsymbol{SMN} = [sm_1, sm_2] \qquad \boldsymbol{PNN} = [pn_1, pn_2] \qquad \boldsymbol{PTN} = [pt_1, pt_2] \tag{2-8}$$

In Figure 2.8, for the error of behavior eating, the reason being considered is that the decision of start moment based on cumulative distribution function of ***PM*** always drop behind actual situation. To solve this issue, the new parameter *ad* is introduced to adjust the ***SMN*** as Eq. (2-9):

$$\boldsymbol{SMN} = [sm_1+ad,\ sm_2+ad,\ \dots,\ sm_n+ad] \tag{2-9}$$

The decision of *ad* is also calculated by *PSO* method. Therefore, the solution of ***PNN&PTN***, *ad* would be decided together by minimal objective function value. Figure 2.10 shows the simulation results of ***PM*** and ***PM'*** after the adjustment of behavior start moments and it demonstrates higher accuracy than before.

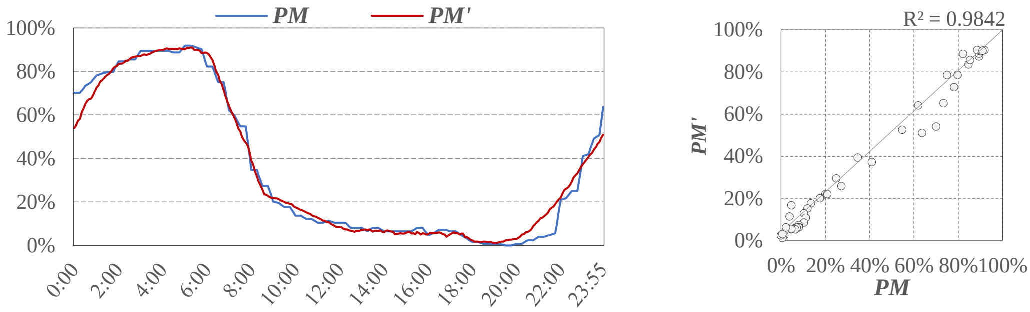

Figure 2.9 Comparation of *PM'* after corrected and *PM* (sleeping)

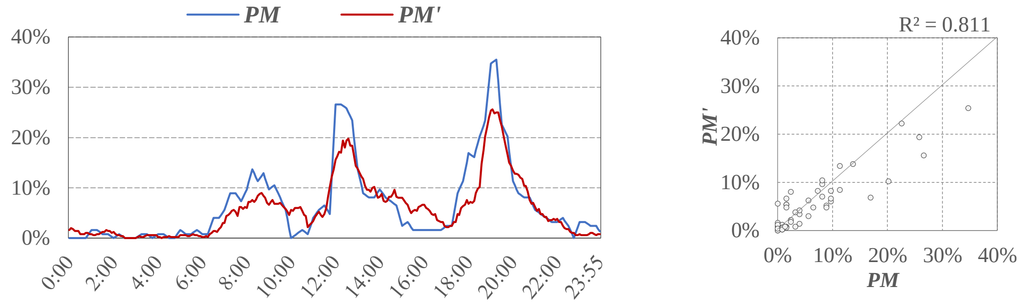

Figure 2.10 Comparation of *PM'* after corrected and *PM* (eating)

Process of searching the suitable parameters

Due to the need to calculate ***PNN&PTN*** corresponding to two types of days for five categories of occupants, the computational workload is substantial. To enhance the efficiency and accuracy of the calculation process, after debugging, the *PSO* algorithm's final number of iteration s was adjusted to 30, with each iteration containing 1,000 particles. With the continuous advancement in iteration, the result of ***PM'*** converges towards ***PM***, as illustrated in the Figure 2.11 (using behavior sleep of work-male in resting day as an example).

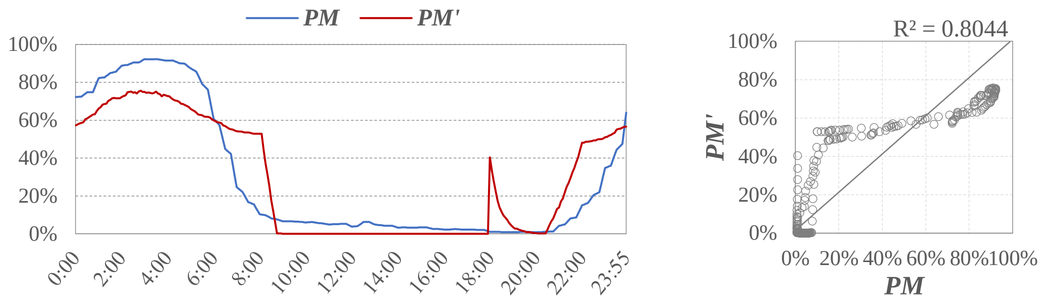

a) Comparation of ***PM'*** and ***PM*** (Iteration – 3)

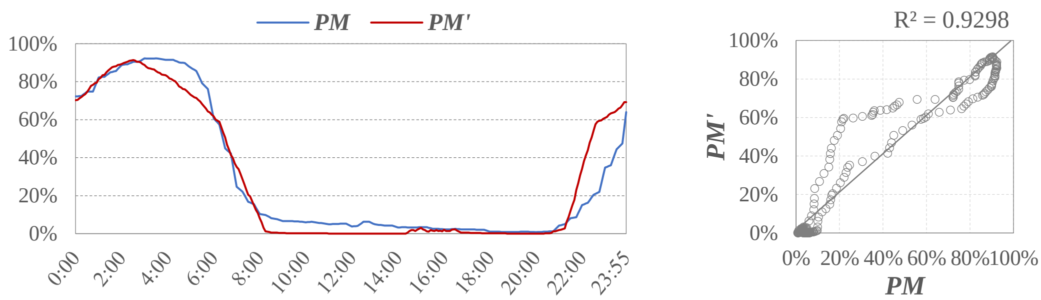

b) Comparation of ***PM'*** and ***PM*** (Iteration-10)

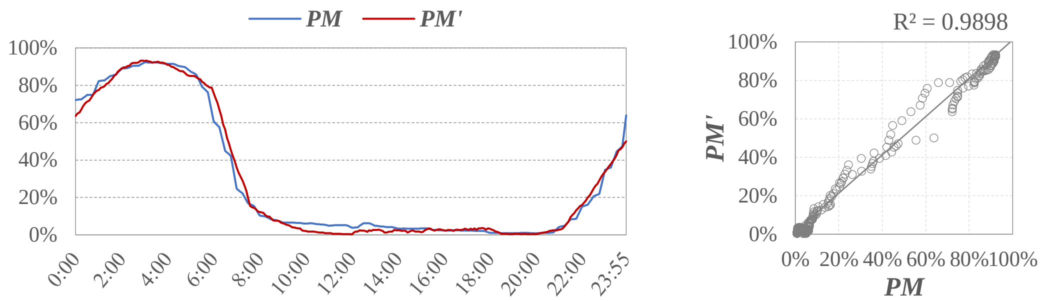

c) Comparation of ***PM'*** and ***PM*** (Iteration – 30)

Figure 2.11 Comparation of *PM'* after corrected and *PM* by advancement of *PSO* iteration (sleep of working-male in resting day)

2.3.3 Results of proposed model

In Figure 2.12-2.16, comparation of ***PM'*** and ***PM*** of 5 type occupants include working-male, housewife, child, teenager and elder are shown, each color block shows the probability that a behavior is undertaken at corresponding period of day. The result shows that ***PM'*** agreed well with ***PM*** and it confirms proposed model's accuracy.

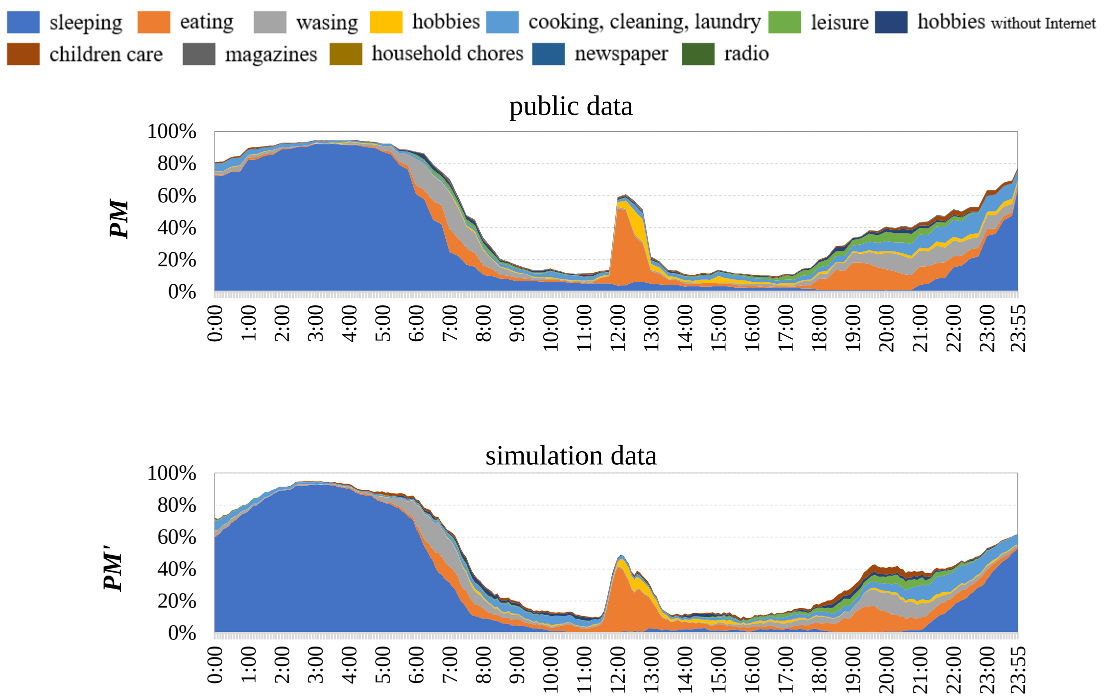

Figure 2.12 Comparation of *PM* and *PM'* (working-male, working day)

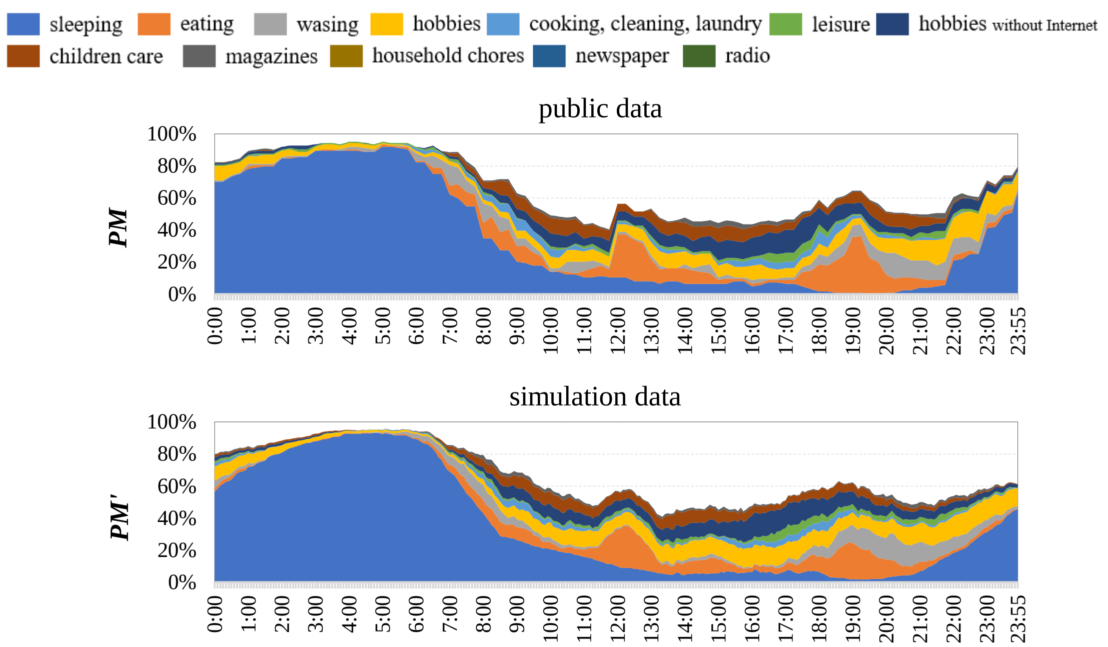

Figure 2.13 Comparation of *PM* and *PM'* (working-male, resting day)

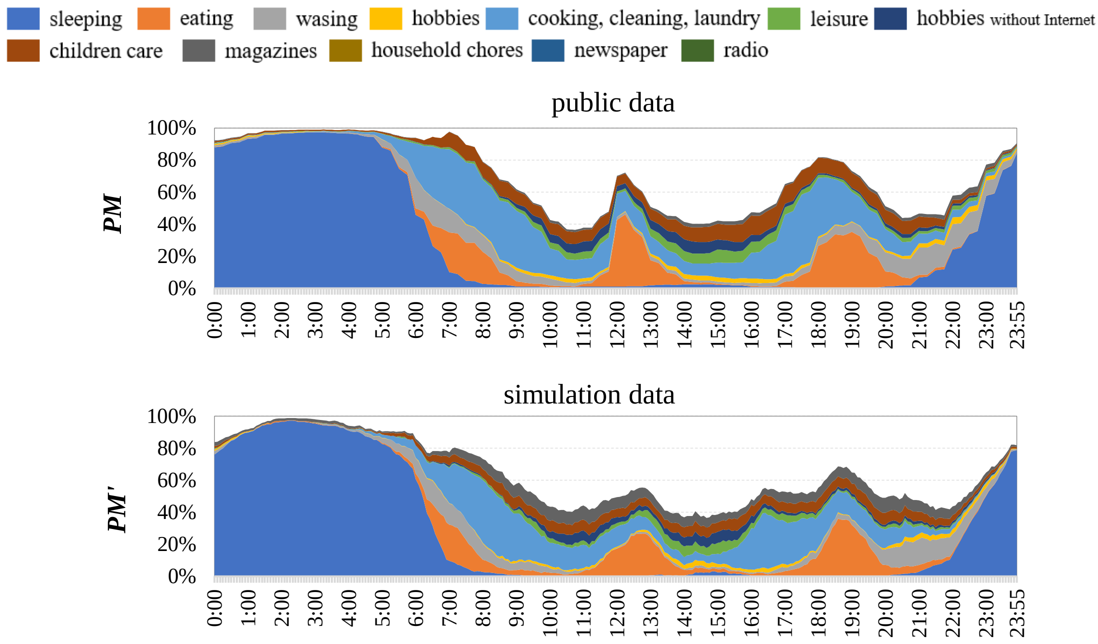

Figure 2.14 Comparation of *PM* and *PM'* (housewife, working day)

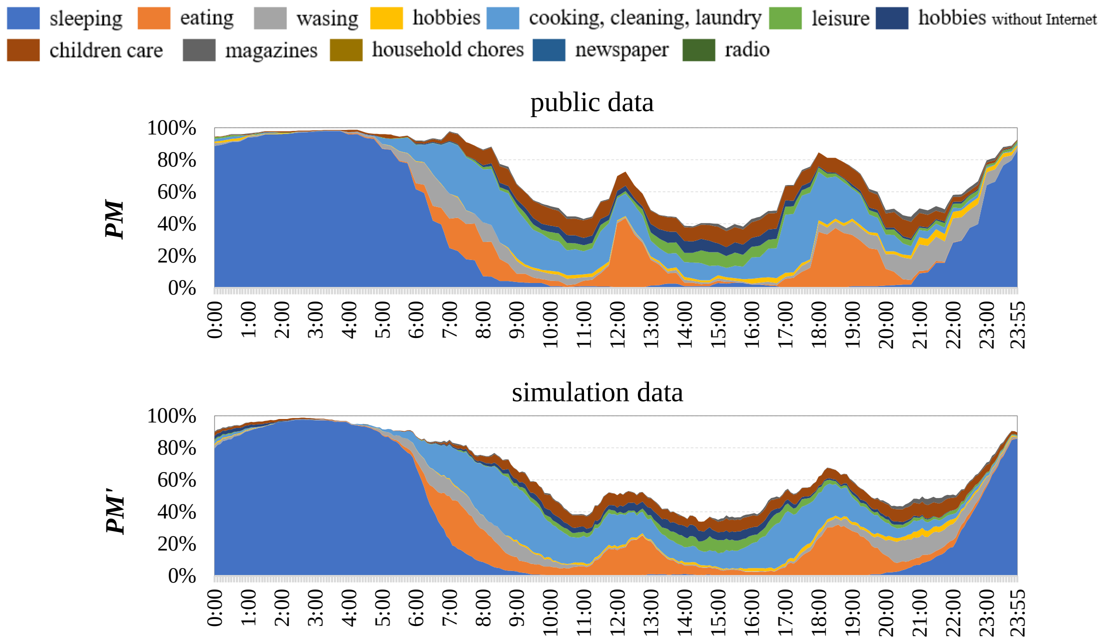

Figure 2.15 Comparation of *PM* and *PM'* (housewife, resting day)

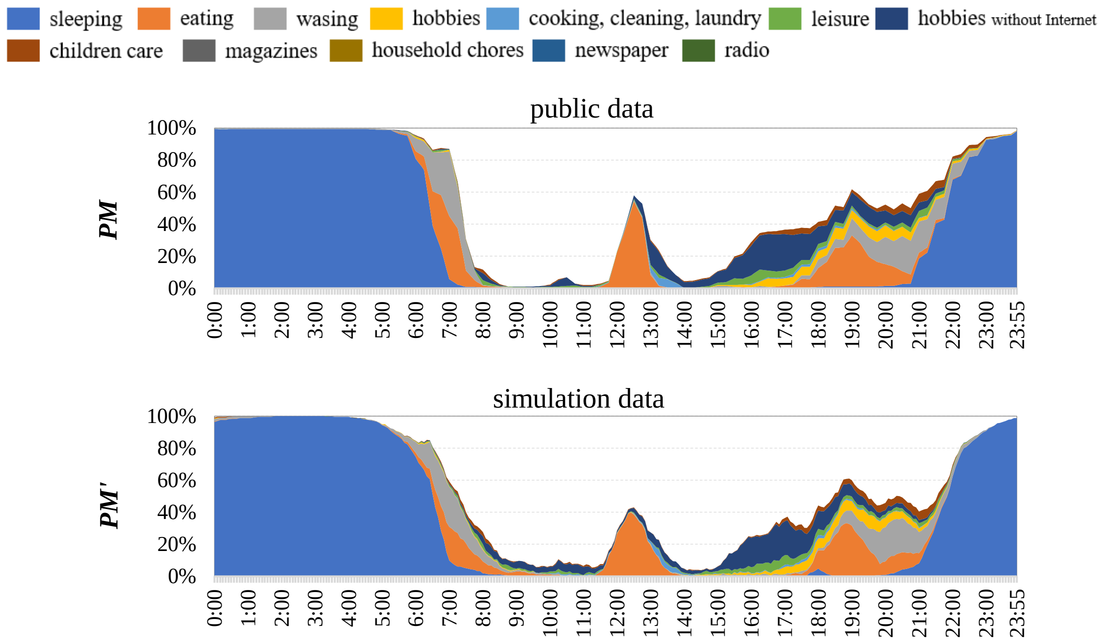

Figure 2.16 Comparation of *PM* and *PM'* (child, working day)

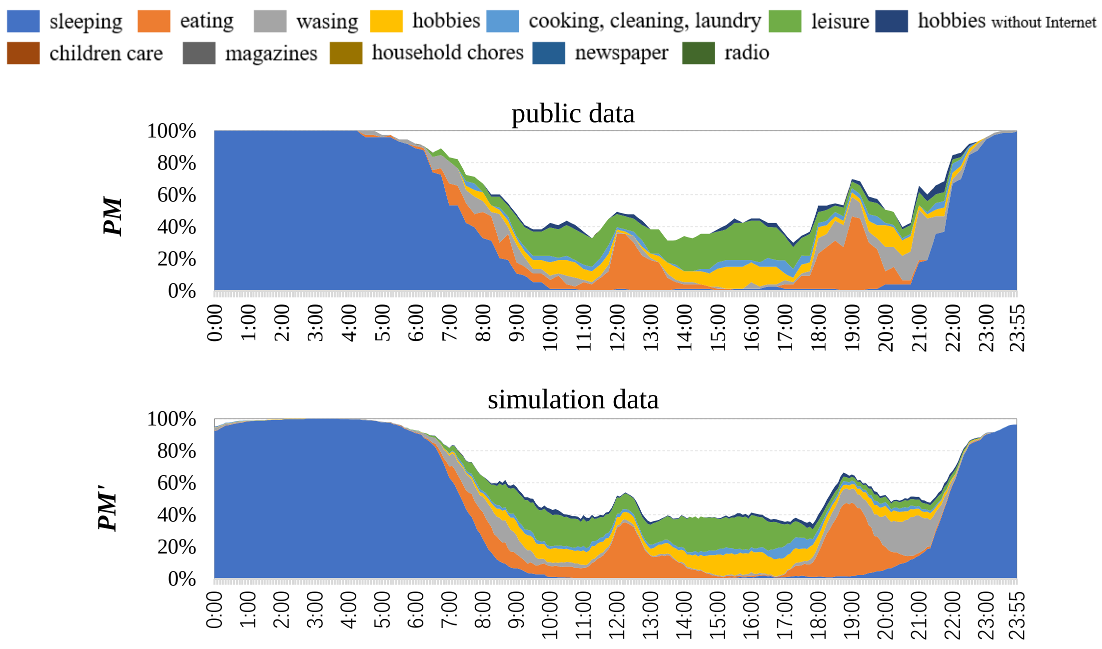

Figure 2.17 Comparation of *PM* and *PM'* (child, resting day)

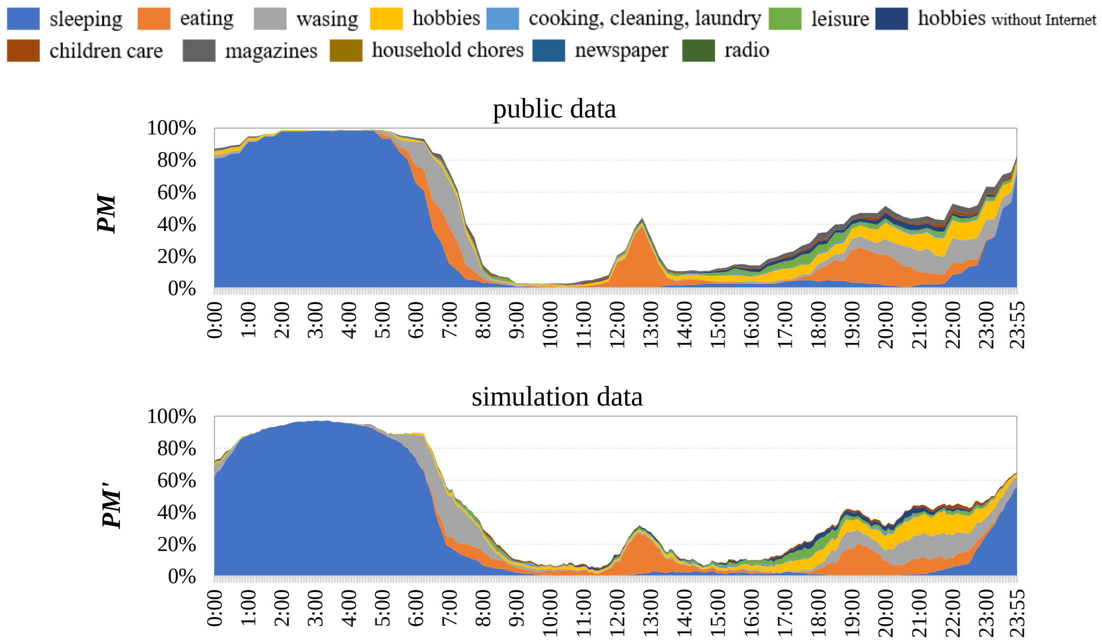

Figure 2.18 Comparation of *PM* and *PM'* (teenager, working day)

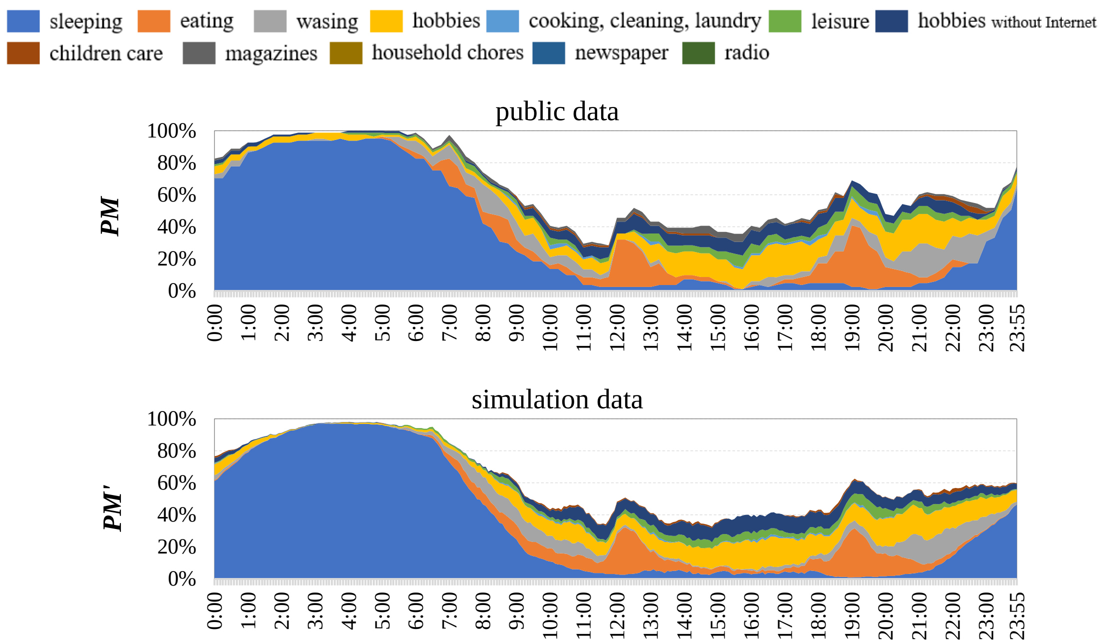

Figure 2.19 Comparation of *PM* and *PM'* (teenager, resting day)

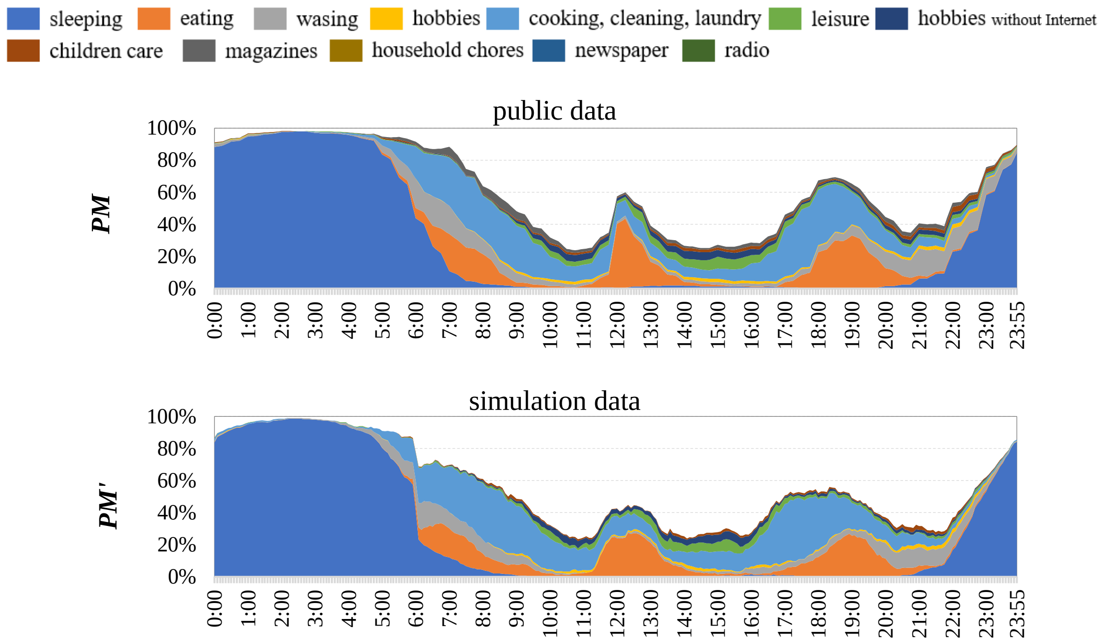

Figure 2.20 Comparation of *PM* and *PM'* (elder, working day)

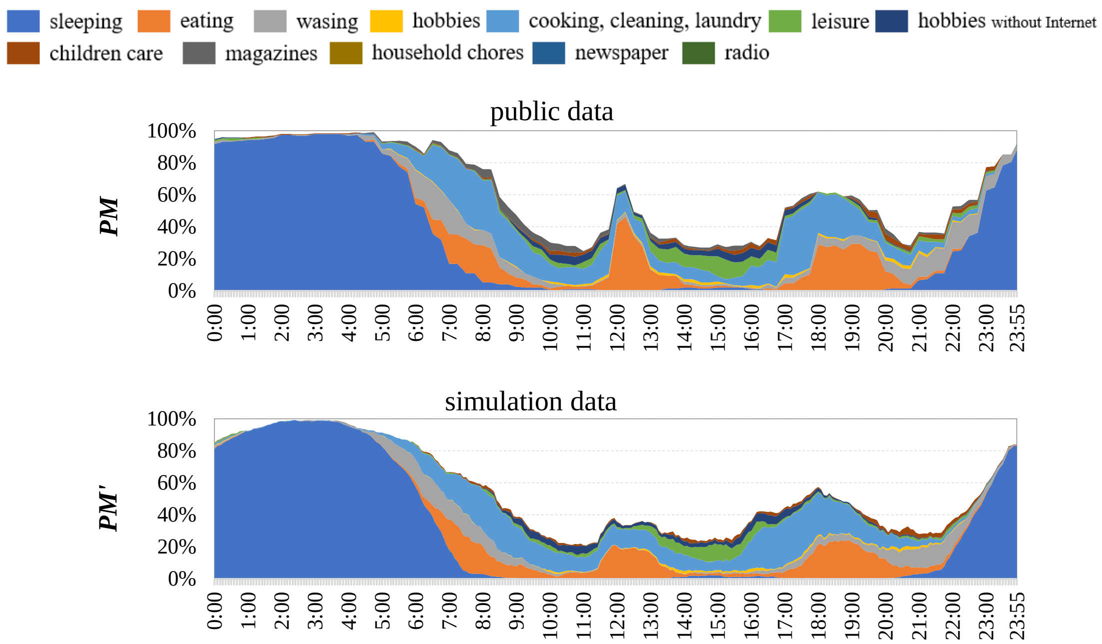

Figure 2.21 Comparation of *PM* and *PM'* (elder, resting day)

2.3.4 Simulation results of household

In the context of simulating electricity demand for residential buildings, it is imperative to incorporate the behavior schedules of household members. While the proposed model is capable of accurately simulating the behavior schedules for each type of occupant, the current limitation lies in the absence of connections among these results. This renders the outputs impractical for direct use, as the behaviors of household members are inherently interconnected. Consequently, a model is proposed to filter and match the generated results, addressing this issue.

According to [7], Japanese household members typically dine together and perform washing up individually. Leveraging this pattern, the generated results for each type of occupant, particularly those with significant numbers, are filtered and matched to construct behavior schedules for a household. It's noted that the initiation time and duration of eating, as well as bathing, may vary among household members, reflecting the natural diversity in their routines.

The detail process of the proposed model is explained as follow:

The objective is to choose appropriate behavior schedules from over 1000 simulation results for each type of occupant to create composite behavior schedules for a household. For this purpose, the *PSO* algorithm is employed to search for suitable solutions. The candidate solution for behavior schedules, identified by their respective IDs for each member, is defined as

$$[x_1, x_2, \ldots, x_n]$$

$(1 <= x_1, x_2, \ldots, x_n <= 1000$, where n is the number of household members)

and the objective function is formulated as Eq. (2-10).

$$y = T_{\text{bath}} - T_{\text{eating}} \tag{2-10}$$

T_{bath}: Duration time that more than two members are bathing at the same time by candidate solution.

T_{eating}: Duration time that more than two members are eating at the same time by candidate solution.

In accordance with [8], within each member, a candidate solution exhibits better fitness when there is minimal overlap in bath behaviors and increased overlap in eating behaviors occurring simultaneously. It is important to note that this process aims not to find the single best solution, but rather to identify a set of suitable solutions with a specified quantity.

The behavior schedules of two households, each consisting of three and five members, respectively, were examined for both working days and resting days. The households in the first case comprised a working male, a housewife, and one child; in the second case comprised two elders, a working male, a housewife, and one child. Figures 2.22-2.29 illustrate five combinations of behavior schedules generated through random matching and with the assistance of the *PSO* algorithm.

For a precise comparison of results, the average ratios of time spent on bath and eating (defined as the time collectively spent by more than two members engaging in the same behavior relative to the

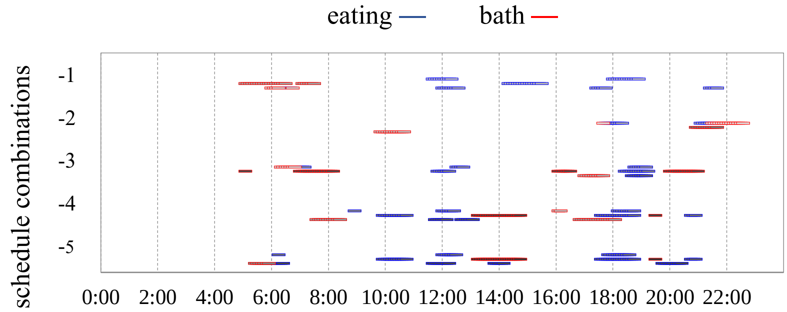

Figure 2.22 Behavior schedules combination of a household with 5 people in working-day (matching randomly)

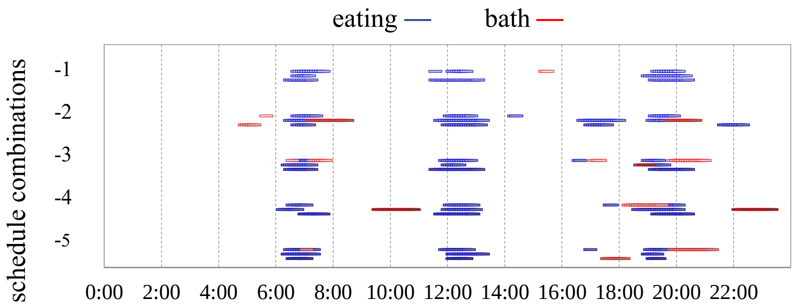

Figure 2.23 Behavior schedules combination of a household with 5 people in working-day (matching by *PSO*)

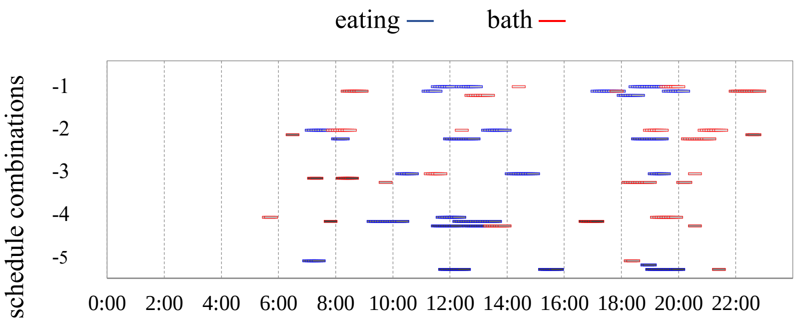

Figure 2.24 Behavior schedules combination of a household with 5 people in resting-day (matching randomly)

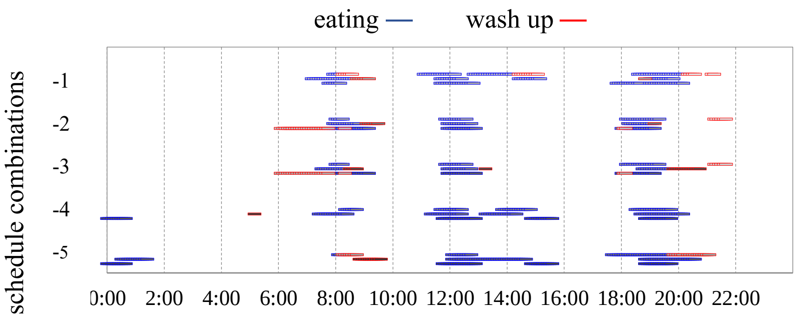

Figure 2.25 Behavior schedules combination of a household with 5 people in resting-day (matching by *PSO*)

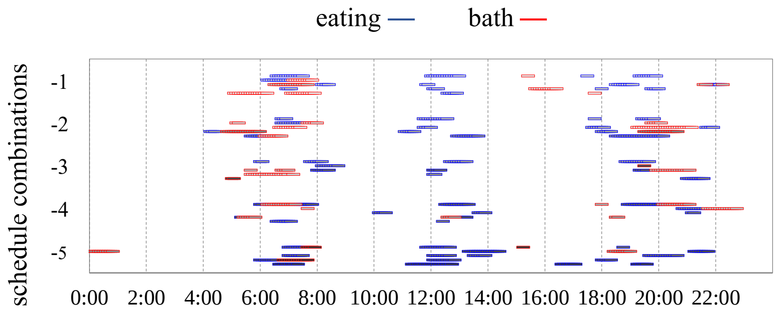

Figure 2.26 Behavior schedules combination of a household with 5 people in working-day (matching randomly)

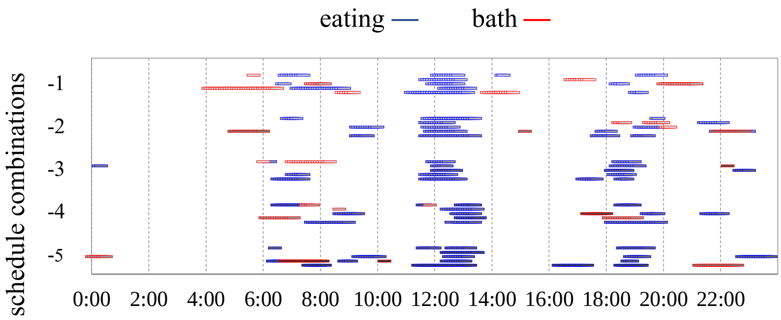

Figure 2.27 Behavior schedules combination of a household with 5 people in working-day (matching by *PSO*)

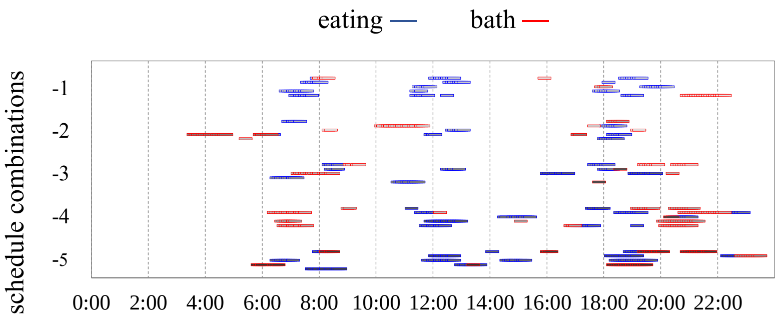

Figure 2.28 Behavior schedules combination of a household with 5 people in resting-day (matching randomly)

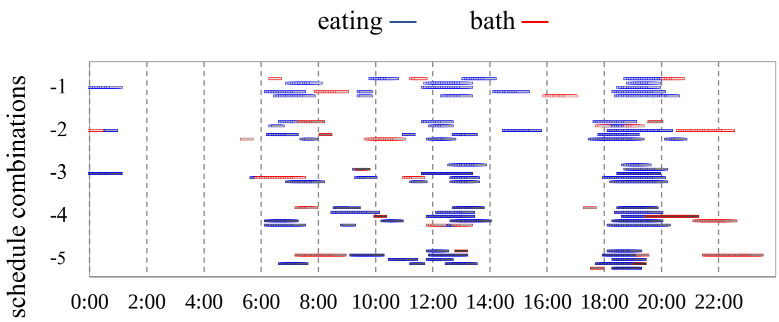

Figure 2.29 Behavior schedules combination of a household with 5 people in resting-day (matching by *PSO*)

total time for that behavior) for the five schedule combinations are calculated and presented in Figure 2.30.

It can be inferred that, in comparison to random matching, the *PSO* algorithm leads to a concentration of eating behaviors by each member during the same periods, resulting in larger R_{eating} values. Conversely, the bath behaviors are distributed across different periods, leading to smaller R_{bath} values. This alignment with the fundamental characteristics of household members' lives validates the effectiveness of our model in generating behavior schedules of household.

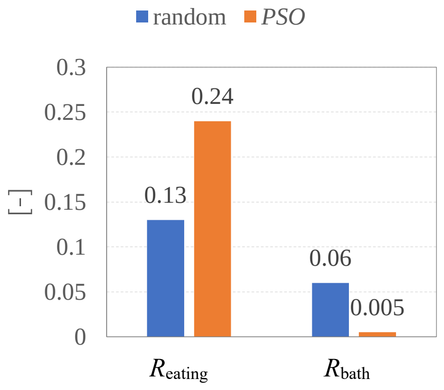

a) 3 people household in working day

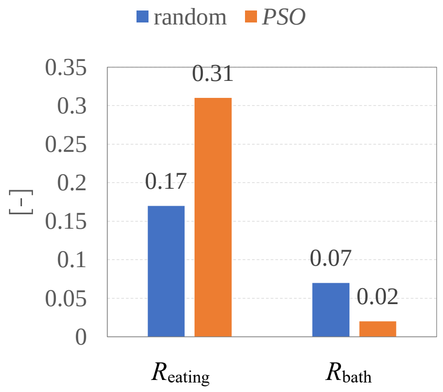

b) 3 people household in resting day

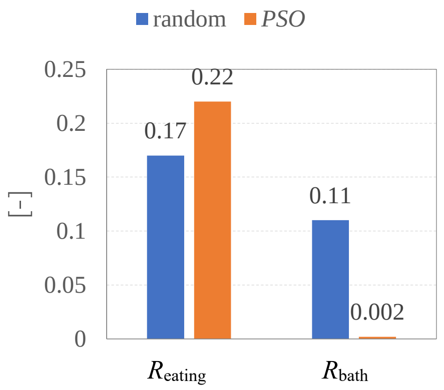

c) 5 people household in working day

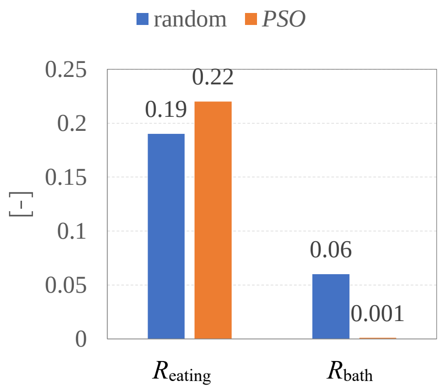

d) 5 people household in resting day

Figure 2.30 Comparation of R_{eating} and R_{bath} in two household and two days by matching randomly and *PSO*

2.4 Conclusions

This chapter proposes a model based on public data to generate occupants' behavior schedules and subsequently formulate behavior schedules for household members. The proposed model could be used in energy demand estimation of residential buildings in urban scale. In contrast to existing research on behavior models, this model possesses the following distinctive features:

- Generating occupants' behavior schedules solely based on publicly available stochastic data (public data), without the need for extensive statistical analysis of large volumes of raw *Time Use Data* (*TUD*). This approach simplifies the behavior model, rendering it more efficient and accessible, particularly in regions where comprehensive *TUD* may not be readily accessible.
- The model does not involve classifying behaviors or setting specific numbers and durations for behavior occurrences. This characteristic serves to eliminate errors arising from subjective assumptions, thereby enhancing the accuracy and objectivity of the model.
- The model employs the Dynamic Time Warping (*DTW*) and Particle Swarm Optimization (*PSO*) algorithms to determine the appropriate number of behavior occurrences and percentages of occurrence durations. This approach aims to closely align simulation results with public data, ensuring a more accurate representation of real-world behavior patterns.
- The model determines the initiation moments of behaviors by referencing the cumulative distribution of public data. In cases where the simulation results deviate from the public data, the initiation moments calculated through the method are adjusted using the *PSO* algorithm to enhance the agreement between the model outcomes and public data.
- The model considers the interconnection of behaviors among household members. Through the *PSO* algorithm, it seeks the optimal combination of generated behavior schedules from each occupant to formulate combinations of household members' behavior schedules.

However, certain drawbacks exist in the proposed model.

For a single occupant:

a) In public data, there are periods, specifically from 12:00 to 12:30 and 22:00 to 22:30, where the probabilities of eating and sleeping exhibit a rapid increase. Unfortunately, the simulation results do not accurately capture this phenomenon.

b) The model lacks consideration for the interaction between individual behaviors. For example, individuals typically tend to engage in sleeping after bath, but the current simulation fails to effectively capture the seamless transition between sleeping and bath within a single schedule.

For household with several members:

c) The current model only considers behaviors related to eating and bath, omitting other behaviors such as watching TV. The inclusion of additional behaviors poses a challenge, as the complexity of matching suitable behavior schedules increases with the number of considered behaviors.

d) As shown in results, household members tend to have lunch together on working days, which is inconsistent with reality. The discrepancy arises because the public data records for eating behaviors do not distinguish between being at home and going out. Addressing this issue is crucial in the context of energy simulation for residential buildings.

There are also some details need to be explained. Firstly, using the *PSO* algorithm alone enables the determination of the start moment of each behavior occurrence (***SMN***), but the incorporation of cumulative distribution of probabilities of adopting a given behavior (***PM***) assists in narrowing the search range and expedites the solution. Secondly, in addition to simulating behavior schedules solely based on historical public data, the model holds potential for anticipating future changes in people's behavior by adjusting the input public data. For instance, modifications could be made to reflect shifts in working times at home, influenced by factors such as the COVID-19. This adaptive capability enhances the model's relevance in dynamic scenarios. Finally, when compared with similar studies utilizing *Time Use Data* in other countries, such as research in UK [3] and US [11], the simulation results underscore the unique characteristics of Japanese occupant behaviors.

In the future, we plan to address the mentioned drawbacks to enhance the model.

To address drawback *a)* and *b)*, a more comprehensive analysis of public data will be conducted, particularly focusing on specific time periods. Subsequently, different weights will be assigned to these time intervals in the simulation process. This approach will enable model to better capture the variations in behavior probabilities, thereby improving the accuracy of our model's predictions.

For drawback *c)*, it will be addressed by considering a broader range of behaviors and exploring the integration of more efficient algorithms.

About final drawback *d)*, the classification of indoor behaviors will be enhanced by incorporating more detailed distinctions based on occupant types and target days.

Additionally, it is crucial to acknowledge that behavior schedules cannot be directly applied in the electricity demand estimation model without considering appliances' operation possibilities aligned with specific behaviors. The research on the correlation between behavior and appliances' operation is introduced in the next chapter.

Reference

[1] G. Happle, J. A. Fonseca, and A. Schlueter, "A review on occupant behavior in urban building energy models," Energy & Buildings, vol. 174, pp. 276-292, Sept. 2018.

[2] J. Tanimoto, A. Hagishima, and H. Sagara, "Validation of methodology for utility demand prediction considering actual variations in inhabitant behavior schedules," Journal of Building Performance Simulation, vol. 1, no. 1, pp. 31-42, Mar. 2008.

[3] I. Richardson, M. Thomson, and D. Infield, "A high-resolution domestic building occupancy model for energy demand simulations," Energy and Building, vol. 40, no. 8, pp. 1560-1566, Feb. 2018.

[4] J. Widén, et al., "Constructing Load Profiles for Household Electricity and Hot Water from Time-Use Data – Modelling Approach and Validation," Energy and Building, vol. 41, no. 7, pp. 753-768, Mar. 2009.

[5] Y. Yamaguchi and Y. Shimoda, "Evaluation of behavior model of occupants in home based on Japanese national time use survey," Proceedings of Building Simulation 2015: 14th Conference of IBPSA, Dec. 2015, pp. 2897-2904.

[6] Y. Yamaguchi and Y. Shimoda, "A stochastic model to predict occupants' activities at home for community-/urban-scale energy demand modelling," Journal of Building Performance Simulation, vol. 10, no. 5-6, pp. 565-581, Jun. 2017.

[7] Y. Li, Y. Yamaguchi, and Y. Shimoda, "Impact of the pre-simulation process of occupant behavior modelling for residential energy demand simulations," Journal of Building Performance Simulation, vol. 15, no. 3, pp. 287-306, Mar. 2021.

[8] Japan Broadcast Institution (NHK), National Lifetime Survey in 2020, Japan. https://www.nhk.or.jp/bunken/yoron-jikan/

[9] H. Sakoe and S. Chiba, "Dynamic programming algorithm optimization for spoken word recognition," IEEE Transactions on Acoustics, Speech, and Signal Processing, vol. 26, no. 1, pp. 43-49, Feb. 1978

[10] J. Kennedy and R. Eberhart, "Particle swarm optimization," Proceedings of ICNN'95 – International Conference on Neural Networks, pp. 1942-1948, Nov. 1995

[11] L. Diao, Y. Sun, Z. Chen, and J. Chen, "Modeling energy consumption in residential buildings: A bottom-up analysis based on occupant behavior pattern clustering and stochastic simulation," Energy and Building, vol. 147, pp. 47-66, July 2017.

Chapter-3

Simulation model & results of residential buildings' electricity demand

3.1 Introduction

In this chapter, the 5-minutes interval electricity demand simulation model of urban residential buildings is developed, and the electricity demand of residential buildings are simulated by proposed model in urban scale and street level area scale of target city.

Due to the vast number of urban residential buildings, simulation of every single house in the city and presenting the results is impractical. Additionally, the time-series electricity demand of a single residential building is hard to understand precisely because it is highly depending on the factors like occupant behaviors, which vary from one household to another. Therefore, the challenge of the proposed model lies in streamlining the volume of calculations while ensuring accuracy by leveraging the characteristics of residential electricity demand.

To address this issue, rather than focusing on individual one, using a cluster of all residential buildings in the target area as the research object, would be more feasible. This approach has the following advantages:

- The aggregated electricity demand of houses is relatively stable and more predictable.
- Simulating results by areas makes it easier to compare different areas among cities.
- Supplied object of some decentralized devices (e.g., cogeneration system) is multiple houses rather than one.

Therefore, the simulation target of this model has shifted from individual house to cluster of houses.

3.1.1 Previous research

As obtaining measured electricity data for buildings at an urban scale is challenging in most cases, an efficient model is necessary to understand the electricity demand of buildings, especially residential buildings. There are many research papers about approaches of making urban buildings energy model, Swan and Ugursal [1] reviewed these research paper's approaches and categorized them as top-down and bottom-up approaches. Shimoda et al. [2] explained bottom-up approach accounts for the energy consumption of each end-use (like appliances, air-conditioner, lighting, etc.), it is effective for targets of assessment that share different end-uses. In detail, Abbasabadi et al [3] further divided the bottom-up approach to data-driven and simulation methods. Data-driven models, such as machine learning, perform well and show good accuracy. However, the result is highly based on the dataset features, making it challenging to forecast future energy demand with changes in factors such as the acceleration of high thermal performance house construction. Additionally, most cities currently lack access to sufficient urban energy data. Therefore, not only data-driven models, but simulation models are also necessary.

One type of simulation model is called an archetype. This model develops a limited set of archetype houses to represent a great number of residential buildings. These archetypes share similar features, including geometric, thermal characteristics, and operating parameters, as explained by Parekh et al. [4]. It should be noted that these archetype houses are generated based on several assumptions, which simplify the real situation. These methods of generating archetype buildings are termed stock modeling, as described by Shimoda et al. [2], and they play an important role in determining the quality of the simulation. In the past studies using archetype methods, apart from building size and shape, stock modeling that considers space heating load, involving house thermal performance and internal gains, has received considerable attention. For example, Streicher et al. [5] proposed a bottom-up model to analysis the space heating and cooling load of Swiss residential buildings using 54 archetypes. The heating loads were disaggregated to show the contributions from the construction year and various components like walls, windows, roof and floor. Lavagna et al. [6] modeled EU residential housing stock with 24 representative dwellings based on building typology, occupant number, lifetime, glazing, space heating and other factors. Mata et al. [7] classified residential buildings in four European countries by building type, construction year, climate region and the main fuel source. However, the life behavior schedule of occupants, which determines whether to activate the air-conditioning and consume electricity, had not been considered in the above-mentioned research studies. Shimoda et al. [2] indicated that it is common for the operation of air conditioning to be continuous in Europe and North America, suggesting that space heating and cooling loads have little connection with occupant behavior. This is different compared to Asia countries like Japan. Dealing with this problem, the household type and occupant's life schedule were considered in their model. In detail, they first developed a model to generate various life schedules that record occupants' behaviors during the daytime [8]. These schedules were then utilized to determine the operational status of air-con, appliances, and lighting in houses within their energy simulation model. In [9] they simulated the energy demand at the postcode district level at a national scale with detailed archetypes of Japanese residential buildings. Ueno et al. [10] proposed a similar model that considers household type and occupant's life schedule to estimate the electricity demand of residential buildings on several example districts.

Using archetype simulation models, the studies had conducted simulations at different scales, including national scale ([2], [5], [6], [7]) and district scale ([9], [10]). However, the research object was a single unit, such as an entire nation, city or district, due to the availability and ease of obtaining the dataset. These studies didn't demonstrate differences in energy demand caused by variations between different areas. While there were also many studies that simulated several areas and displayed maps of residential energy use intensity, some issues still exist. For example, Jones et al. [11] simulated the energy demand of houses for all parts of Neath Port Talbot in the UK, but the resolution of the demand is at a yearly level and is unable to show energy demand in short time intervals. Yamaguchi et al. [9] simulated all postcode-level districts in Japan. Due to the extensive computational requirements for the entire country, the simulation focused on 500 randomly selected households per district, presenting only the average energy demand per household.

In summary, existing models for urban houses' electricity demand are limited by computational scale, making it challenging to apply calculations to all houses throughout the entire city. Therefore, this chapter develops a model using the archetype simulation method to estimate the electricity demand of houses and across all areas of the target city.

3.1.2 Overview

Figure 3.1 illustrates the overview of the proposed model.

Firstly, necessary public statistic data have been collected. Secondly, several archetype houses (each archetype represent one type of houses) have been set to represent the housing stock in Japan. In detail, each archetype is assigned with unique characteristic, including house type (apartment / detached), floor area and combination of household member with specific attributes like age, gender and employment / school status. Thirdly, several proposed data processing models are developed to estimate the number of real object houses classified in each archetype house (number of each archetype house), the distribution of construction years for the housing stock under three cases (case_2020, case_2025 and case_2025_ retrofit).

Depending on whether it is affected by thermal performance, the house's electricity demand is divided into two categories as appliances (including lighting and ventilation) and air-conditioning, which need to be simulated separately.

In appliances category, the electricity simulation model utilizes occupant behavior schedules, probabilities of appliances usage, and appliances power settings in current (case_2020) and future (case_2025 and case_2025_ retrofit) to simulate appliances electricity consumption.

In the air-conditioning category, due to the influence of thermal performance of house's construction, electricity demand needs to be calculated based on the heating load. Firstly, calculating the heating load of archetype house with standard thermal performance based on the current temperature and future predicted temperatures. Because multiple occupant behavior schedules are utilized, each archetype house receives multiple heating load results, combined with appliances' electricity calculated by the same behavior schedule, forming its respective database.

When simulating the residential electricity demand in the target area, simulation results are randomly selected from these databases in quantities corresponding to the estimated number of each archetype house. Due to differences in thermal performance, the heating load of a real house may vary from that of its corresponding archetype house. Therefore, the heating load of the real houses should be corrected from the archetype house's heating load based on the estimated results of construction year in each case.

Then, utilizing current and future air-conditioner electricity models, the electricity consumption of the air-conditioning is then calculated based on the corrected heating load. By adding the electricity demand of appliances, the total electricity demand of real houses in target area is determined.

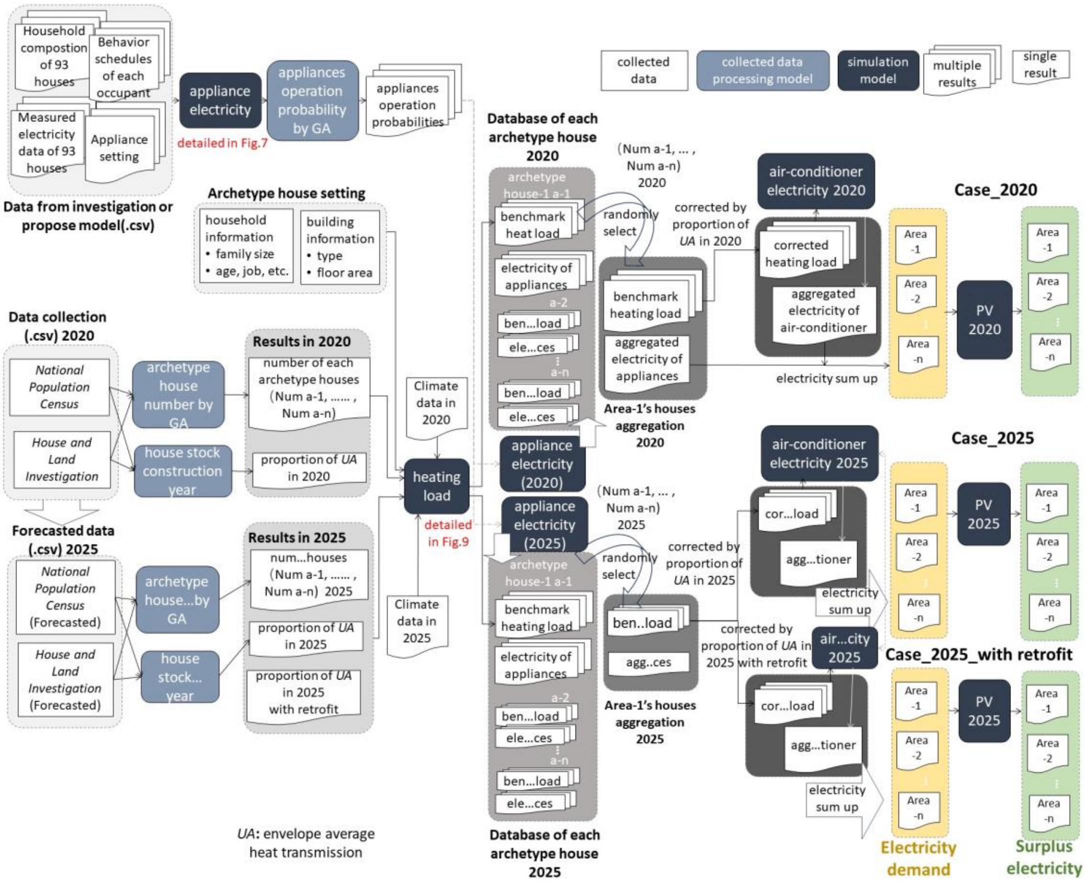

Figure 3.1 Overview of the process of electricity simulation model of houses in urban

3.2 Data preparation

3.2.1 Calculation setting

To develop estimation models for the number of each archetype house and construction year, public statistical data include Population Census [12], House and Land Investigation [13] of each survey year that have been collected. The content of collected data is shown in Tables 3.1, 3.2, 3.3. Additionally, measured 30-minute interval electricity consumption data from 93 households in Ozasa residential area has been collected to develop appliances operation probabilities model and verify the simulation results.

Table 3.1 List of data used by National Population Census in 2020 (current)

Content		Symbol
Household Number (street-level)	total	h_t
	household member: 1-6	$h_{1\text{-}6}$
	household member: elder single	h_e
	household member: couple only	h_{2c}
	household member: elder couple only	h_{2ce}
	household member: couple and child	h_{cc}
	house type: apartment	h_{ap}
	house type: detached	h_{de}
Population (street-level)	total	p_t
	male	p_m
	female	p_f
	male-child (under 15 years)	p_{mc}
	male (15-65 years)	p_{ma}
	elder-male (above 65 years)	p_{me}
	female-child (under 15 years)	p_{fc}
	female (15-65 years)	p_{fa}
	elder-female (above 65 years)	p_{fe}
	marital status	p_{ms}
	apartment	p_{ap}
	detached	p_{de}
Ratio (district-level)	one-parent /couple, children household	R_{op}
	employed female / female (15-65 years)	R_{ef}

To begin the simulation, it is necessary to set the archetype houses to represent the entire residential sectors. In detail, the archetype house could be divided into two parts, including building type side and household side. For the building type side, Shimoda et al. [14] developed an end-use residential energy model called TREES and classified the Japanese residential buildings into 12 archetypes which are used in this study. Table 3.4 and Figure 3.2 show the detail information of these houses include floor plan, rooms with air-conditioner (red part). For the household side, according to [14], and to simplify the model, the households in the target city are classified into 12 categories. Considering the constraints of house floor plan and area on the household size, some combinations with small number in statistical data, like single member household living in a detached house, are not considered. Therefore, 21 archetype houses (c_0-c_{20}) consisting of household and building types are shown in Table 3.5.

Table 3.2 List of data used by National Population Census in several years (1995, 2000, 2010, 2015, 2020)

Content	Symbol	
Household number (street-level)	total number in target year	h_{ty}
Population (street-level)	migration people moved in during the past 5 years of target year	p_y^{in}
	average household size in target year	p_{hy}

Table 3.3 List of data used by National House and Land Investigation in several years (1995, 2000, 2010, 2015, 2020)

Content	Symbol	
House number (street-level)	houses built during the past 5 years of target year in house stock	B_y
	demolished houses during the past 5 years of target year	D_y

Table 3.4 Building type and area of archetype houses

Apartment(A), Detached (D)

Building type	Total floor area(m^2)	Floor area of air-conditioned rooms	Building type	Total floor area(m^2)	Floor area of air-conditioned rooms
A-1	(<20)	9.72	D-1	(<40)	9.72, 8
A-2	(20-40)	9.72, 8	D-2	(40-60)	9.72, 9.72, 8
A-3	(40-60)	9.72, 12.96	D-3	(60-80)	12.96, 9.72, 9.72
A-4	(60-80)	16.2, 12.96, 8	D-4	(80-100)	16.2, 12.96, 8
A-5	(80-100)	22.68, 12.96, 8	D-5	(100-120)	16.2, 12.96, 9.72
A-6	(>100)	22.68, 12.96, 9.72, 8	D-6	(>120)	22.68, 16.2, 12.86, 8

a) apartment houses

b) detached houses

Figure 3.2 Floor plan of 12 archetype houses

Table 3.5 Archetype houses setting

Apartment(A), Detached (D)

male(m), work-female(f) elder(e), housewife(h), child(c)

Archetype-ID	Building Type	Household member
c_0	A1, A2	m1
c_1	A1, A2	f1
c_2	A1, A2	e1
c_3	A1, A2	m1, f1
c_4	A2, A3	m1, h1
c_5	A2, A3	f1, c1
c_6	A2, A3	e2
c_7	A3, A4, A5	m1, f1, c1
c_8	A3, A4, A5	m1, h1, c1
c_9	A5, A6	m1, h1, c2
c_{10}	A6	m1, h1, c3
c_{11}	A6	m1, h1, c2, e2
c_{12}	D1, D2	m1, f1
c_{13}	D1, D2	m1, h1
c_{14}	D1, D2	f1, c1
c_{15}	D1, D2	e2
c_{16}	D2, D3, D4	m1, f1, c1
c_{17}	D2, D3, D4	m1, h1, c1
c_{18}	D4, D5, D6	m1, h1, c2
c_{19}	D4, D5, D6	m1, h1, c3
c_{20}	D4, D5, D6	m1, h1, c2, e2

In this research, the target city is Fukuoka, located in the southwestern part of Japan. Figure 3.3 shows the basic information includes location, the administrative division of the city and climate [15]. The city experiences a warm climate during the year and the longest hours of sunshine in spring. It is divided into seven administrative districts (Distict-1 to District-7) and 1051 street-level areas. District-2 and District-3 represent the central urban areas. Detailed information about the seven districts is provided in Table 3.6.

a) location of target city in Japan

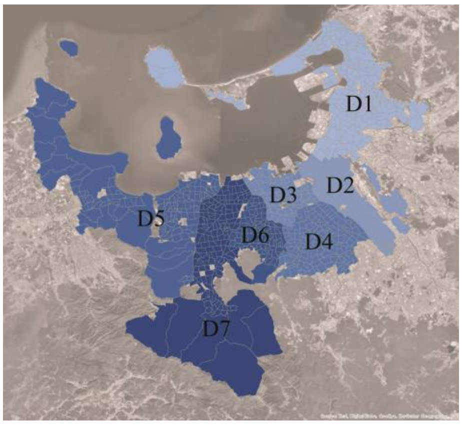

b) administrative districts of target city

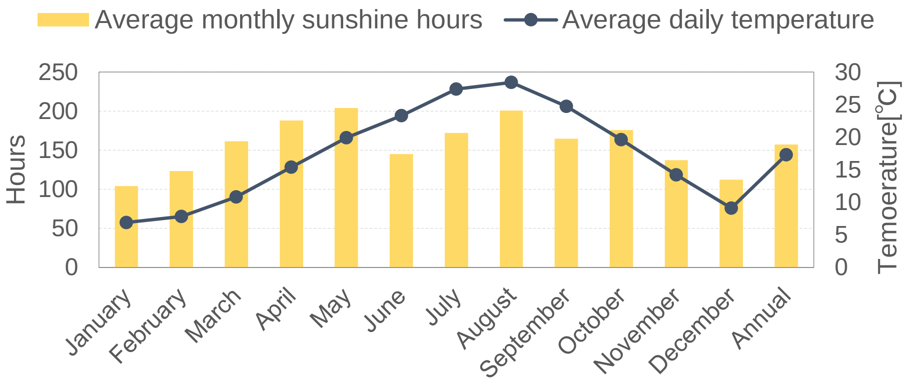

c) Average daily temperatures and sunshine hours in each month of target city

Figure 3.3 Basic information of target city

Table 3.6 Basic information of 7 districts in target city (2020)

District-ID	Population	Household	House (total)	Detached house
District-1	315,893	156,362	146,370	36,740
District-2	235,319	154,640	149,390	13,810
District-3	192,654	127,391	118,620	8,180
District-4	264,517	129,031	124,280	33,540
District-5	208,225	95,698	91,360	29,780
District-6	125,958	67,367	64,820	16,800
District-7	220,201	100,635	97,460	29,650

3.2.2 Number of each archetype house (case_2020)

Since the public statistic data for each attribute of house or occupant is published separately, cross-referencing records is unavailable, making it impossible to directly understand the number of each archetype house. Therefore, a model is developed to estimate the number of each archetype house according to public statistical data in the target area. The method of this model involves calculating the total number of households and the total population of different types of occupants separately based on the tentative solutions of each archetype house number, which are generated randomly. The fitness of these solutions (the errors between public statistical data and estimated data based on solutions) are evaluated and the tentative solutions are improved for better solutions with smaller errors using Genetic Algorithm (GA) [16]. Before starting the algorithm, to reduce the calculation count, some constraints on the solutions are determined to decrease the number of generated tentative solutions. In detail, the solutions are generated and refined within a specific range, as defined by the methods outlined in Table 3.7, using public statistical data. For example, the number of households whose member is a single working person (calculated by c_0 plus c_1) is calculated by subtracting single elder member households (h_{1e}) from single member households (h_1). During the algorithm process, an object function is necessary to evaluate the fitness of solutions. Therefore, the sum of errors calculated by Eq. (3-1) is utilized as the object function. Table 3.8 shows each error [e_0, e_1, …, e_6], which represents the ratios of the public statistical values to the aggregated household and population numbers according to the solutions. The combination of solutions with minimum function result has the best fitness and is chosen as a result in this calculation iteration.

$$E = e_0+e_1+e_2+e_3+e_4+e_5+e_6 \tag{3-1}$$

As one of street-level area, the GA process and inferred results of Hakozaki-1, District-1 are shown in Table 3.9 and Figure 3.4. In the iteration-91, all errors fall within the range of 0.8 to 1.2, indicating that these results can be considered as the inferred results of various archetype houses in this example area.

Most target areas could obtain results with small errors (each e is in the range (0.8, 1.2)) within 100 iterations with GA. Figure 3.5 shows comparisons of each type of public statistic data with estimation results in 1051 street-level areas of the target city (one point represents one area). In these results, the statistical number of children is generally less than the estimated results. One possible reason is that the age of children in public statistical data is under 15 years without including all children, which is a weakness of this model. Additionally, it should be noted that only household type is considered in this model without involving floor area. After estimation, the number of different floor areas (like A1, A2) of one combination (like c_1) is distributed proportionally.

Figure 3.6 shows the estimated quantities of archetype houses in the seven districts of target city. It could be observed that single-person household (c_0, c_1, c_2) comprise a significant proportion.

Table 3.7 Specific household number calculation method

Household type	Archetype houses-ID	Calculated by public data
one-person	$c_0 + c_1$	$= h_1 - h_{1e}$
two-persons (both working)	$c_3 + c_4 + c_{12} + c_{13}$	$= (h_{2c} - h_{2ce})\, R_{ef}$
two-persons (one working)	$c_5 + c_{14}$	$= (h_{2c} - h_{2ce})\ (1 - R_{ef})$
two-persons (elders)	$c_6 + c_{15}$	$= h_{2ce}$
three-persons (two working)	$c_7 + c_{16}$	$= h_3\ (1 - R_{ef})$
three-persons (one working)	$c_8 + c_{17}$	$= h_3\ R_{ef}$
four-persons	$c_9 + c_{18}$	$= h_4$
five-persons	$c_{10} + c_{19}$	$= h_5$
six-persons	$c_{11} + c_{20}$	$= h_6$

Table 3.8 Errors' calculation method

Item	Errors' calculation method
Household Number	$e_0 = (h_{ap} + h_{de}) / (c_0 + c_1 +, \ldots, + c_{20})$
Population (apartment)	$e_1 = p_{ap} / (c_0 + c_1 + c_2 + 2(c_3 + \ldots + c_6) + 3(c_7 + c_8) + 4c_9 + 5c_{10} + 6c_{11})$
Population (detached)	$e_2 = p_{de}\ / (2(c_{12} + c_{13} + c_{14} + c_{15}) + 3(c_{16} + c_{17}) + 4c_{18} + 5c_{19} + 6c_{20})$
Population (male)	$e_3 = p_{ma}\ / (c_0 + c_3 + c_4 + c_7 +, \ldots, + c_{13} + c_{16} +, \ldots, + c_{20})$
Population (elder)	$e_4 = (p_{me} + p_{fe})\ / (c_2 + c_{15} + 2\ (c_6 + c_{11} + c_{15} + c_{20}))$
Population (female)	$e_5 = p_{fa} / (c_1 + c_3 + c_4 + c_5 + c_6 +, \ldots, + c_{14} + c_{16} +, \ldots, + c_{20})$
Population (children)	$e_6 = (p_{mc} + p_{fc}) / (c_5 + c_7 + c_8 + c_{14} + c_{16} + 2(c_9 + c_{11} + c_{18} + c_{20}) + 3(c_{10} + c_{19}))$

Table 3.9 Solutions of all archetype houses and errors at each iteration (Iteration-1,2, …,91) of an example street-level area (Hakozaki-1, District-1)

Iteration-1											
solu-	c_0	c_1	c_2	c_3	c_4	c_5	c_6	c_7	c_8	c_9	c_{10}
tions	1347	914	404	62	89	76	125	13	203	67	8
	c_{11}	c_{12}	c_{13}	c_{14}	c_{15}	c_{16}	c_{17}	c_{18}	c_{19}	c_{20}	
	3	58	10	130	26	30	84	69	3	4	
errors	E	e_0	e_1	e_2	e_3	e_4	e_5	e_6			
	1.88	1.32	1.49	0.98	1.09	0.9	0.95	1.81			
Iteration-2											
solu-	c_0	c_1	c_2	c_3	c_4	c_5	c_6	c_7	c_8	c_9	c_{10}
tions	1389	759	301	240	88	34	69	48	161	123	16
	c_{11}	c_{12}	c_{13}	c_{14}	c_{15}	c_{16}	c_{17}	c_{18}	c_{19}	c_{20}	
	2	38	1	25	96	4	38	52	6	6	
errors	E	e_0	e_1	e_2	e_3	e_4	e_5	e_6			
	1.49	1.24	0.97	0.94	1.17	0.72	0.86	0.43			
⋮											
Iteration-91											
solu-	c_0	c_1	c_2	c_3	c_4	c_5	c_6	c_7	c_8	c_9	c_{10}
tions	1250	691	301	97	132	125	93	2	112	113	27
	c_{11}	c_{12}	c_{13}	c_{14}	c_{15}	c_{16}	c_{17}	c_{18}	c_{19}	c_{20}	
	5	16	0	31	127	69	49	1	9	1	
errors	E	e_0	e_1	e_2	e_3	e_4	e_5	e_6			
	0.94	0.82	1.1	0.91	0.9	0.87	0.84	1.18			

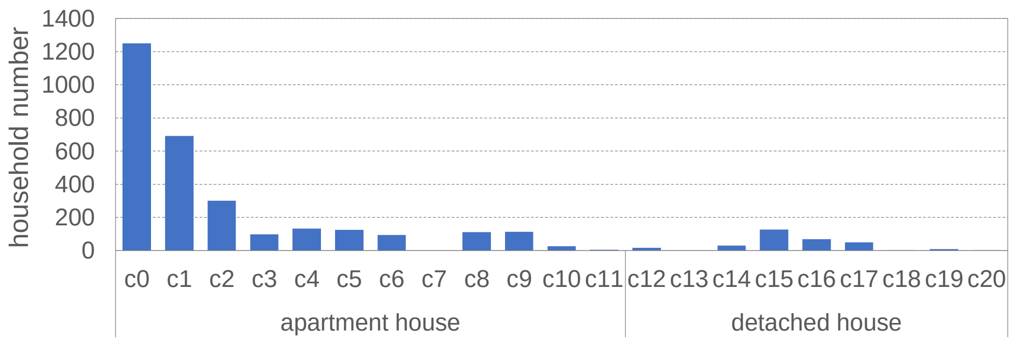

Figure 3.4 Number of each type of archetype houses in Hakozaki-1, District-1 (Solutions in Iteration-91)

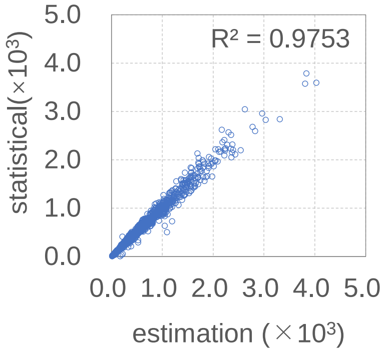

household number

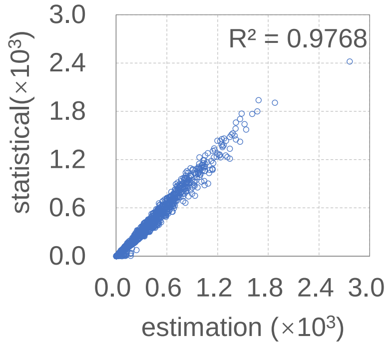

population (apartment)

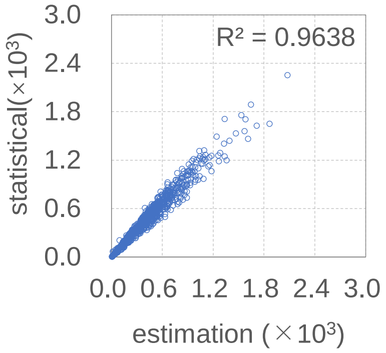

population(detached)

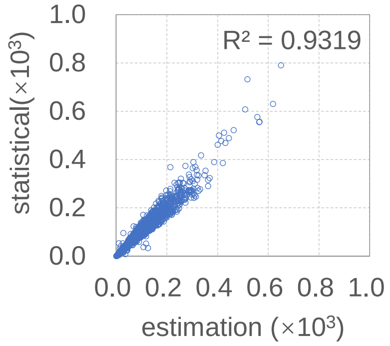

population (working-male)

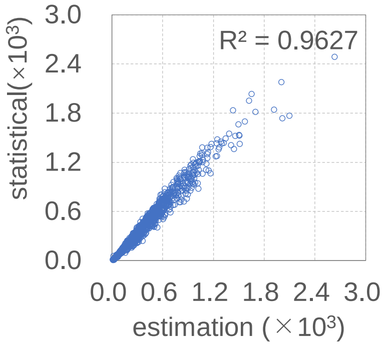

population (elder)

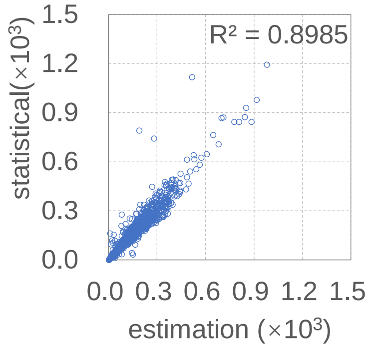

population (working-female, housewife)

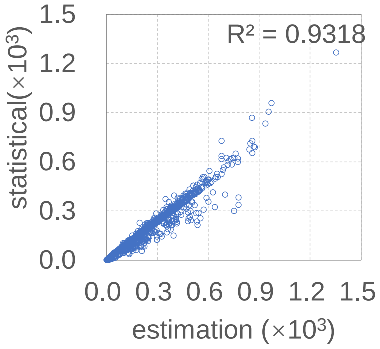

population (children)

Figure 3.5 Comparation of public statistical data with estimations of all street-level areas

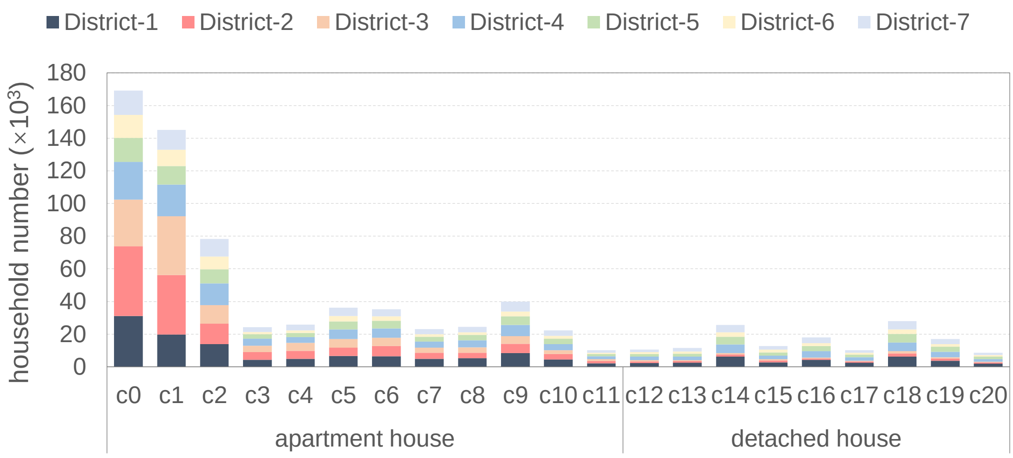

Figure 3.6 Number of each type of archetype houses in each district of target city

3.2.3 Construction year of current houses stock (2020)

The electricity consumption of the air-conditioner is directly determined by the heating load, which is related to the thermal performance of house. Considering the thermal performance of house is highly dependent on the construction year, and construction years of houses stock varies from area to area. Therefore, it is necessary to estimate the construction years of the house stock in target street-level areas.

$$h_y^{in} = \frac{p_y^{in}}{p_{hy}} \tag{3-2}$$

$$b_y = \frac{h_y^{in}}{\sum h_y^{in}} \cdot B_y \tag{3-3}$$

$$r_y = \frac{h_y}{h_{y-5}} \tag{3-4}$$

$$b_y' = b_y \cdot r_y \tag{3-5}$$

$$r_y' = \frac{e^{r_y} - e^{-r_y}}{e^{r_y} + e^{-r_y}} \tag{3-6}$$

$$r_y'' = r_y' \cdot K_y \tag{3-7}$$

$$b_y'' = b_y \cdot r_y'' \tag{3-8}$$

p_y^{in}: migration people moved in target street-level area in the target period
p_{hy}: average family size in target street-level area in the target period
B_y: built houses in district-level area in the target period
h_y: household number in street-level area in the target interval period

To deal with this problem, a model is proposed to estimate the current construction years of the house stock using National House and Land Investigation [13] in the past several years. Since used data is published every five years and begun in 1995 (data in 2005 is not published), the period of construction year is set as ~1995, 1995~2000, 2005~2010, 2010~2015, 2015~2020. Significantly, this model assumes that in the target area, the number of built houses in target period (b_y) is correlated with the migration households, which had moved in (h_y^{in}) and calculated by Eq. (3-2). In detail, in the target period, b_y is calculated by distributing houses stock built in district-level area (B_y) according to the ratio of h_y^{in} to the sum migration households of all street-level areas in this district-level area ($\sum h_y^{in}$) by Eq. (3-3). However, considering that urban areas vary widely, for the developed downtown areas with many households, the land has been highly used, even h_y^{in} is very large, these households can rent or purchase the existing houses, it is not mean b_y is large too. Instead, the situation in undeveloped countryside areas is different. Therefore, the change rate of households (r_y) calculated by Eq. (3-4), is used to correct b_y into b_y' in Eq. (3-5). It should be noted that r_y in some areas would exceed 1. This means b_y' would exceed h_y^{in} by Eq. (3-5), which is not possible. Therefore, it is necessary to limit r_y to r_y' whose range is (0~1) by hyperbolic tangent function (tanh) in Eq. (3-6). Finally, to verify the model, sum of all street-level area estimation results ($\sum b_y'$) calculated by Eq. (3-5) is compared with B_y. The result shows that $\sum b_y'$ is far from B_y. To improve the model, r_y' is further corrected into r_y'' with K_y, as shown in Eq. (3-7). Then, b_y'' is calculated by r_y'' as shown in Eq. (3-8). Figure 3.7 shows the improved results after correction, demonstrating the effectiveness of this approach.

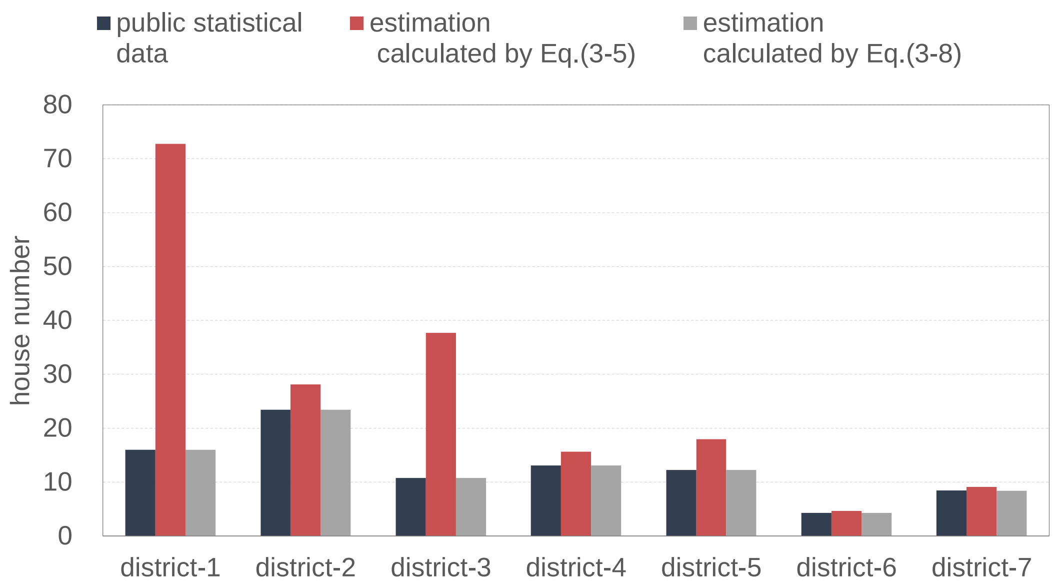

Figure 3.7 Estimation houses number compared with statistical data of all districts in target city

3.2.4 Newly built, demolished house (2025)

To forecast newly built houses in 2025, the required public statistic data include h_{2025}, p_{2025}^{in}, p_{h2025}, B_{2025}, which is predicted by linear regression of the past several years 'data. Through the above process in Section 3.2.3, b_{2025}"is calculated.

Considering the future scenario, not only b_{2025}", but also forecast demolished houses (d_y) and retrofitted houses (re_y) in 2020~2025 is necessary. To forecast d_y" (corrected d_y), similar to the proposed model in Section 3.2.3, d_y" is correlated with the migration households that had moved out (h_y^{out}). The calculation method of h_y^{out} is shown in Eq. (3-9). With the same process in Section.3.2.3, d_y" is calculated by Eq. (3-10, 3-11). The average life of Japanese houses is 30-40 years, therefore, d_y" is only considered for houses built before 1995. For re_y, it is hard to forecast with the public statistic data directly, therefore, scenario of re_y would be discussed.

Combining the results in Section 3.2.3, Figure 3.8 shows the estimation results of several construction periods of house stock and forecasted newly built houses, demolished houses and households moving in/out in example street-level area.

$$h_y^{out}=\left|\left|h_y-h_{y\text{-}5}\right|-h_y^{in}\right| \tag{3-9}$$

$$d_y=\frac{h_y^{out}}{\sum h_y^{out}}\cdot D_y \tag{3-10}$$

$$d_y" = d_y\cdot r_y" \tag{3-11}$$

D_y: demolished houses in district-level areas in the target period

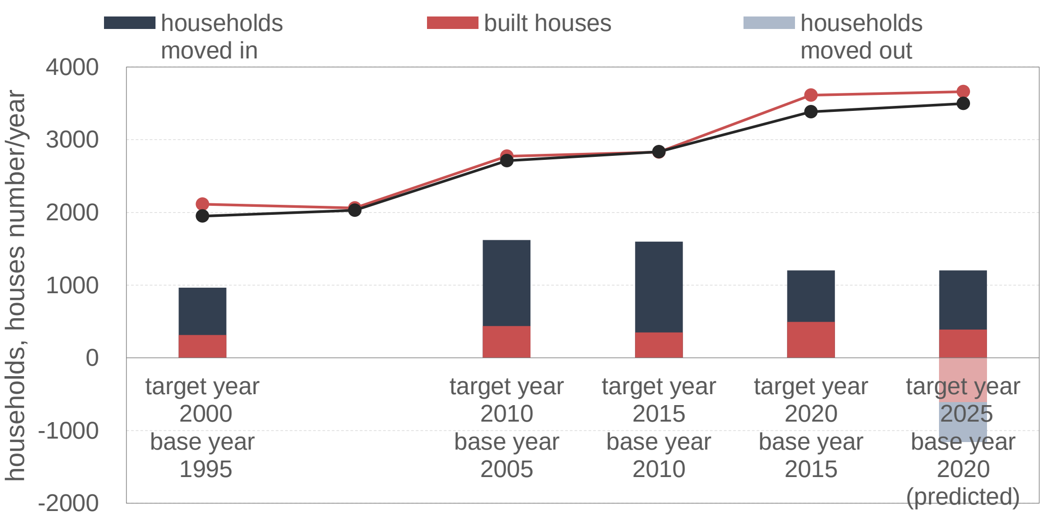

Figure 3.8 Estimation of households and houses number in several years and built, demolished houses during several periods in example street-level area.

Using the above calculation process, the changes in the number of households, newly built houses, and demolished houses between case_2025 and case_2020 for all street-level area are illustrated in the Figure 3.9. There are several conclusions of simulation result.

Firstly, for the households' change, 73% of areas in target city are increasing, most of these are concentrated in the center of the city (District-2) and west (District-5). On the contrary, areas where the households decreased are mainly on the fringes and south (District-6,7) of the city. Secondly, the distribution of newly built and demolished houses shows significant differences due to the differences of people migration in different urban area. Compared the results of downtown (District-3) with suburbs (District-1,2,4,5,6,7), the ratio of newly built houses to household number in suburbs and downtown are 9.9%, 5.3% and the demolished houses are 4.2% and 4.5%. These results show that in target city, there is greater construction progress in suburbs and almost the same demolish progress in suburbs and downtown in period of 2020 to 2025.

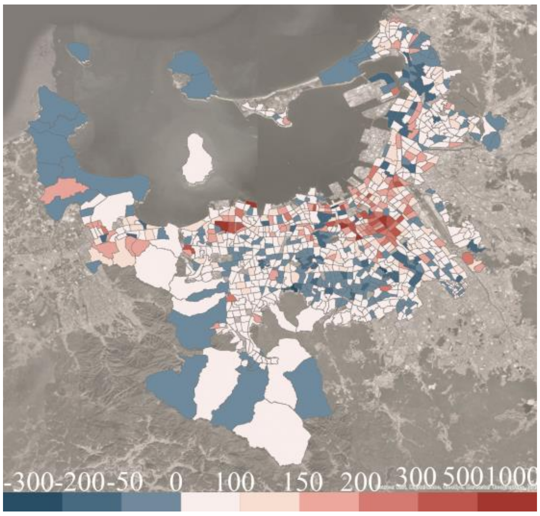

a) household number change

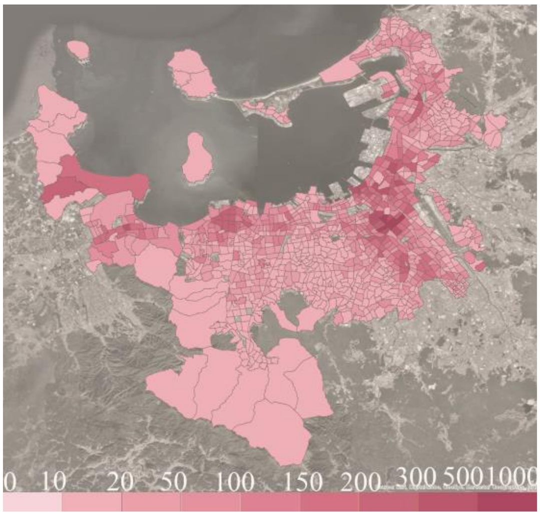

b) newly built houses

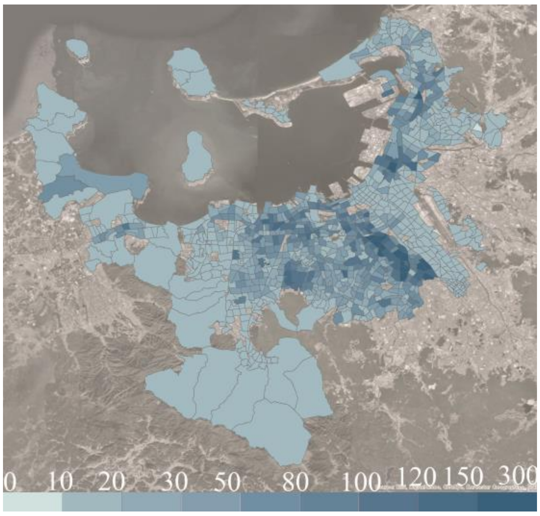

c) demolished houses

Figure 3.9 Variation of household number, newly built, demolished houses of all street-level areas compared case_2025 to case_2020

3.2.5 Thermal performance of houses

In Japan, the Residential Envelope Average Heat Transmission Coefficient (UA) [W/m^{2}K], is proposed to evaluate the thermal performance and energy-saving effectiveness of houses. This coefficient is calculated using Eq. (3-11)

$$UA = Q / Ae \tag{3-11}$$

Q: total amount of heat lost by the building [W/K]

Ae: envelope area [m^2]

Specifically, thermal performance standards for houses in Japan are classified into seven levels (level_1 to level_7), each associated with various UA values. These values are determined based on the climate zone classification of the target city [17]. According to [18], the distribution of houses across various thermal performance standards varies according to their construction years, as illustrated in Table 3.10. Utilizing this proportional distribution, the estimated distribution of houses across construction years and thermal performance standards for the target city in 2020 (case_2020) and 2025 (case_2025) is illustrated in Figure 3.10.

Additionally, the Japanese government aims to achieve a minimum of 30% of houses reaching at least level-4 in the housing stock by 2025, as outlined in [19]. To achieve this goal, it is essential to consider not only newly built and demolished houses but also retrofitting existing ones. Therefore, a house retrofitting scenario for 2025 (case_2025_retrofit) has been established, with 30% of housing stock getting level_4. Figure 3.10 shows the distribution of houses across different thermal performance standards with three cases. It shows that when considering only newly built and demolished houses (case_2025), the proportion of each thermal performance standard in the housing stock remains essentially similar to the current situation (case_2020) and falls short of the target set in (case_2025_retrofit). Achieving the target requires significant efforts in retrofitting existing houses. In detail, the number of retrofitted houses in each street-level area are shown in Figure 3.11.

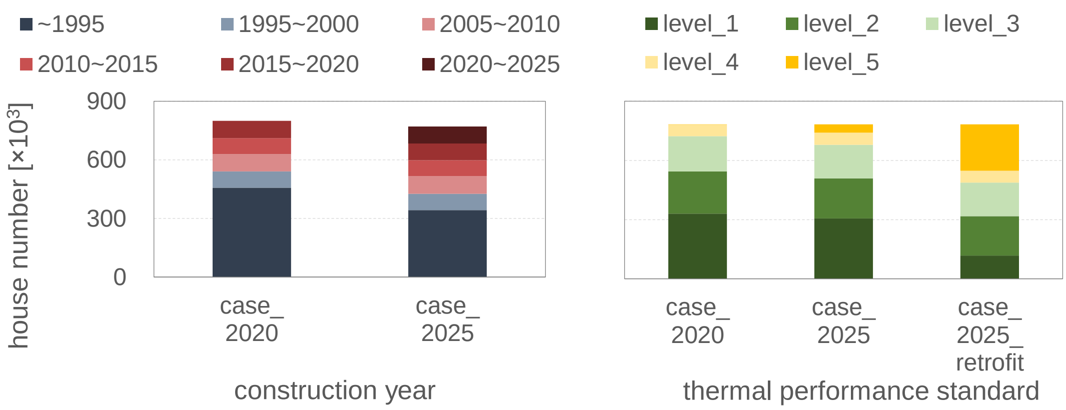

Figure 3.10 House number of each construction year, thermal performance standard of target city in case_2020, case_2025, case_2025_retrofit

Table 3.10 Ratio of different thermal performance standard based on construction periods

construction year	level_5 UA=0.6	level_4 UA=0.87	level_3 UA=1.54	level_2 UA=1.8	level_1 UA=2.57
Apartment					
1980-1985	0	0	0	0	100
1986-1990	0	0	0	20	80
1991-1995	0	0	0	37	63
1996-2000	0	0	16	42	41
2001-2005	0	1.5	36	41	21
2006-2010	0	7.4	41	40	11
2011-2015	0	12.2	49.6	33.6	4.6
2015-2020	2	70	28	0	0
2020-2025	75	25	0	0	0
Detached					
construction year	level_5 UA= 0.6	level_4 UA= 0.87	level_3 UA= 1.54	level_2 UA= 1.8	level_1 UA=2.57
1980-1985	0	0	0	5	95
1986-1990	0	0	0	30	70
1991-1995	0	0	0	45	55
1996-2000	0	0	25	45	30
2001-2005	0	4.8	45	36.6	13.6
2006-2010	0	24.1	45	28.2	2.9
2011-2015	0	39.7	40.8	16.2	2.7
2015-2020	25	60	15	0	0
2020-2025	80	20	0	0	0

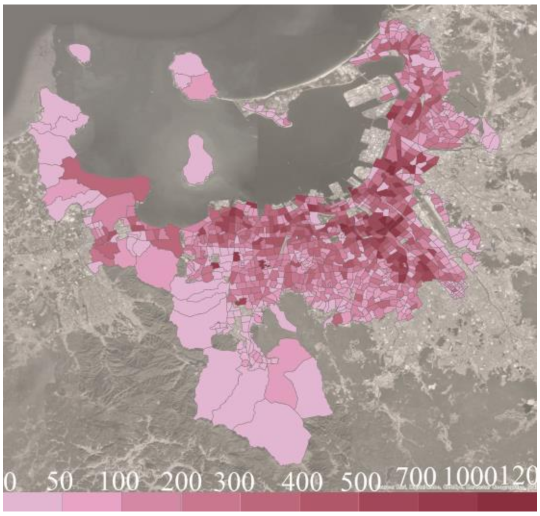

Figure 3.11 Retrofitting houses of all street-level area in case_2025_retrofit

3.3 Electricity simulation model

3.3.1 Occupant behavior schedule model

As mentioned in Chapter 2, the operation of various appliances, lighting, etc. is determined by the occupant's behavior, therefore it is necessary to initially estimate the behavior schedules of household members based on their attributes. The Particle Swarm Optimization (PSO) algorithm is employed to simulate behavior schedules based on public statistical data considering factors such as the occupant's type and whether it is a working or resting day. For a detailed explanation of the simulation process, refer to [20].

3.3.2 Appliances operation probabilities model

While the above model simulates the behavior schedules of occupants, it's important to note that these schedules may not align with appliance operating schedules. For example, cookers may not always used before eating behavior of occupants. Therefore, it is still necessary to determine the probability of appliance operation based on occupant behavior. Due to the differences in habits among people, it is impossible and meaningless to estimate the probabilities of appliances operation of each household. In this model, the operation probabilities of appliances and lighting for multiple households have been estimated with GA based on 93 households' measured electricity data. The obtained results are then utilized in the estimation at the urban scale. It should be noted that in Japan, there is minimal air-conditioner operation during spring and autumn. Consequently, when considering the measured electricity in April, it is assumed to be consumed only by appliances and lighting, excluding air-conditioner.

The detail estimation processes are outlined below:

At iteration-1, 10000 candidate solutions (solution-1, solution-2, …, solution-10000) are generated randomly, each solution includes candidate operation probabilities of each appliance and lighting during the daytime based on occupant behaviors (e.g., at solution-1, there is an 81.7% probability of using IH cooker before behavior-eating in occupant's schedule). Using these solutions, the electricity consumption of households is simulated individually, and the difference between the simulation results and measured data is employed as the objective function to evaluate the fitness of these candidate solutions. As showed in Table 3.11, in the process of deriving the next-iteration candidate solutions, through cross-combining and mutating the candidate solutions from the previous iteration in the direction of minimizing the objective function, the objective function values of the candidate solutions in the next iteration continuously decreases compared to the previous iteration. Figure 3.12 shows the simulation results using example solutions (solution-a, solution-b and solution-c) at iteration-1, iteration-50 and iteration-150. The simulation results based on example solutions at iteration-150 closely match the measured data. However, it's crucial to note that the results from the measured data represent only one case of urban houses. Therefore, all solutions at iteration-150, instead of selecting the best one, are used for simulating electricity consumption at the urban scale for houses.

It's important to note that solutions with good fitness do not necessarily represent the actual probability of each appliance and lighting operation. These results are a combination of all probabilities, aimed at making simulation outcomes closely align with the measured data of the houses group. While the electricity data of this houses group may not perfectly mirror that of other groups across all urban areas, it is reasonable to believe that it reflects the fundamental temporal characteristics of electricity demand for other house groups at an urban scale.

Table 3.11 Solutions (s-1, s-2, …, s-10000) of usage probabilities of some appliances, lighting and objective function's values at iteration-0, iteration-50, iteration-150 (I-0, I-50, I-150)

I-0	IH cooker	micro-wave	dishwasher	…	daytime lighting	objective function	R^2
s-1	81.7%	36.8%	40.2%	…	55.5%	1890	0.12
s-2	40.9%	45.2%	32.8%	…	93.%	1941	0.21
…	…	…	…	…	…	…	…
s-10000	52.4%	76.5%	4.6%	…	82.5%	1445	0.08

⋮

I-50	IH cooker	micro-wave	dishwasher	…	daytime lighting	objective function	R^2
s-1	5.6%	1.9%	3.2%	…	32.6%	872	0.22
s-2	9.8%	15.6%	4.3%	…	82.5%	863	0.25
…	…	…	…	…	…	…	…
s-10000	2.5%	4.9%	3.8%	…	47.8%	804	0.22

⋮

I-150	IH cooker	micro-wave	dishwasher	…	daytime lighting	objective function	R^2
s-1	3.5%	2.3%	3.1%	…	61.3%	463	0.71
s-2	2.8%	2.7%	3.3%	…	52.6%	424	0.76
…	…	…	…	…	…	…	…
s-10000	5.4%	1.8%	2.4%	…	54.2%	477	0.72

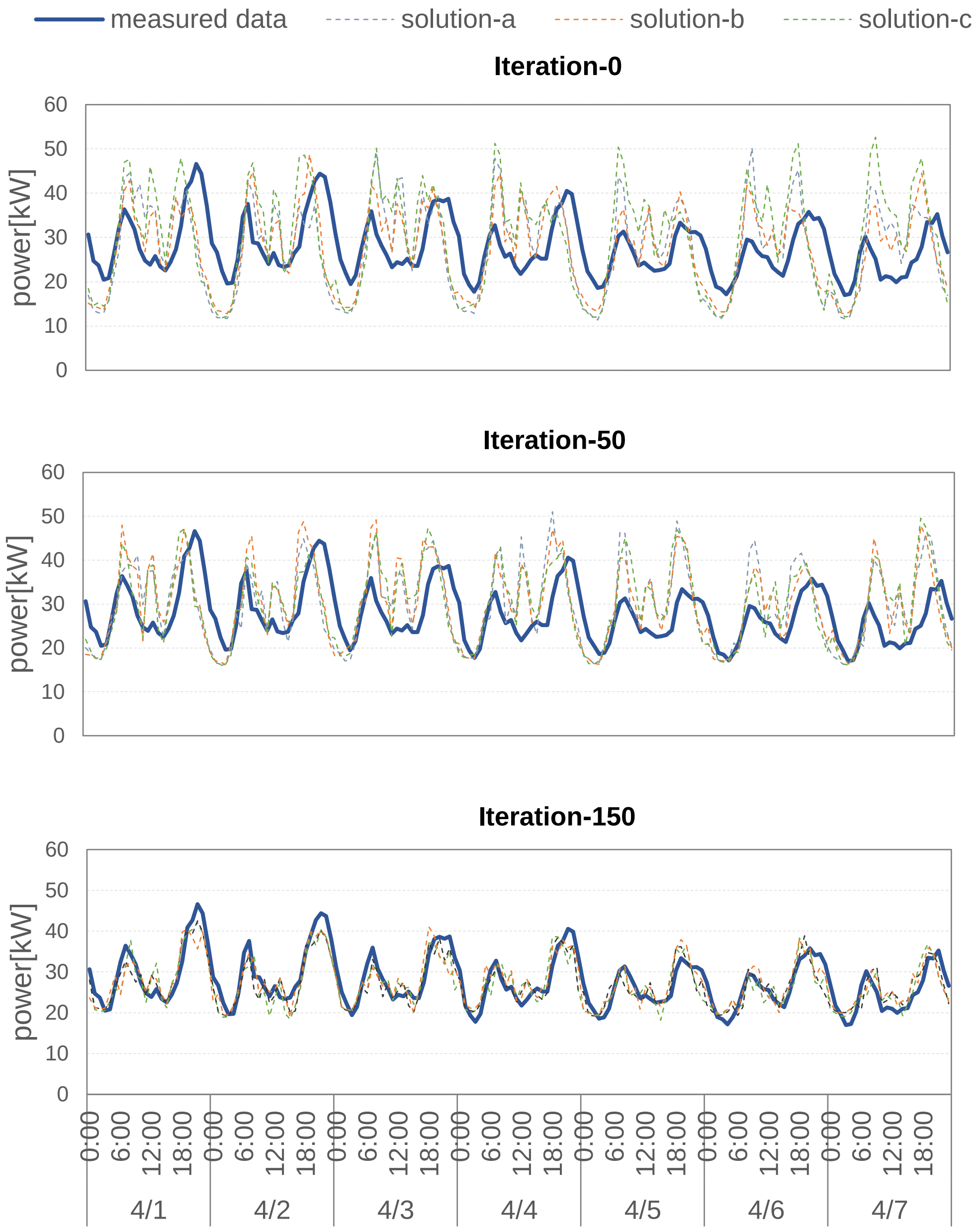

Figure 3.12 Measured data and simulation results by example solutions (solution-a, solution-b, solution-c) at iteration-0, iteration-50 and iteration-150

3.3.3 Appliances electricity simulation model

Figure 3.13 shows the calculation process of appliances (including lighting and ventilation) electricity.

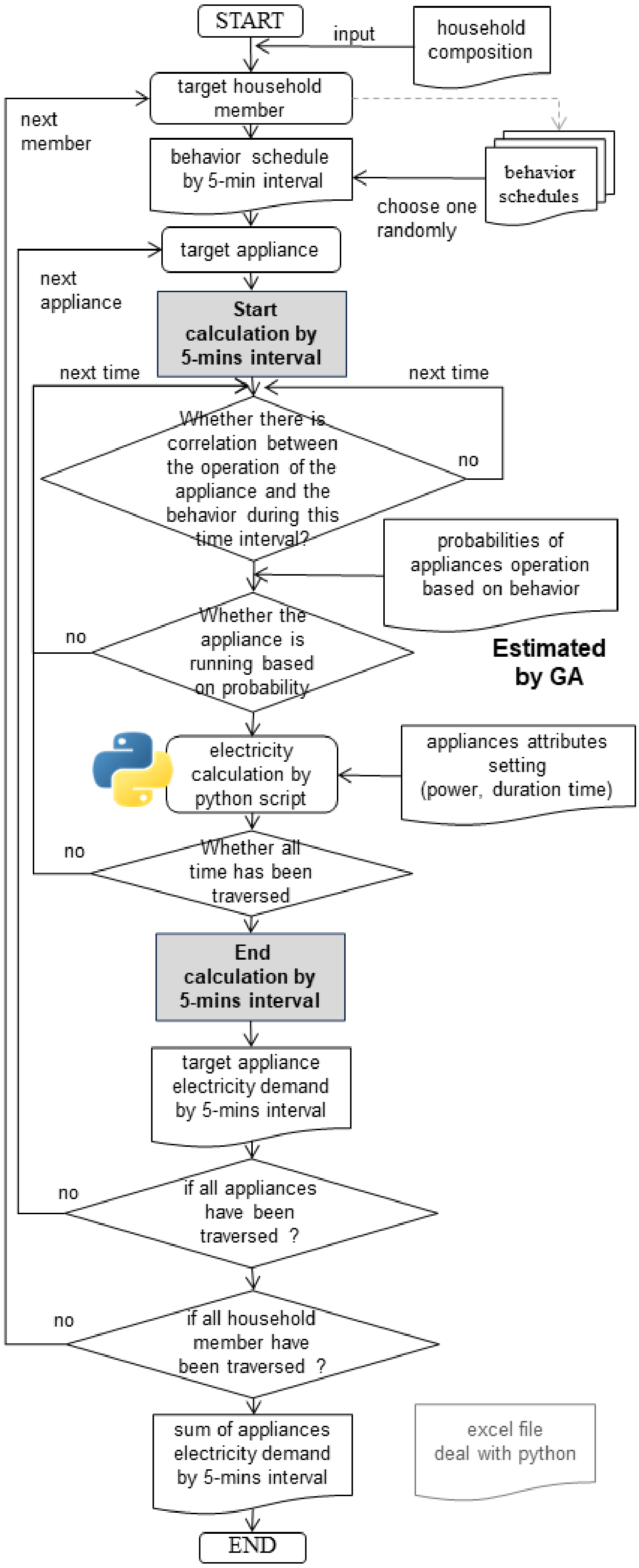

Figure 3.13 Calculation process of appliances, lighting and ventilation electricity

The detailed calculation process is introduced as follow:

Household appliances can be categorized into three types based on their usage patterns. Type one, exemplified by rice cookers and washing machines, is decided to be operated before or after the occupant's behavior and has a relatively stable duration time. Type two, represented by TVs and computers, is decided to be operated during people's behavior. Type three, such as refrigerators, operates all day and has no direct relation with people's behavior. Therefore, only the duration time of type one should be specified.

Based on the household composition, randomly select behavior schedules of household members (detailed in chapter 2). These behavior schedules are used to determine the operating schedules of several household appliances of type one and type two.

Table 3.12 shows the simulation settings of these appliances. The simulation of each household appliance is determined based on its ownership rate. Traverse the behavior schedule by 5-minute intervals of one day. For appliances of type one, if the behavior (such as eating) at this specific moment is associated with the use of household appliances (such as rice cooker, IH cooker, etc.), determine whether the appliance is activated before or after that moment based on the probability of its usage. For appliances of type two, determine whether the appliance is activated at that moment based on the probability of its usage. Once the operation of this appliances is decided, its operating power and duration are obtained as random numbers following a normal distribution within the specified range. During the operation period, the activation is no longer determined based on the behavior schedule of this individual member or other houses members. For appliances of type three, these appliances always operate continuously.

After traversing the schedules of all appliances and household members, the total time-series electricity demand for all appliances is calculated, resulting in the appliances electricity demand of one house.

Table 3.12 Appliances simulation setting

Item	ownership rate [%]	Rating Power [W]	Lasting [min]	Timing
rice cooker	100	700-1400	45-50	before eating
IH cooker	29.2	700-1700	10-15	before eating
microwave	99.1	1200-1400	0.5-5	before eating
dishwasher	34.4	600-800	55-65	after eating
vacuum cleaner	94.8	10-300	5-10	cleaning
washing machine	100	200-1200	30-40	washing
iron	90.0	900-1400	6-8	household chores
hairdryer	85.6	1000-1400	-	after bath
TV	96.2	40-600	-	TV
computer	78.5	60-90	-	working at home, hobby
refrigerator	99.6	150-300	-	-
warm toilet seat	64.1	300-1400	-	-

The detailed process of determining appliances' power is introduced in the following:

Firstly, the rating powers (P_s) of all type appliances from various households are determined randomly within the range of maximum and minimum rating powers [21]. Secondly, considering the actual power of appliances is not always at rating power, the electricity consumption of appliances is simulated using measured data ($P(t)_s$ and P_m), as described by Eq. (3-12).

$$P(t)_s = \frac{P(t)_m \, P_s}{P_m} \tag{3-12}$$

$P(t)_s$: electricity consumption by simulation

$P(t)_m$: electricity consumption by on-site measurement

P_s: appliances rating power determined randomly

P_m: appliances rating power on-site measurement

The power of lighting (P_l) and ventilation (P_v) considering the room area, is calculated by Eq. (3-13, 3-14).

$$P_l = 5.3 \cdot A_r + 21.298 \tag{3-13}$$

$$P_v = h \cdot A_r \cdot 0.5 \tag{3-14}$$

A_r: area of lighting room [m^2]

h: Floor height [m]

In general, the lighting operation schedule is often related to time and occupants' behavior schedule in past research. However, occurrences such as lighting being on during the daytime or being inadvertently left on are not uncommon. This research addresses this phenomenon by adjusting the probability of lighting operation, introducing a distinction from past research.

3.3.4 Air-conditioner electricity simulation model

In this section, the simulation model for air-conditioning electricity is explained separately, including the heating load schedule, decision of operation, and electricity calculation parts.

Heating load model

Unlike appliances whose powers are almost constant, the power consumption of air conditioning is determined by the heating load, which varies with factors such as temperature, room areas, houses' thermal performance, internal heat gain, and so on. To calculate the heating load, the software New HASP/ACLD [22] is utilized to simulate the benchmark heating load of target houses based on basic information, including temperature, household, and building details. For example, Figure 3.14 shows the detailed building structure information of archetype house with *UA* of 0.87. Subsequently, considering the internal heat gain from occupants and appliance operation, a heat balance model for rooms is developed to calculate the handled heating load schedule of the air conditioner.

Firstly, iterating through these 5-minute interval benchmark heating load schedules with internal heat gain and appliance operation. When the benchmark heating load exceeds the capacity of air-conditioner, the handle heating load equals to the capacity of the air-conditioner. When the benchmark heating load is less than the capacity but exceeds it by 20%, the handled heating load equals to benchmark heating load. When the load is less than 20% of the capacity, the handled heat load is 0.

All rooms with air-conditioner in the target house are traversed to obtain the handled heating load schedules.

The detailed process is illustrated in Figure 3.15.

Gross floor area	S= 98 m²
volume	B= 254.8 m³

part	material	thickness [m]	Thermal conductivity [W/(mK)]	Thermal Resistance [m²K/W]	heat transfer coefficient [W/(m²K)]	Correction by thermal bridge	Aria [m²]	H Coefficient of temperature difference	K×A×H [W/K]
Roof	Ri Resistance of heat transfer			0.11					
	plasterboard	0.012	0.17	0.0706					
	styrene foam board (extrusion)	0.045	0.037	1.2162					
	airspace			0.0860					
	plywood	0.012	0.19	0.063					
	asbestos straight	0.012	1.2	0.010					
	Ro Resistance of heat			0.04					
			Sum	1.601	0.625	0.735	62.9	1	46.244
Extarnal Wall	Resistance of heat transfer (inside)			0.111111					
	plasterboard	0.012	0.17	0.0706					
	styrene foam board (extrusion)	0.045	0.037	1.2162					
	airspace			0.0860					
	plywood	0.009	0.19	0.047					
	mortar	0.03	1.5	0.020					
	Ro Resistance of heat			0.04					
			Sum	1.595	0.627	0.717	144	1	103.320
Window (double insulating glass)	Resistance of heat transfer (inside)			0.11					
	glass	0.003	1	0.003					
	airspace	0.012		0.17					
	glass	0.003	1	0.003					
	Ro Resistance of heat			0.04	2.54				
			Sum	0.326	2.954	2.954	28	1	82.417
Floor	Resistance of heat transfer (inside)			0.11					
	plywood	0.01	0.19	0.053					
	airspace			0.0860					
	plywood	0.012	0.19	0.063					
	styrene foam board (extrusion)	0.055	0.037	1.486					
	airspace			0.0860					
	concrete	0.3	1.4	0.214					
	Ro Resistance of heat			0.04					
			Sum	2.143	0.467	0.597	62.9	0.7	26.283
Heat Loss by heat transfar Σ A*K*H									258.265
Total area of envelope									297.861
UA								①/②=	0.8671

Figure 3.14 Detailed building structure information of archetype house

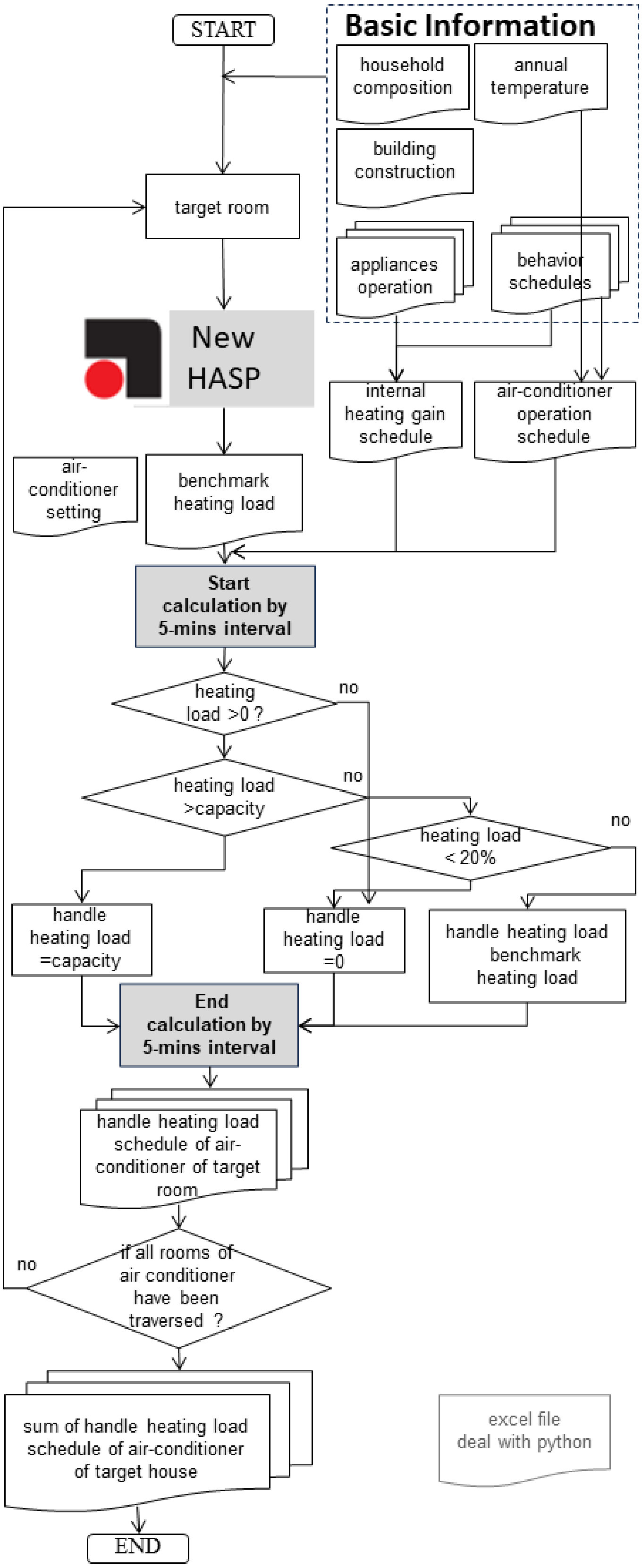

Figure 3.15 Heating load simulation process

Decision of operation

Once the air-conditioner is determined to be operated, it would generate electricity consumption according to the results of the handled heating load schedules. It's important to note that the decision-making process for air-conditioner operation is considerably more complex compared to appliances and lighting. This complexity arises for two main reasons: firstly, the operation of the air con is influenced by various factors such as the time of day, air temperature, set temperature, and personal habits, making it challenging to determine the probabilities of operation. Secondly, in the case of GA, it is necessary to compare results from numerous candidate solutions to find the best solution. However, due to computational limitations, obtaining numerous heating load calculation results is difficult. In this study, the operating probability (P_i) is calculated by Eq. (3-15) referring to [23]. Table 3.13 presents the base probabilities in different periods of a day.

$$P_i = P_T \cdot \frac{T_i - T_{ri}}{T_b - T_{ri}} \tag{3-15}$$

P_i : probability of using air-conditioner by temperature at time *i*

P_T : base probability according to time periods of a day

T_i : air-temperature at time *i*

T_b : air-temperature when 100% operating air-conditioner

T_{ri} : set temperature of air-con at time *i*

Table 3.13 Base probability (P_T) according to time periods of a day

Period		Usage probability by time [%]	
		heating	cooling
0:00-5:00	night period	50	20
5:00-10:00	waking up period	30	5
10:00-13:00	going out until lunch	35	5
13:00-16:00	after noon until returning home	35	10
16:00-19:00	child's return period	40	20
19:00-21:00	meals, baths	50	40
21:00-24:00	leisure time after returning home	60	60

Handled heating load of houses in example weeks of summer and winter.

Based on the calculation process described above, Figures 3.16-3.21 present handled heating load results of six archetype houses (apartment houses includes A-1_F1-1, A-3_F3-1, A-6_F6-1 and detached houses include D-1_F2-1, D-3_F3-1 and D-6_F6-1) in summer and winter example weeks. These results are calculated by sample behavior schedules.

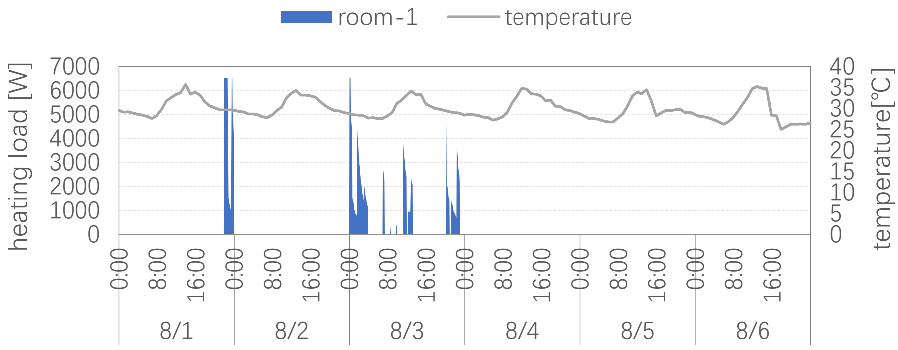

a) summer

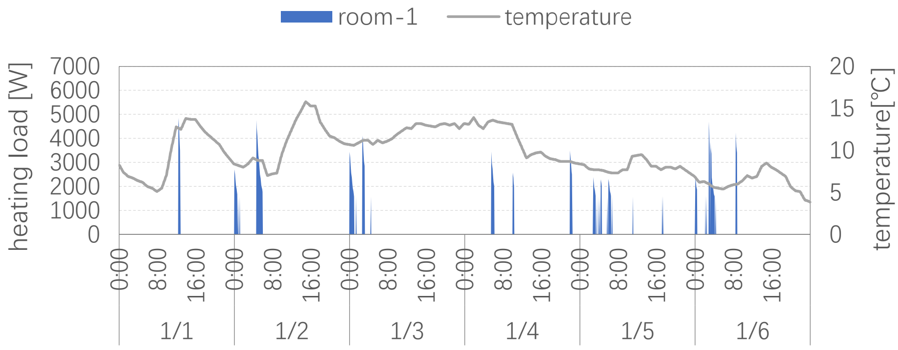

b) winter

Figure 3.16 Example handled heating load schedules of A-1_F1-1

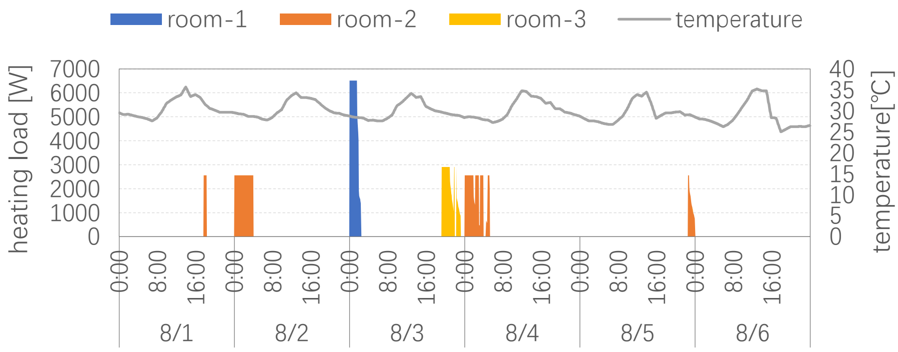

a) summer

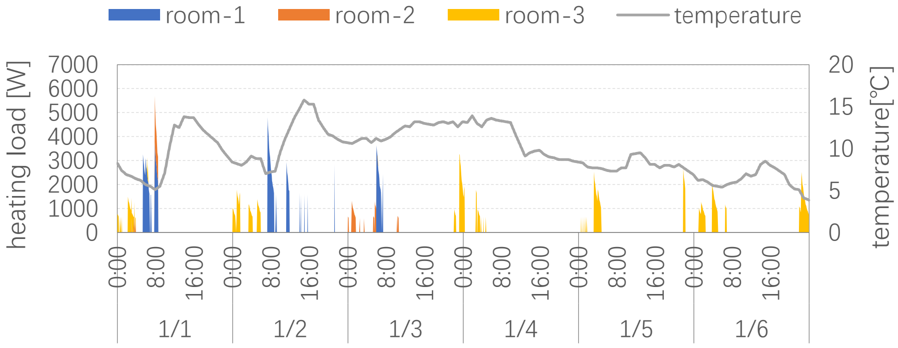

b) winter

Figure 3.17 Example handled heating load schedules of A-3_F3-1

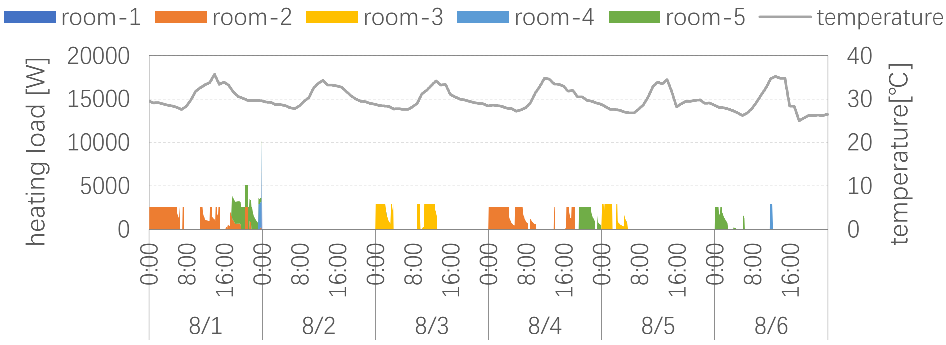

a) summer

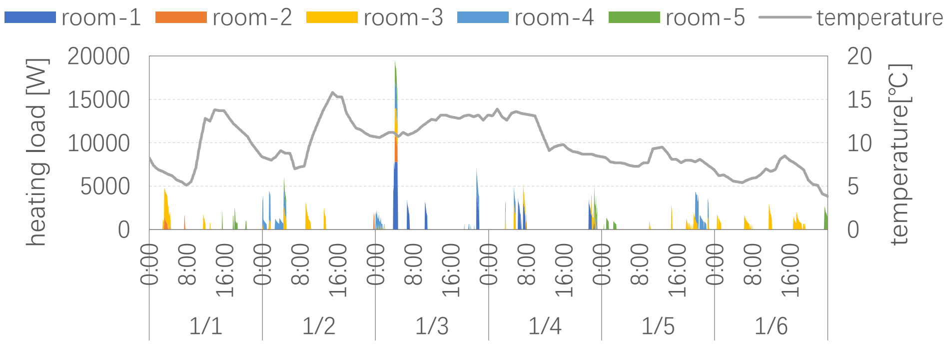

b) winter

Figure 3.18 Example handled heating load schedules of A-6_F6-1

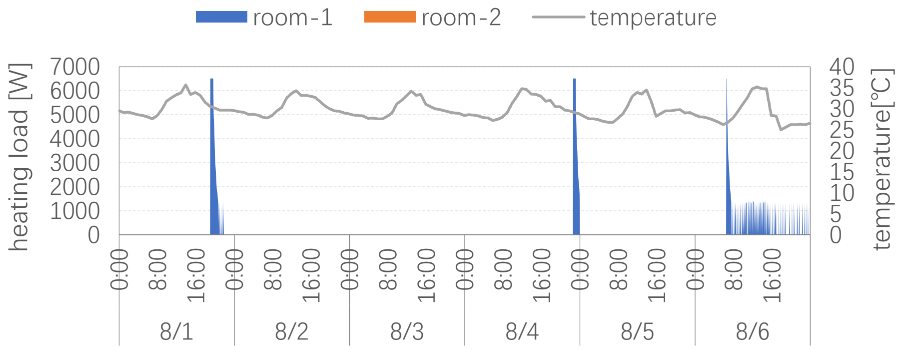

a) summer

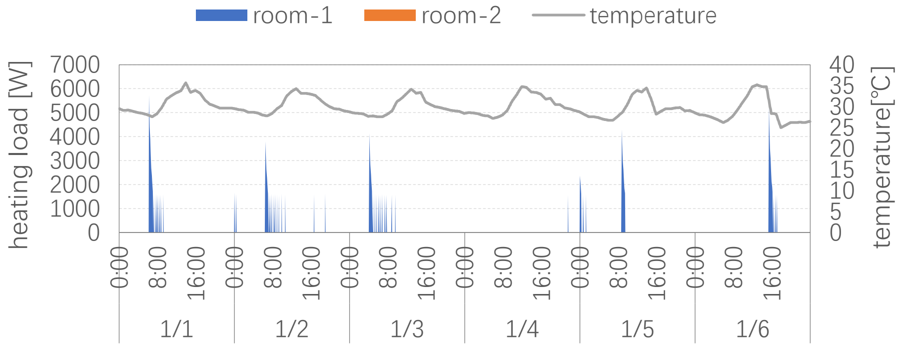

b) winter

Figure 3.19 Example handled heating load schedules of D-1_F2-1

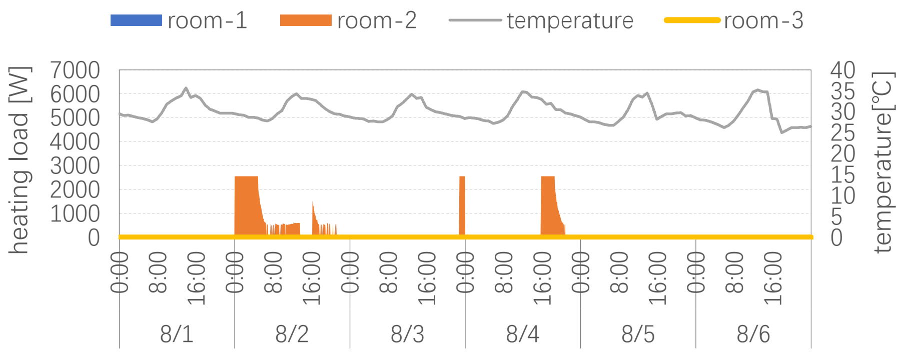

a) summer

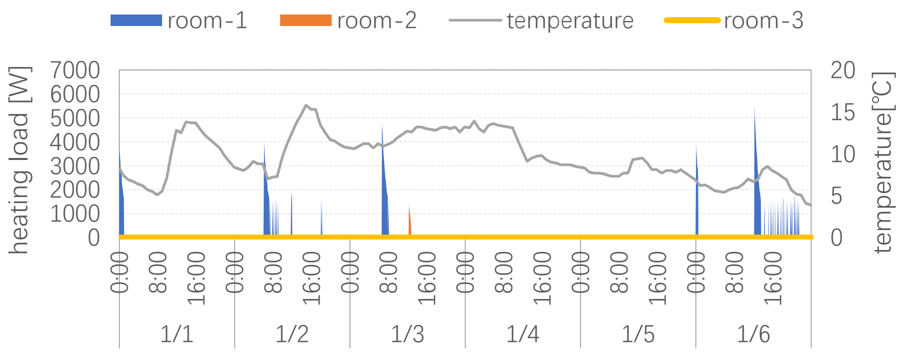

b) winter

Figure 3.20 Example handled heating load schedules of D-3_F3-1

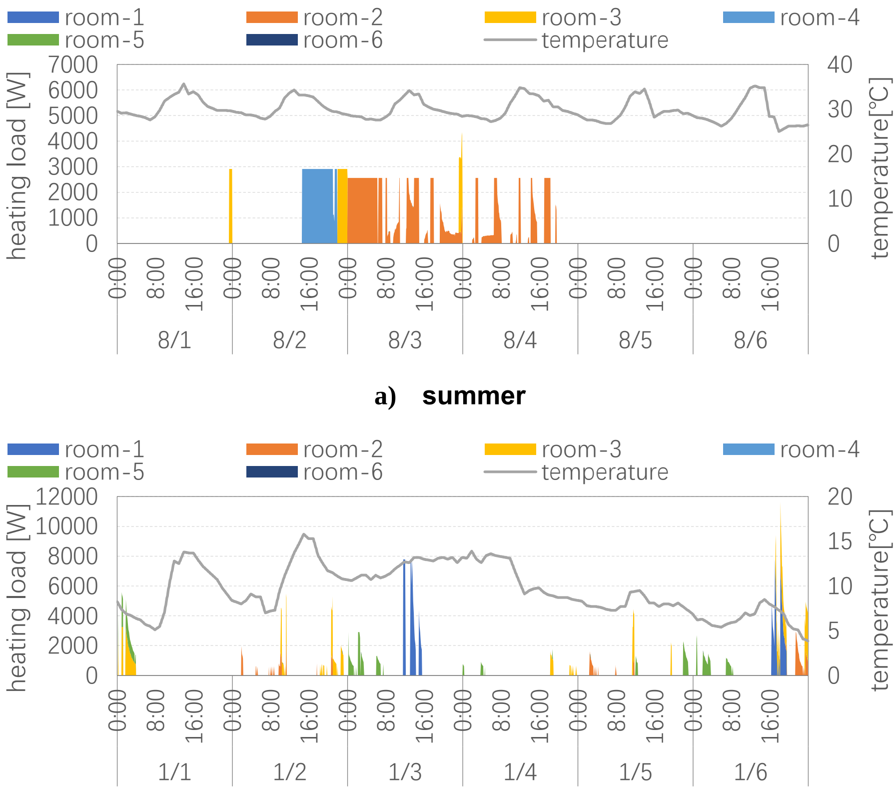

a) **summer**

b) **winter**

Figure 3.21 Example handled heating load schedules of D-6_F6-1

Correction for heating load based on UA

Based on the estimation results of the UA values in section 3.2.5, the heating load of archetype houses are adjusted to obtain the heating load results of actual houses according to the different UA values as shown in Table 3.14 [24].

Table 3.14 Regression Formula of load ratio and area or UA ratio compared with archetype house.

Type	Ratio (y)	Ratio (x)	Regression Formula
	cooling-load	area	$y = -0.14x^2+0.8x+0.3$
apartment	heating-load	area	$y = -0.72x+0.26$
	cooling-load	UA	$y = -0.15x^2+0.88x+0.3$
	heating-load	UA	$y = 0.7x+0.37$
detached	cooling-load	area	$y = -0.11x^2+0.84x+0.3$
	heating-load	area	$y = 0.69x+0.28$
	cooling-load	UA	$y = -0.1x^2+0.99x+0.2$
	heating-load	UA	$y = 0.003x^2+0.68x+0.4$

Electricity calculation

Based on the air-conditioner heating load results, the electricity consumption is calculated using temperature, rating capacity, maximum capacity and rating COP (Coefficient of Performance) of the air-conditioner. According to the area of target room, the air-conditioners with different capacities are selected as shown in Table 3.15. The heating load of heating is equivalent to sensible heating load; the heating load of cooling is equivalent to sum of sensible heating load and latent heating load. The calculation process of heating and cooling are explained in Eq. (3-15) to Eq. (3-26) and Eq. (3-27) to Eq. (3-37).

Table 3.15 Air-conditioner performance based on room area.

Air-conditioner ID	Room area [m^2]	COP cooling	COP heating
1	8	5.21	4.05
2	9.72	5.17	3.99
3	12.96	5.00	3.78
4	16.2	5.09	3.58
5	19.44	4.36	3.37
6	22.68	4.14	3.17

$$R = R_{\text{sensible}} \tag{3-15}$$

$$R_c = R \,/\, (\text{Cafh}\times\text{Cdf}) \tag{3-16}$$

$$\text{qrmaxh} = \text{heatrtd} \,/\, \text{heatmax} \tag{3-17}$$

$$R_d = R_c \,/\, \text{heatmax} \tag{3-18}$$

$$\text{a}_0 = (-1.17\times\text{heatrtd}+6.55)\times T^2 + (0.08\times\text{heatrtd}-0.47)\times T - 0.002\times\text{heatrtd}+0.01 \tag{3-19}$$

$$\text{a}_1 = (2.59\times\text{heatrtd}-12.86)\times T^2 + (-0.19\times\text{heatrtd}+0.94)\times T + 0.004\times\text{heatrtd}-0.02 \tag{3-20}$$

$$\text{a}_2 = (-2.04\times\text{heatrtd}+10.61)\times T^2 + (0.15\times\text{heatrtd}-0.68)\times T - 0.002\times\text{heatrtd}+0.02 \tag{3-21}$$

$$\text{a}_3 = (0.37\times\text{heatrtd}-1.09)\times T^2 + (-0.03\times\text{heatrtd}+0.11)\times T + 0.0006\times\text{heatrtd}-0.004 \tag{3-22}$$

$$\text{a}_4 = (-0.09\times\text{heatrtd}+0.59)\times T^2 + (0.002\times\text{heatrtd}-0.01)\times T + 0.00005\times\text{heatrtd}-0.0003 \tag{3-23}$$

$$\text{fh}_1 = \text{a}_4 R_d^4 + \text{a}_3 R_d^3 + \text{a}_2 R_d^2 + \text{a}_1 R_d + \text{a}_0 \tag{3-24}$$

$$\text{fh}_2 = \text{a}_4\times\text{qrmaxh}^4 + \text{a}_3\times\text{qrmaxh}^3 + \text{a}_2\times\text{qrmaxh}^2 + \text{a}_1\times\text{qrmaxh} + \text{a}_0 \tag{3-25}$$

$$E_{ac} = \text{fh}_1 \,/\, \text{fh}_2\times\text{heatrtd} \,/\, \text{heatcop} \tag{3-26}$$

$$R = R_{\text{sensible}} + (-R_{\text{latent}}) \tag{3-27}$$

$$R_c = R \,/\, (\text{Cafc}\times\text{Chm}) \tag{3-28}$$

$$\text{qrmaxc} = \text{coolrtd} \,/\, \text{coolmax} \tag{3-29}$$

$$R_d = R_c \,/\, \text{coolmax} \tag{3-30}$$

$$\text{a}_1 = (-0.20\times\text{coolrtd}+0.48)\times T^2 + (-0.00036\times\text{coolrtd}+0.05)\times T \tag{3-31}$$

$$\text{a}_2 = (0.04\times\text{coolrtd}+0.23)\times T^2 + (0.002\times\text{coolrtd}-0.04)\times T \tag{3-32}$$

$$\text{a}_3 = (0.15\times\text{coolrtd}-1.07)\times T^2 + (-0.009\times\text{coolrtd}+0.07)\times T \tag{3-33}$$

$$\text{a}_4 = (-0.06\times\text{coolrtd}+0.35)\times T^2 + (0.0004\times\text{coolrtd}-0.0021)\times T \tag{3-34}$$

$$\text{fh}_1 = \text{a}_4 R_d^4 + \text{a}_3 R_d^3 + \text{a}_2 R_d^2 + \text{a}_1 R_d + \text{a}_0 \tag{3-35}$$

$$\text{fh}_2 = \text{a}_4\times\text{qrmaxc}^4 + \text{a}_3\times\text{qrmaxc}^3 + \text{a}_2\times\text{qrmaxc}^2 + \text{a}_1\times\text{qrmaxc} \tag{3-36}$$

$$E_{ac} = \text{fh}_1 \,/\, \text{fh}_2\times\text{coolrtd} \,/\, \text{coolcop} \tag{3-37}$$

R:	Time-series heating load	T:	Time-series temperature
R_{sensible}:	Time-series sensible heating load	R_{latent}:	Time-series latent heating load
Cafh:	Capacity correction coefficient for indoor unit air volume (heating)	coolrtd:	Rated cooling capacity
Cdf:	Defrost ability correction factor	coolmax:	Maximum cooling capacity
heatrtd:	Rated heating capacity	E_{ac}:	Time-series electricity demand of air-conditioner
heatmax:	Maximum heating capacity		
heatcop:	Heating COP	coolcop:	Cooling COP

By this calculation process, the results of air conditioner electricity demand calculated by the sample handled heating loads in Figures 3.16-3.21, combined with household appliance electricity demand, are shown in Figures 3.22-3.27 respectively. The results indicate significant disparities in both numerical values and time periods of air conditioning electricity consumption, driven by differences in the set temperature of the air conditioner and occupants' behavior schedules. This also suggests that for individual house, the time-series electricity demand is unpredictable.

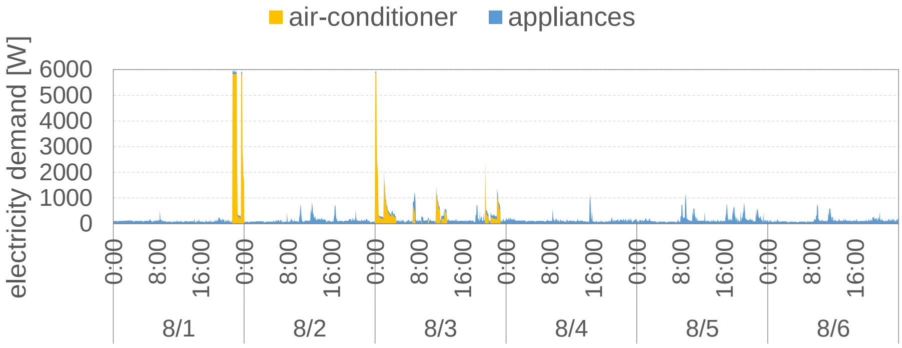

a) summer

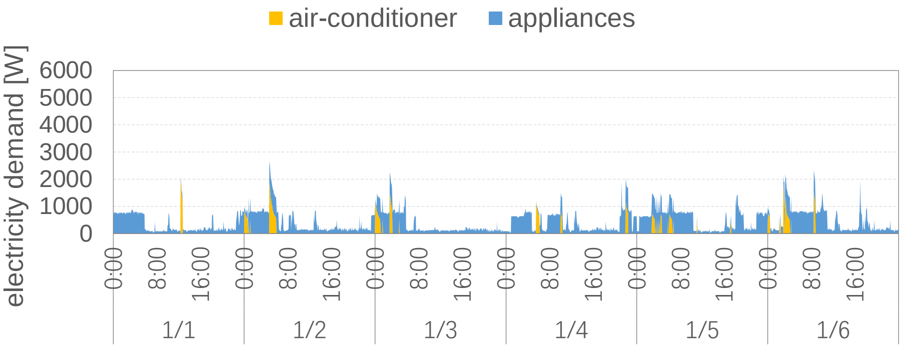

b) winter

Figure 3.22 Electricity demand by example handled heating schedules. (A-1_F1-1)

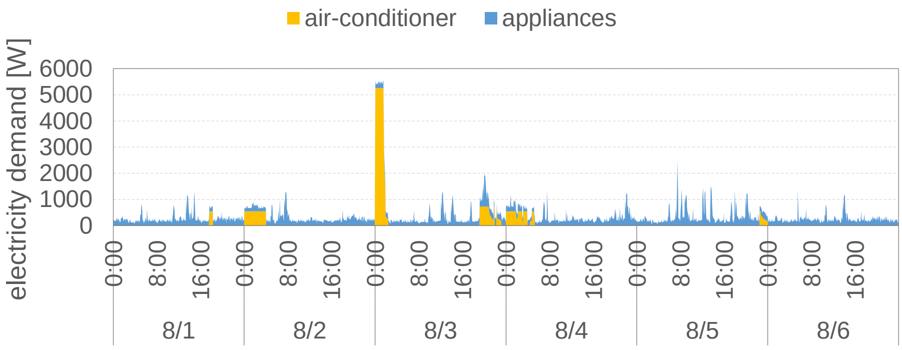

a) summer

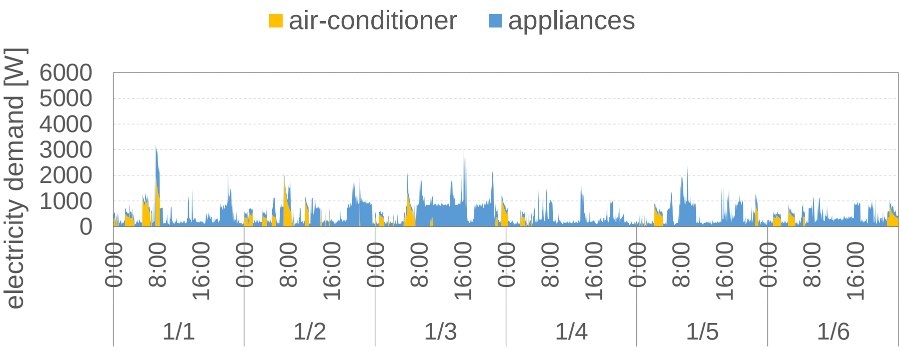

b) winter

Figure 3.23 Electricity demand by example handled heating schedules. (A-3_F3-1)

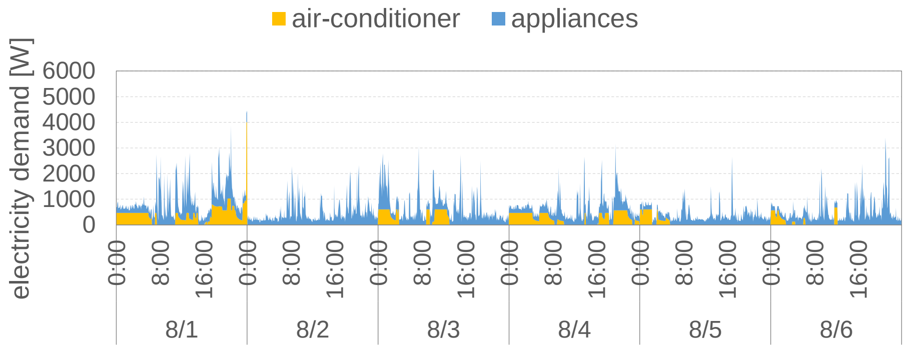

a) summer

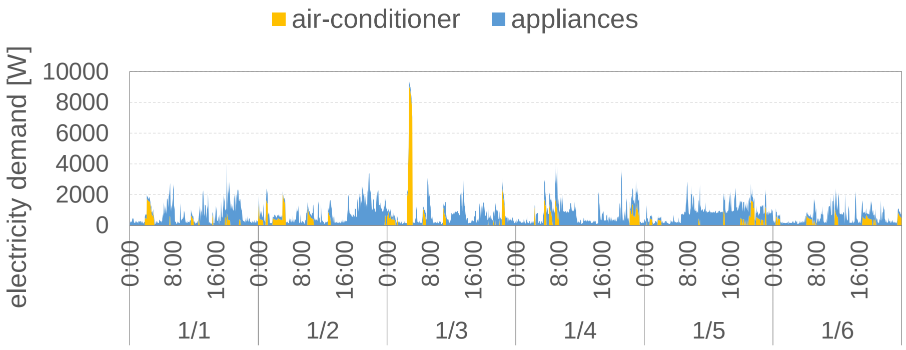

b) winter

Figure 3.24 Electricity demand by example handled heating schedules. (A-6_F6-1)

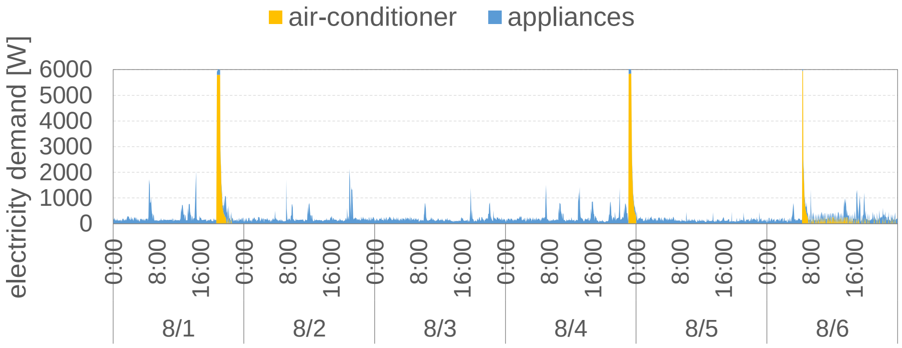

a) summer

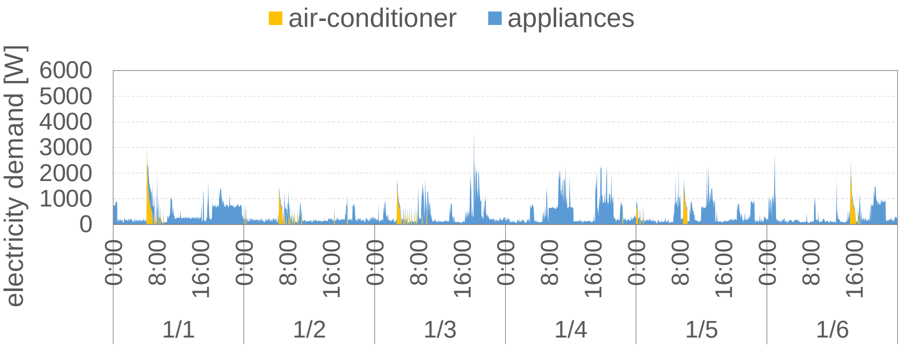

b) winter

Figure 3.25 Electricity demand by example handled heating schedules. (D-1_F2-1)

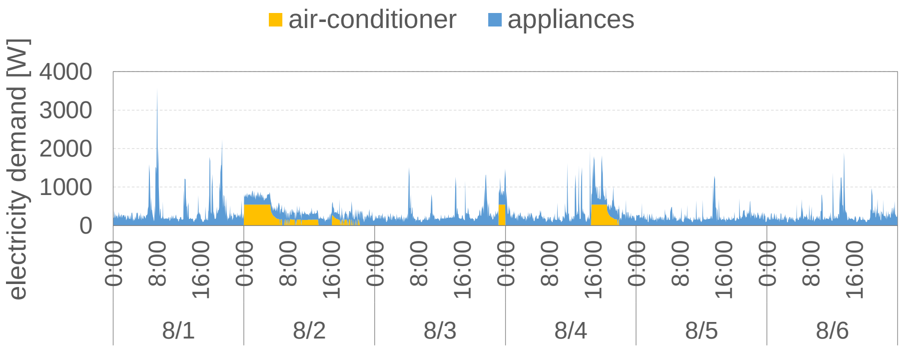

a) summer

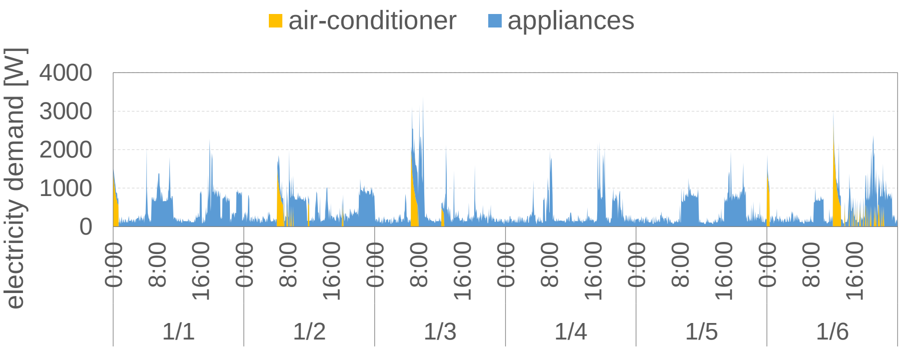

b) winter

Figure 3.26 Electricity demand by example handled heating schedules. (D-3_F3-1)

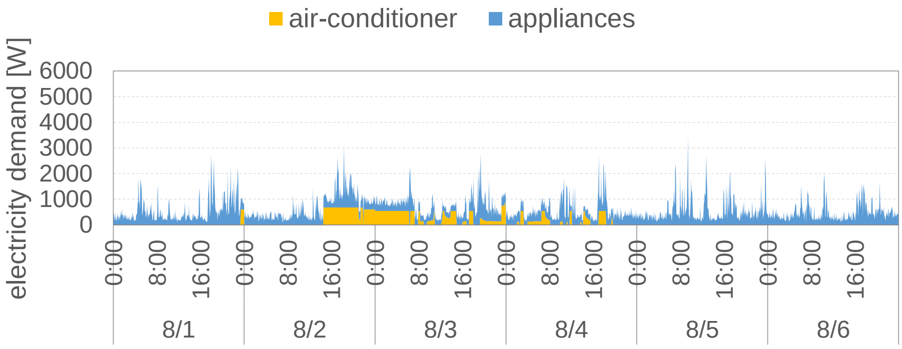

a) summer

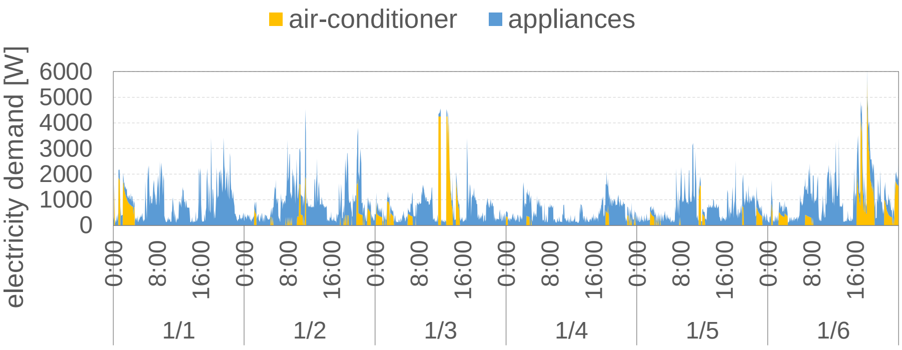

b) winter

Figure 3.27 Electricity demand by example handled heating schedules. (D-6_F6-1)

3.3.5 Verification

In the Section 3.3.2, GA was employed to adjust the simulation results of electricity demand for 93 households, ensuring a close match with the measured data in April. Therefore, the accuracy of the model has been validated for the spring and autumn seasons (excluding air conditioning part). In this section, the model is further enhanced by incorporating the air-conditioning part, extending the validation to the summer and winter seasons. Figure 3.28 presents a comparison between the hourly interval simulation results and measured data for weekdays and weekends during the summer and winter seasons, confirming the accuracy of the model.

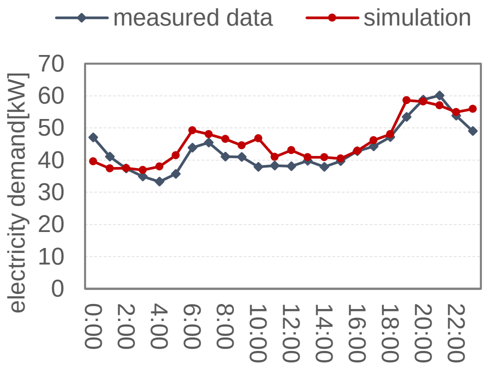

a) working-day in summer (R^2=0.75)

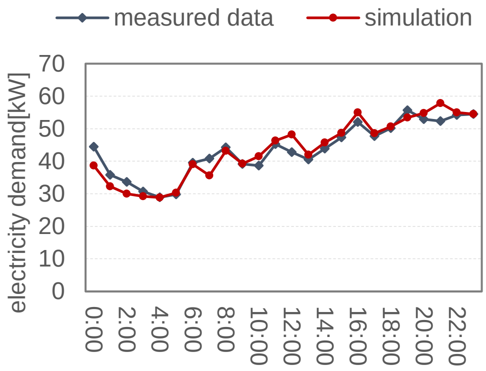

b) Resting-day in summer (R^2=0.87)

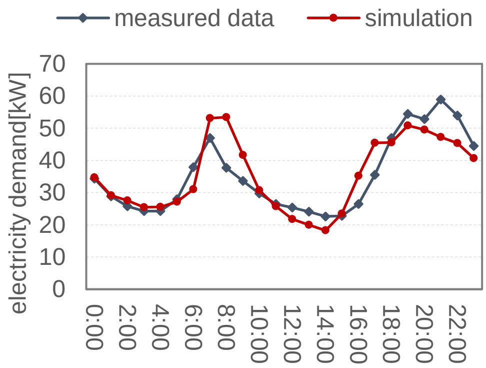

c) working-day in winter (R^2=0.73)

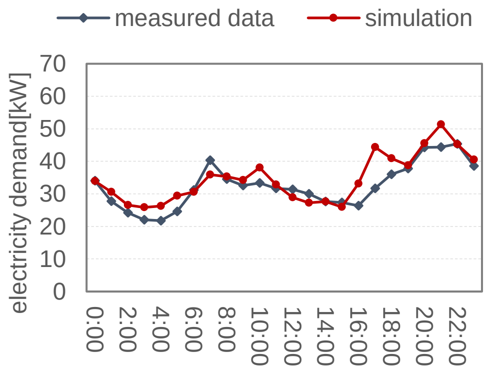

d) Resting-day in winter (R^2=0.74)

Figure 3.28 Simulation results of example days in summer, winter compared with actual data

The simulation results and measured data are also compared and verified in the form of monthly totals, as shown in Figure 3.29. The error over the year noted to be 1.45%. Due to the lack of classification of measured data based on electricity usage types, this simulation compares the proportions of each electricity usage type with the simulations in [25] and the data from The Energy Data and Modeling Center (EDMC) [26], as illustrated in Figure 3.30. There is difference between the simulation results and reference in the ratio of air-conditioning electricity to appliances electricity. This difference could potentially be attributed to the fact that the simulation in [27] is based on the entire Japanese housing stock, whereas the simulation targets in this proposed model are newly constructed houses, which exhibit higher thermal performance compared to the average standard.

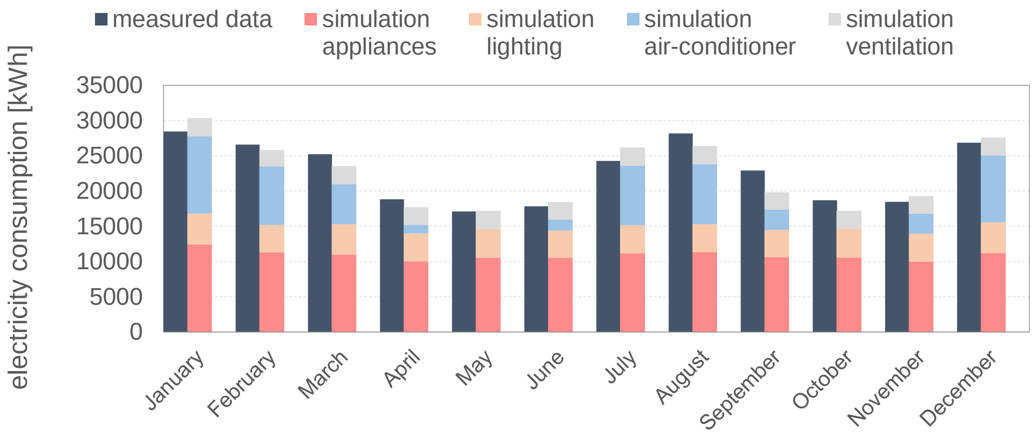

Figure 3.29 Comparation with electricity consumption simulation results with measured data of 93 households in each month

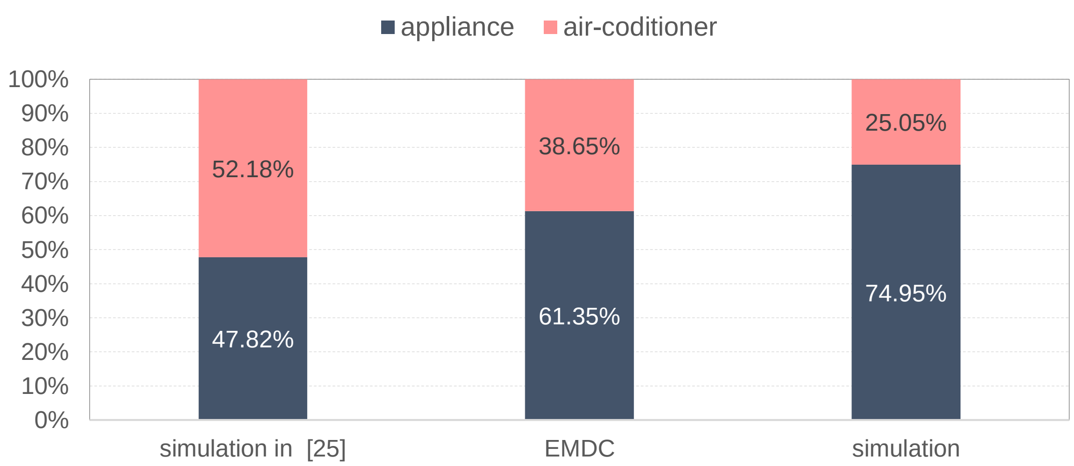

Figure 3.30 The comparison of the proportions of annual electricity consumption for household appliances and air conditioner with three cases

3.4 Simulation results of electricity demand

3.4.1 Urban scale

According to the estimation results of each archetype house's number in target area (Section 2.2.3), the above process, which obtains the electricity demand results for individual houses, is performed with corresponding quantities and aggregated to derive the total electricity consumption of houses in the target area. In this section, the results of two cases (case_2025 and case_2025_retrofit) will be discussed. To simulate these cases in 2025, predicted weather data in [28] and parameters of more efficient appliances (87.5% power), lighting (84% power) and air-conditioner (107% COP) in [29] are utilized.

In case_2025, the annual electricity consumption of the target urban houses is 2319.4 GWh. In case_2025_retrofit, considering houses retrofitting, the annual electricity consumption is 2141.4 GWh, reflecting a reduction of approximately 7.6% compared to case_2025. The air-conditioner electricity demand in summer (June, July and August) decreased from 180.5 GWh to 125.7 GWh and decreased from 359.1 GWh to 252.6 GWh in winter (October, November and December), resulting in a reduction ratio of 30% as shown in Figure 3.31. Figure 3.32 presents the hourly electricity consumption comparison results in example week between two cases for the summer and winter of 2025.

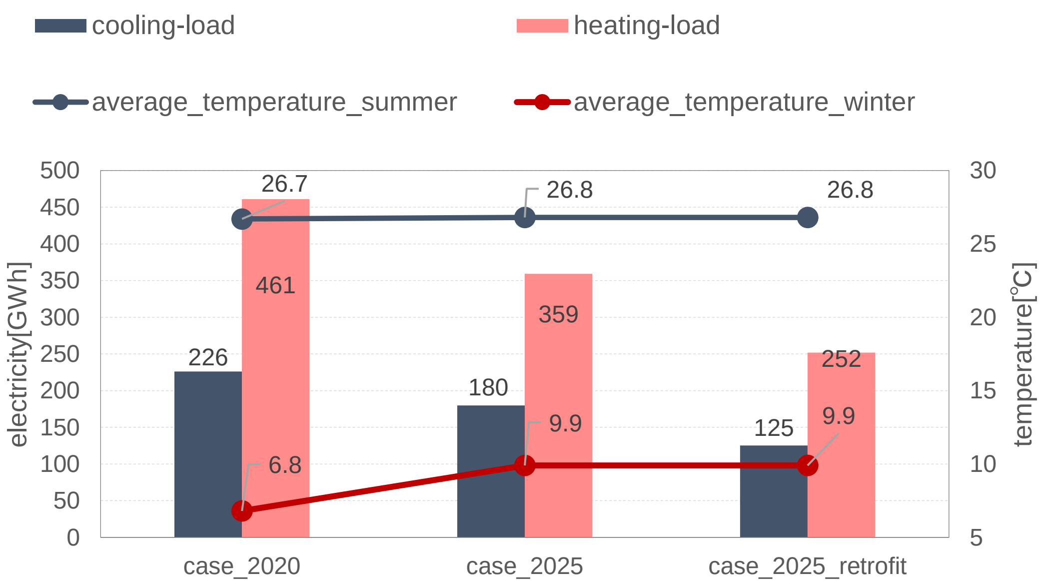

Figure 3.31 Air-conditioning electricity of houses and average temperature in target city during summer and winter with three cases

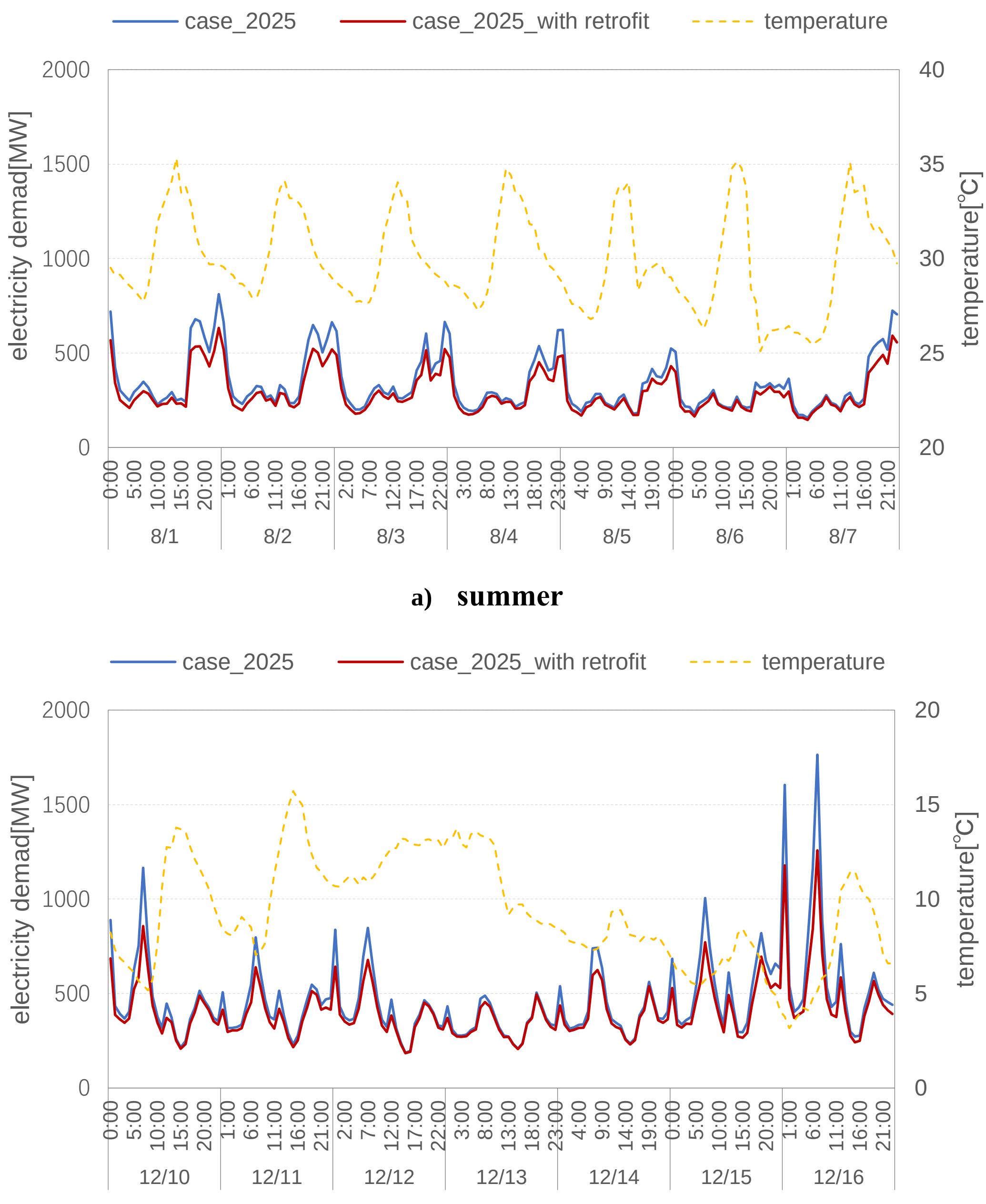

a) summer

b) winter

Figure 3.32 Hourly electricity demand of houses in target city (case_2025 and case_2025_with retrofit)

3.4.2 Street-level area scale

For each street-level area, Figure 3.33 depicts the summer and winter electricity demand results for both cases along with the corresponding change rates. These figures are drawn by ArcMap software, where each color in the bottom represents a range of energy consumption or change rate levels as shown by the numbers above. The analysis reveals significant variations in electricity demand change rates across areas. In comparison to the case_2025, case_2025_retrofit demonstrates a notable reduction in electricity demand, particularly in the west (District-5) areas.

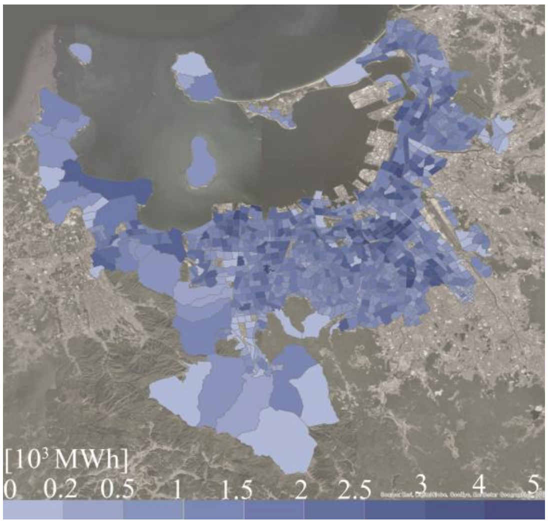

a) electricity demand [MWh] (case_2025)

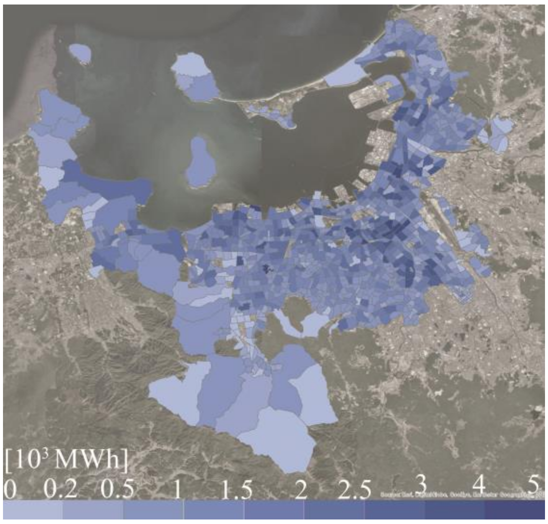

b) electricity demand [MWh] (case_2025_retrofit)

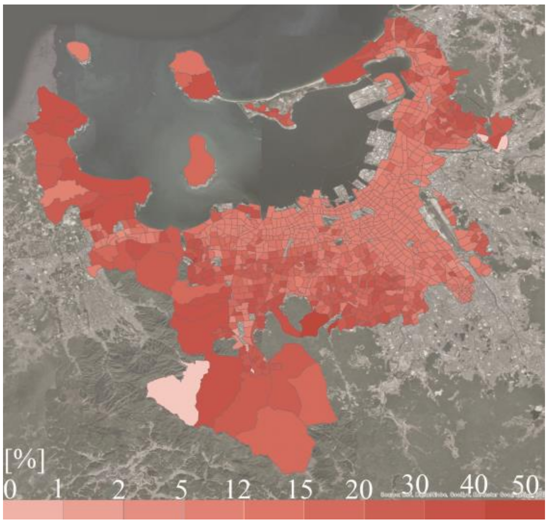

c) electricity demand change rate [%]
compared case_2025_retrofit with case_2025

Figure 3.33 Electricity demand of all areas in two cases and change rates during summer and winter

3.5 Conclusions

In this chapter, a detailed introduction is provided for the simulation model of urban-scale residential electricity demand using the archetype simulation method. The specific process is as follows:

- Collecting public data such as population census and Land and house surveys over multiple years. Then utilizing the Genetic Algorithm (GA) algorithm, the types and quantities of archetype house as well as the distribution of thermal performance levels for each house in each street level area of the target city are calculated for present (case_2020) and future considering retrofitting (case_2025_retrofit) or not (case_2025).
- Based on the extensive occupant's behavior schedules from Chapter 2, along with hourly-interval electricity data for 93 households and power consumption data for various home appliances, the GA is employed to calculate the probabilities of appliances' usage based on the occupant's behaviors. These probabilities are then utilized in the calculation of electricity demand for archetype houses.
- Simulate the electricity demand excluding air-conditioner and heating load for archetype houses, then adjust the heating load for actual houses based on the difference in UA values. Finally, calculate the electricity data for air conditioner.
- The proposed model is firstly used to simulate the hourly electricity demand of 93 households, the results are compared with measured electricity data, which ensures the accuracy of model.
- The total houses' electricity demand for target area is calculated by summing up the estimated electricity demand for various types of archetype houses according to the estimated numbers.

Using the above method, the houses' electricity demand in urban scale and in street-level scale are simulated separately with three cases. These results will be used in Chapter 4 to calculate the surplus electricity for PV generation. Compared to 2020, in the absence of retrofitting, there is approximately a 21% reduction in air conditioning electricity consumption in 2025. With retrofitting considered, there is approximately a 45% reduction in air conditioning electricity consumption. At the street area level, electricity demand in the city center area has been reduced by approximately 10% or less, while in suburban areas, the reduction ranges from 15% to 40%.

Reference

[1] Lukas G. Swan, V. Ismet Ugursal, Modeling of end-use energy consumption in the residential sector: A review of modeling techniques, Renewable and Sustainable Energy Reviews, vol.13, pp.1819-1835, Oct. 2009.

[2] Yoshiyuki Shimoda, Minami Sugiyama, Ryuya Nishimoto, Takashi Momonoki, Evaluating decarbonization scenarios and energy management requirement for the residential sector in Japan through bottom-up simulations of energy end-use demand in 2050, Applied Energy, vol.303, no.1, Dec. 2021.

[3] Narjes Abbasabadi, Mehdi Ashayeri, Urban energy use modeling methods and tools: A review and an outlook, Building and Environment, vol.161, no.15, Aug. 2019.

[4] Anil Parekh, M.A.Sc., P.Eng., Development of archetypes of building characteristics libraries for simplified energy use evaluation of houses, Ninth International IBPSA Conference, Aug.15-18, 2005.

[5] Kai Nino Streicher, Pierryves Padey, David Parra, Meinrad C. Bürer, Stefan Schneider, Martin K. Patel, Analysis of space heating demand in the Swiss residential building stock: Element-based bottom-up model of archetype buildings, Energy and Buildings, vol.184, no.1, pp.300-322, Feb, 2019.

[6] Monica Lavagna, Catia Baldassarri, Andrea Campioli, Serena Giorgi, Anna Dalla Valle a, Valentina Castellani b, Serenella Sala, Benchmarks for environmental impact of housing in Europe: Definition of archetypes and LCA of the residential building stock, Building and Environment, vol.145, pp.260-275, Nov, 2018.

[7] É. Mata, A. Sasic Kalagasidis, F. Johnsson, Building-stock aggregation through archetype buildings: France, Germany, Spain and the UK, Building and Environment, vol.81, pp.270-282, Nov, 2014.

[8] Yohei Yamaguchi, Yoshiyuki Shimoda, A stochastic model to predict occupants' activities at home for community-/urban-scale energy demand modelling, Journal of Building Performance Simulation, vol.10, iss.5-6, pp.565-581, 2017.

[9] Yohei Yamaguchi, Hideaki Takenaka, Ken T. Murata, Yuka Kambayashi, Takeshi Okada1, Ayako Taniguchi-Matsuoka, Yuto Shoda1, Yoshiyuki Shimoda, National-scale application of an activity-based residential building energy model using postcode-level census data, 16th International IBPSA Conference, pp.2326-2333. Aug.15-18, 2019.

[10] Tsuyoshi Ueno, Yasusi Sinohara, Construction and verification of a model for estimating electricity consumption of residential buildings in region for the development of an area energy demand simulation tool, IEEJ Transactions on Power and Energy, vol.142, no.8, pp.366-375, Mar. 2022. (in Japanese)

[11] P J Jones, S Lannon, J Williams, Modelling building energy use at urban scale, 7th International IBSPA conference, August 13-15, 2001.

[12] Statistics Bureau. Ministry of Internal Affairs and Communications. Japan: Population Census.

[13] Statistics Bureau. Ministry of Internal Affairs and Communications. Japan: House and Land

Investigation.

[14] Yoshiyuki Shimoda, Takahiro Asahi, Ayako Taniguchi, Minoru Mizuno, Evaluation of city-scale impact of residential energy conservation measures using the detailed end-use simulation model, vol.32, iss.9, pp.1617-1633, Sep.27, 2007.

[15] Japanese Meteorological Agency. (in Japanese) https://www.jma.go.jp/jma/menu/menureport.html

[16] John H. Holland, Adaptation in Natural and Artificial Systems, 1975.

[17] Ministry of Land, Infrastructure, Transport and Tourism. Establishment of higher grades related to energy saving performance in the housing performance display system. (in Japanese). https://www.mlit.go.jp/policy/shingikai/content/001443042.pdf

[18] Ono Hidemitsu, CHOI Youngjin, Takahashi Kentaro, Ikeda Tomohiro, Ueno Takahiro, Sumiyoshi Daisuke, Optional planning method of urban energy supply based on minute energy demand-Part 2 Development of energy demand estimation method for residential buildings, Society of Air-Conditioning and Sanitary Engineers Conference Academic Lecture Papers 2019 Conference (Sapporo) Academic Lecture Papers, Vol.10, pp.273-276, 2019. (in Japanese)

[19] Minutes of the 208th National Assembly Committee on Land, Infrastructure, Transport and Tourism 2022;14:7-27. (in Japanese)

[20] Wang H, Sumiyoshi D. Development of Occupants' Behavior Model in Urban Scale Using Dynamic Time Warping and Particle Swarm Optimization Algorithms Based on National Lifetime Survey. Proc. 13th ENERGY Int. Conf. Smart Grids, Green Commun. IT Energy-aware Technol 2023:17-22.

[21] Explanation of the energy consumption calculation method used in the judgment criteria of housing project builders. (in Japanese)

[22] Operation manual of NewHASPACLD. (in Japanese)

[23] Takuro Fujii, Yoshiyuji Shimoda, Takao Morikawa, Minoru Mizuno, Development and application of city scale residential energy end-use model by considering with various household categories Part1, J. Environ.Eng., AIJ, no.589, pp51-58, Mar. 2005.

[24] Daisuke Sumiyoshi, Development report of simple residential energy calculation program, Feb 2014. (in Japanese)

[25] Taniguchi-Matsuoka A, Shimoda Y, Sugiyama M, Kurokawa Y, Matoba H, Yamasaki T, Morikuni T, Yamaguchi Y, Evaluating Japan's national greenhouse gas reduction policy using a bottom-up residential end-use energy simulation model, Applied Energy, Vol.279, No.1, 115792, Dec. 2020.

[26] The energy data and modeling center, The Institute of Energy Economics, Japan (2015). EDMC Handbook of Energy & Economic Statistics in Japan (2015), The Energy Conservation Center, Japan.

[27] National Research and Development Corporation Building Research Institute, Technical information regarding evaluation of energy consumption performance in accordance with the 2016 Energy Conservation Standards. (in Japanese).

https://www.kenken.go.jp/becc/house.html

[28] The Agro-Meteorological Grid Square Data. (in Japanese).
https://amu.rd.naro.go.jp/

[29] Takamura S, Yamaguchi Y, Habara H, Shimoda Y, District electricity demand prediction under large diffusion of photovoltaic and energy saving technology, J. Environ. Eng., AIJ, Vol.77, No.680, pp.805-811, Oct. 2012. (in Japanese).

Chapter-4

Simulation model & results of surplus electricity from PV generation and EV charging

4.1 Introduction

In response to the climate crisis, the Japanese government aims to achieve a renewable energy share of 36-38% in the electricity mix by 2030 to mitigate emissions. This ambitious target includes the introduction of 103.5 ~117.6 GW of solar energy [1].

Throughout the process of promoting the widespread adoption of photovoltaic (PV) technology, cities can play a pivotal role. The urban scale is well-suited for integrating local PV generation to meet local demand [2]. By leveraging existing structures, such as rooftops, the installation of PV panels avoids the need for additional land and materials. Additionally, it helps reduce transmission losses associated with supplying electricity to meet local demand [3]. Consequently, the incorporation of PV in urban areas has garnered significant attention [4].

Due to the wide variation in urban contexts, it is essential to assess the solar potential in different urban regions to introduce photovoltaic (PV) systems efficiently and economically. Developing estimation models based on Geographic Information System (GIS) is the primary approach for addressing this issue [5]. For example, Wiginton et al. [6] utilized GIS and object-specific image recognition to identify available rooftop areas for PV deployment in an example region in southeastern Ontario. Bergamasco et al. [7] estimated roof surface availability and PV system efficiency using GIS and a database of the Joint Research Centre of the European Commission. Šúri et al. [8] developed a database of yearly and monthly solar radiation maps with a spatial resolution of 1 km in Europe using GIS with measurements from 566 ground meteorological stations. These studies have contributed to maximizing the introduction of PV in urban areas by identifying PV potentials. However, PV generation has the problem of strong fluctuations depending on weather condition [9]. The temporal disparities between fluctuating PV generation and electricity demand often result in an excess of PV electricity production, referred to as surplus electricity [10].

Surplus electricity is often considered an undesirable factor [10]. This distributed power can be present at anytime and anywhere, significantly increasing the burden on the power grid [7]. Current research on surplus electricity primarily focuses on enhancing self-sufficiency by controlling the supply and demand sides or adapting to demands of other users, limited to specific regions. There is a limited quantitative study on surplus electricity at the urban scale, particularly regarding when and where surplus electricity occurs and its relationship with the corresponding urban context. This information is valuable for providing insights and essential information PV planning [10]. Liao et al. [10] quantified the time-series PV surplus in a high roof-PV penetration scenario in Seoul, Korea. They explored the correction between surplus electricity and several building type. However, the target was limited to two example districts. Gomez-Exposito et al. [11] evaluated storage capacity for balancing surplus electricity with several scenarios of centralized renewables, rooftop PV in case of Spain. While this evaluation operates at a larger scale (national scale), the impact of urban context on surplus electricity was not considered.

The change of urban context cannot be overlooked. For example, in Japan, the government is promoting retrofitting of existing houses with high thermal performance and has legislated that newly built houses must meet specified thermal performance standards from 2025 [12]. It is anticipated that these measures will enhance the thermal performance of the houses and contribute to a reduction in electricity demand of air-conditioning. With the advancement of houses retrofitting, it is expected that the urban context will undergo changes, impacting the spatial and temporal distribution of surplus electricity. Currently, there is a lack of related research on quantifying the impact of changes in urban context on surplus electricity.

On the other hand, there are numerous methods for dealing with surplus electricity. Sending this electricity to urban grid is a commonly used approach, but it poses technical challenges such as voltage and frequency regulation. Due to variations in the condition of electrical infrastructure across different regions, the absorption capacity for maximum surplus electricity differs [13]. Additionally, there are more flexible methods available for managing surplus electricity within local microgrids. With smart devices and communication technologies, PV generation can be controlled by adjusting the power, tilt, and orientation angles of the PV array to meet electricity demand [14]. Another approach involves reallocating some power demands through demand-side management (DSM) to periods of surplus electricity during the day [15]. Furthermore, surplus electricity can be absorbed using battery energy storage and subsequently supplied to loads during periods without renewable generation [16].

With the acceleration of electric vehicles (EVs) development recently, research on utilizing surplus electricity from PV to EV has been extensively conducted. For example, Kawasaki et al. [17] explored the feasibility of achieving urban zero emissions by employing EV charging and discharging to regulate large scale PV generation, with a specific consideration of the economic perspective. Nishinoda et al. [18] evaluated load-leveling effect by using EV batteries to storage surplus electricity in the real-world scenario of installed PV systems in a specific target area. However, the study focused on EV charging using a single PV source. Ichi et al. [19] simulated a smart grid scenario within a residential block, demonstrating the integrated utilization of surplus power generated by multiple residential PVs. The study confirmed the appropriateness of electricity interchange through the smart grid for residential areas characterized by high prevalence of EVs and detached houses, ultimately enhancing the electricity self-sufficiency rate.

Based on existing research, currently there is a lack of quantitative research on the integration of EVs in the urban scale, especially regarding the required quantity of EV integration across different urban areas to fully utilize surplus electricity from PV considering the change of urban context. Therefore, this chapter will utilize the electricity demand results of target city from Chapter 3, combined with the PV model, to simulate the surplus electricity for three cases (cases_2020, case_2025 and case_2025_retrofit) and the required quantity of EVs for fully utilizing this surplus electricity. Furthermore, it will analyze the relationship between these results and the characteristics of residential buildings.

4.2 PV model and surplus electricity

To obtain the surplus electricity, the proposed PV model is used to calculate PV generation. The PV setups for three cases (case_2020, case_2025 and case_2025_retrofit) are outlined as follows:

- case_2020: 9% of detached houses and 0.2% of apartment houses have PV on roofs [20]
- case_2025: Based on case_2020, all newly built detached houses will be installed with PV, and the removal of PV in demolished houses follows the proportion of housing stock in 2020.
- case_2025_retrofit: Same with case_2025.

The PV panel setup area for each house is assumed to be half of the roof area. The power generation is calculated by Eqs. (4-1, 4-2, 4-3).

$$P_{pv} = P_{sol}\, pv_a 180/\cos\left(2\pi pv_g\right)\, pv_{ef} pv_{los} o_{los}\, R_{tem} \tag{4-1}$$

$$R_{tem} = 1 + \alpha_{max}\,(T_{CR} - 25)\,/100 \tag{4-2}$$

$$T_{CR} = T_{OA} + \Delta T \tag{4-3}$$

P_{pv}: PV's generation electricity [kWh]

P_{sol}: slope solar radiation per unit area 5-mins interval

pv_a: PV's area

pv_g: PV's angle (26.1°)

pv_{ef}: conversion efficiency (0.18)

pv_{los}: conversion loss from direct current to alternating current (0.95)

o_{los}: other loss (0.95)

R_{tem}: Loss compensation due to temperature rise

T_{CR}: Weighted average solar module temperature [°C]

T_{OA}: Air-temperature

α_{max}: -0.41[%•°C-1]

ΔT : Weighted average solar module temperature rise value (18.4°C)

Figure 4.1 shows the maximum PV generation power of each area in target city with two cases and the difference between two cases. Due to the current low installation rate of PV in apartment houses (0.2%), the maximum PV power is smaller in urban centers with a higher proportion of apartment houses, whereas the situation is reversed in suburban areas. Under the current rate of houses replacement, in areas where population outflow is more significant and the number of demolished houses exceeds the number of newly built, the disposal of PV panels is higher, leading to a decrease in the maximum PV generation power (bule area).

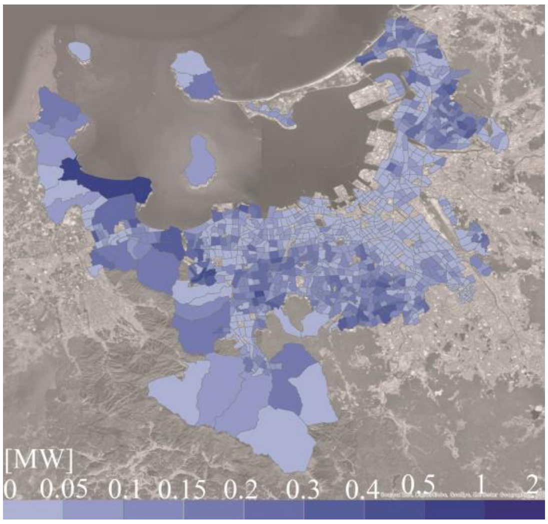

a) Maximum PV generation power in case_2020

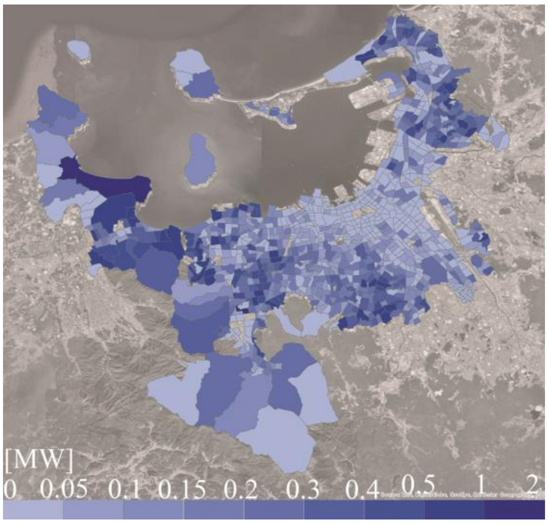

b) Maximum PV generation power in case_2025 and case_2025_retrofit

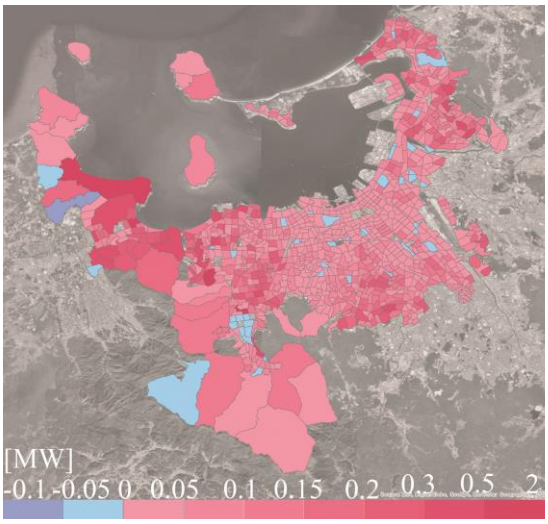

c) Maximum PV generation power change between

case_2020 and case_2025

Figure 4.1 Maximum PV generation power of each area in target city

By proposed PV model, the calculation results are subtracted from the electricity demand results in Chapter 3, yielding the surplus electricity results at 5-minute intervals for all street-level areas of the target city.

This study analyzes the surplus electricity in each street level area of the target city from two aspects: maximum power and duration time. Additionally, the impact of houses retrofitting on surplus electricity based on houses characteristics are also considered.

Figure 4.2 and Figure 4.3 illustrate the maximum power and the duration of surplus electricity occurrence in each street-level area during summer and winter seasons for case_2025 and case_2025_retrofit. Each color in the bottom represents a range of surplus electricity power, duration time or change rate levels as shown by the numbers above. Several conclusions can be drawn regarding geographical features:

- Residential areas in the city center (District-2,3) generate almost no surplus electricity.
- Houses retrofitting is unlikely to generate surplus electricity in areas where surplus electricity does not occur.
- Areas with higher maximum surplus power experience a more significant increase in the duration of surplus electricity occurrence due to houses retrofitting.
- In terms of occurrence duration, the peripheral areas of the city have longer durations compared to the internal regions, while there is no apparent geographical difference in terms of maximum power.

a) maximum surplus power [W/m²] (case_2025)

b) maximum surplus power [W/m²] (case_2025_retrofit)

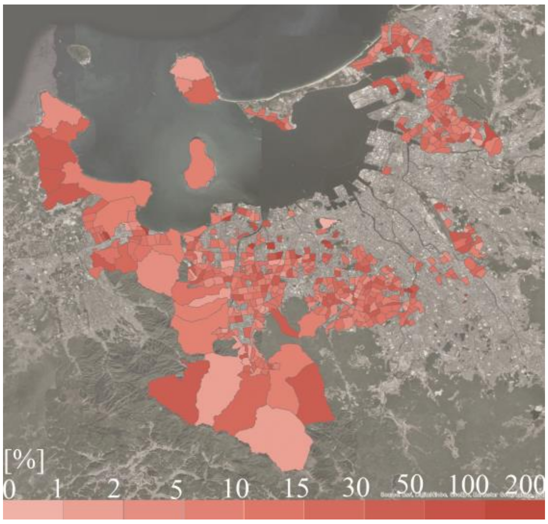

c) change rate [%] between two cases.

Figure 4.2 Maximum surplus electricity power of all areas and the comparison between case_2025_retrofit and case_2025 during summer and winter

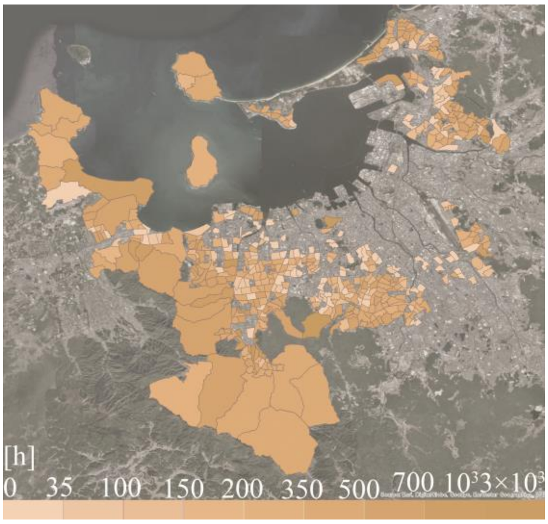

a) surplus power duration [h] (case_2025)

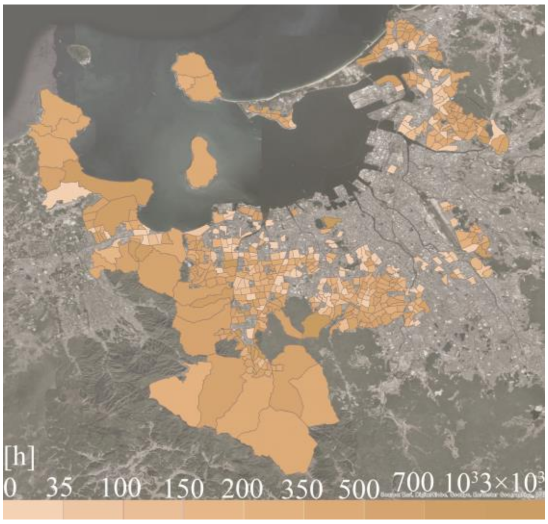

b) surplus power duration [h] (case_2025_retrofit)

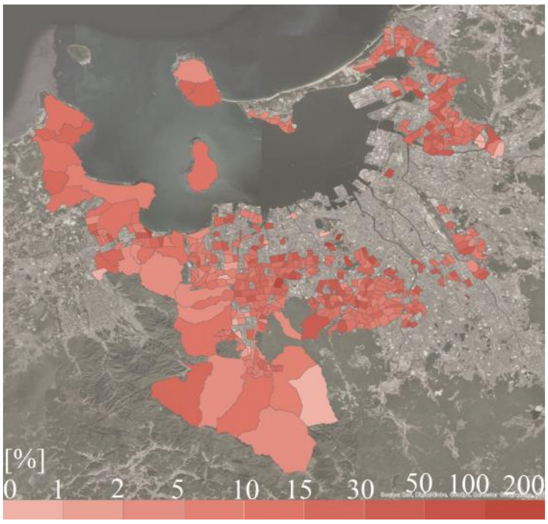

c) change rate [%] between two cases

Figure 4.3 Surplus electricity duration of all areas and the comparison between case_2025_retrofit and case_2025

Figure 4.4 shows the cumulative amount of the number of street level areas experiencing surplus electricity and occurrence durations in the whole city. In case_2025, the longest duration of surplus electricity occurs in most areas at 11:00 in the spring. In case_2025_retrofit, the chances of surplus electricity occurrence increase during the summer, reaching the same level as in the spring.

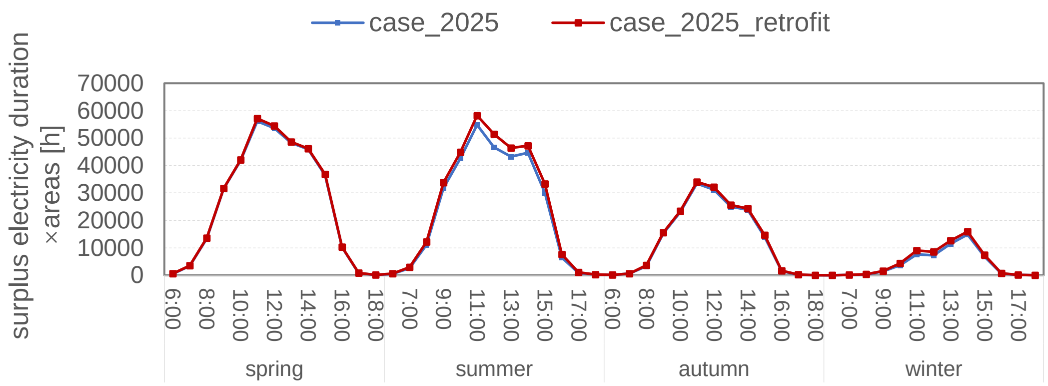

Figure 4.4 Cumulative amount of the number of street level areas experiencing surplus electricity and occurrence durations in summer and winter period (case_2025 and case_2025_retrofit)

A detailed analysis is conducted on the relationship between the urban context (including characteristics of houses such as proportion of detached houses, average household size and average construction year) and surplus electricity (maximum power per square meter of houses and duration time) during the summer and winter periods.

In terms of maximum power, Figures 4.5, 4.6 illustrate that areas with a higher proportion of houses and a larger average construction year generate higher power, and houses retrofitting leads to a more significant increase. Figure 4.7 indicates that there is not a significant correlation between household size and power.

Figure 4.5 Maximum surplus electricity during summer and winter and proportion of detached houses with two cases in 2025

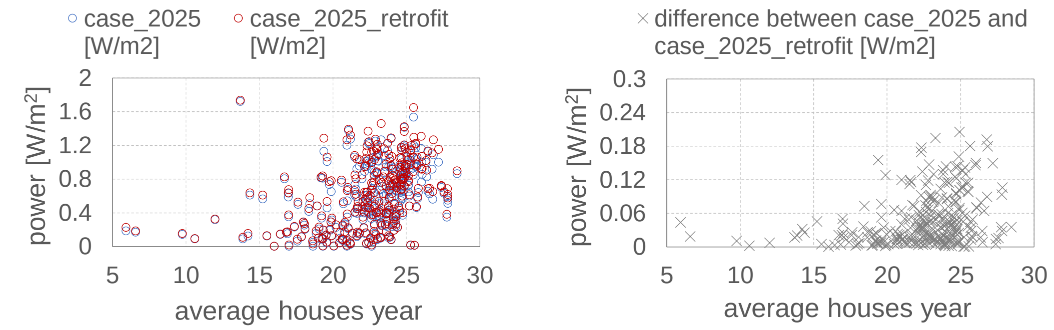

Figure 4.6 Maximum surplus electricity during summer and winter and average construction year with two cases in 2025

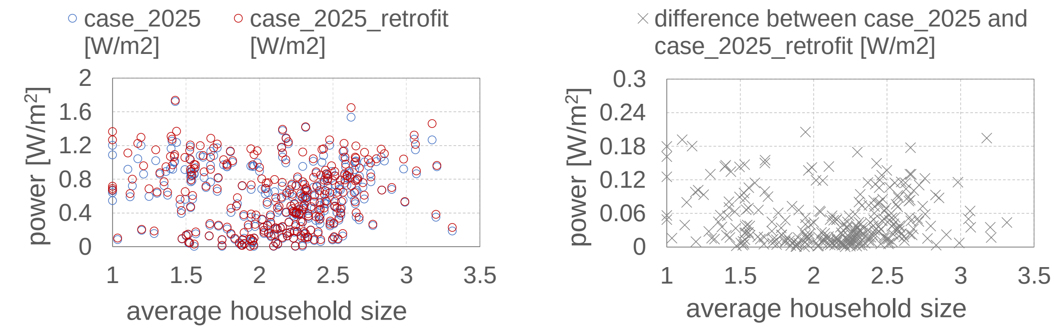

Figure 4.7 Maximum surplus electricity during summer and winter and average household size with two cases in 2025

Figures 4.8, 4.9 4.10 present the results for duration, depicting similar characteristics to maximum power. This implies that for areas with a lower proportion of detached houses and a smaller average construction year, the improvement in duration is more pronounced during houses retrofitting.

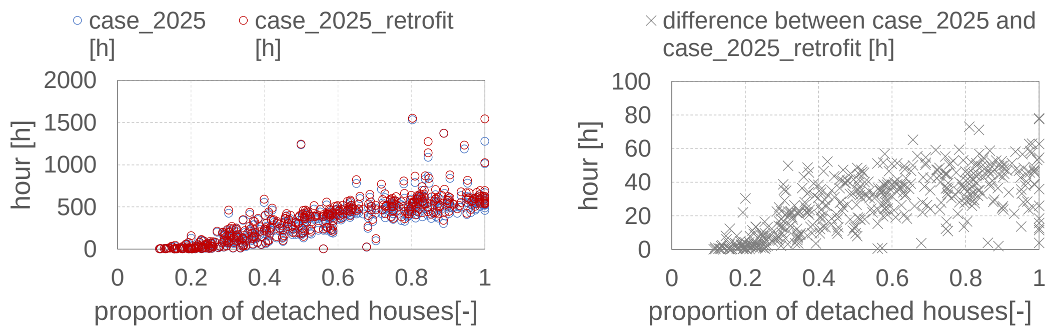

Figure 4.8 Surplus electricity duration time during summer and winter and proportion of detached houses with two cases in 2025

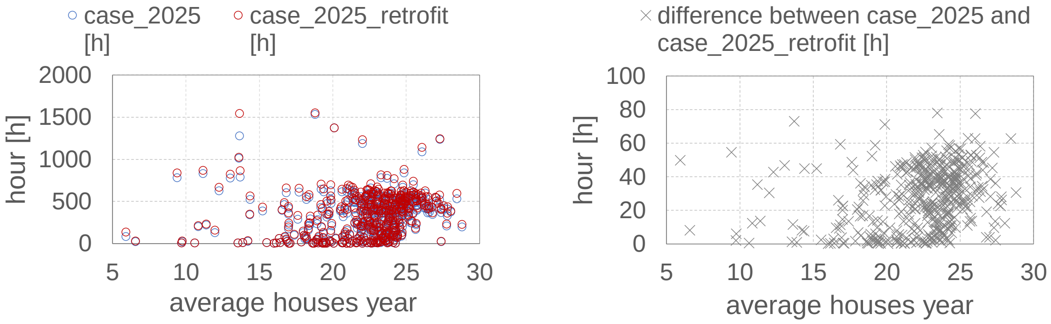

Figure 4.9 Surplus electricity duration time during summer and winter and average construction year with two cases in 2025

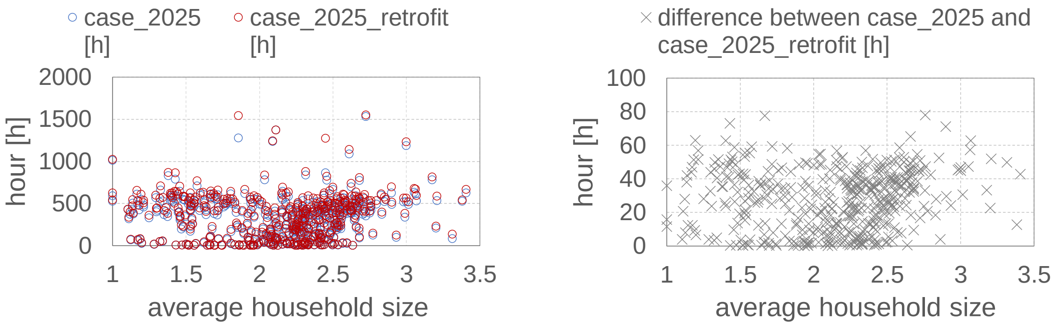

Figure 4.10 Surplus electricity duration time during summer and winter and average household size with two cases in 2025

4.3 EV model and minimum EVs introduction rate

This section provides a detailed introduction to the EV model utilizing surplus electricity for charging, as well as the minimum EV introduction rates required for each area to fully consume the surplus electricity.

4.3.1 Data collection

To assess the electricity consumption of EVs driving on urban scale, it is imperative to acquire data on the origin and destination of the EVs, along with the corresponding distances traveled. The origin and destination are designated as specific street-level areas. The probabilities representing the likelihood of individuals using cars for commuting and private purposes between different administrative districts are referring to [21]. The destination for each street-level area is randomly selected within its associated district. Distances between individual street-level areas are determined using road distance data from Google Maps. For example, the distances from the target area in District-2 to other street-level areas in Fukuoka are depicted in Figure 4.11.

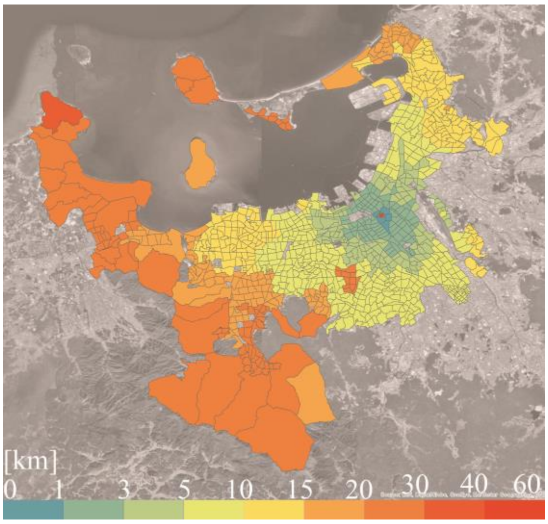

Figure 4.11 Districts and distances between all areas to sample area in target city [km]

As shown in Figure 4.12, the in/out house status of EV is determined based on the behavior schedules of occupants, including working male, working female, housewife, and elders as introduced in Chapter 2.

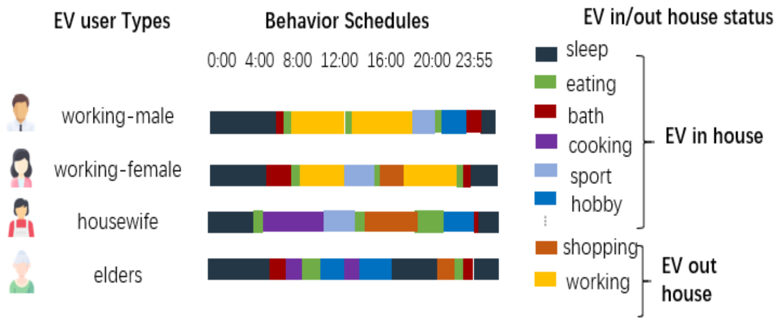

Figure 4.12 Conceptual diagram of behavior schedules and EV

4.3.2 Calculation process of EV charging and discharging

Figure 4.13 shows an image of EV's running, charging and discharging of one day in this simulation. In this scenario, households possessing EV only own one, and the user is randomly selected from household members. When the EV is at home, it could charge or discharge using power stations (EVPS) installed in each house. Conversely, when the EV is away from home, it consumes electricity while in operation.

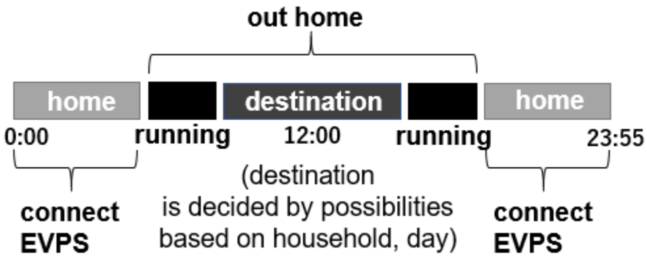

Figure 4.13 Image pf EV charge/discharge during a day

Figure 4.14 shows battery's capacity settings and limitation on discharge and forced charging electricity [22]. According to [22], if the battery's charge level falls below 30%, the discharge process is halted. Additionally, when the electricity level drops below the minimum required amount to ensure a round trip to the destination (E_{min}, calculated by Eq. (4-1)), the battery is forced to charge.

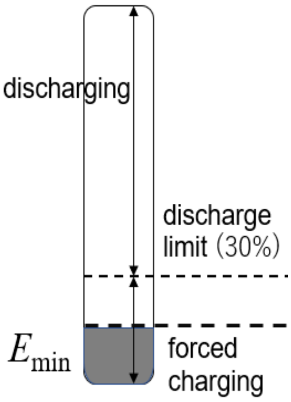

Symbol	Content
d_{kWh}	Distance traveled per kWh
	Spring/Autumn: 7.9 km/kWh
	Summer: 6.3 km/kWh
	Winter: 4 km/kWh
V	Average speed: 20.2 km/h
E_r	Rated charging/discharging power of EVPS: 6 kW
E_{str}	EV battery capacity: 40 kWh
F_{loss}	Natural loss rate: 5.9×10^{-6}

Figure 4.14 Capacity settings and conceptual diagram of EV storage batteries

Figure 4.15 shows the calculation process of EVs charge/discharge and the impact of EVs charge/discharge on houses electricity supply and demand in target area. In detail, firstly, prepared data include household number, attributes, behavior schedules, surplus electricity of houses in the past research are input into the model. Then the in/out house status of EV is determined by the occupant's behavior schedules. To calculate charge power (P_{cg}), if surplus power is available, Eq. (4-2) is employed, utilizing surplus electricity power (P_{sur}), number of EVs in houses of target area (N_{ev_cg}) and charging possible power (P_{cg_po}, calculated by Eq. (4-3)). If no surplus electricity exists, according to [23] when time-series CO_2 emission indicator (indicator that shows how much CO2 is emitted to supply 1kWh of electricity generation [kg-CO_2/kWh], I_{CO2}) of the system power is greater than 0.55 or I_{CO2} is smaller than 0.45 but remained electricity in battery ($E_{rem}(t)$) is less than Emin, then P_{cg} would be equal to P_{cg_po}. To calculate discharge power (P_{dcg}), when EV is in house, no surplus electricity exists, I_{CO2} is greater than 0.55 and $E_{rem}(t)$ is greater than Emin, P_{dcg} would calculate by Eq. (4-4) with P_{sur}, number of EVs discharged at houses in the area (N_{ev_dcg}) and charging possible power (P_{dcg_po}, calculated by Eq. (4-5)). $E_{rem}(t)$ is calculated by Eq. (4-6) with power conditioner charge load factor (Lcg(t), calculated by Eq. (4-7)), power conditioner discharge load factor ($L_{dcg}(t)$, calculated by Eq. (4-8)), power conditioner charge efficiency ($pcs_{cg}(t)$, calculated by Eq. (4-9)), power conditioner discharge efficiency ($pcs_{dcg}(t)$, calculated by Eq. (4-10)), power of driving (P_{d_dcg}, calculated by Eq. (4-11)) and power of natural loss (P_{n_dcg}, calculated by Eq. (4-12))

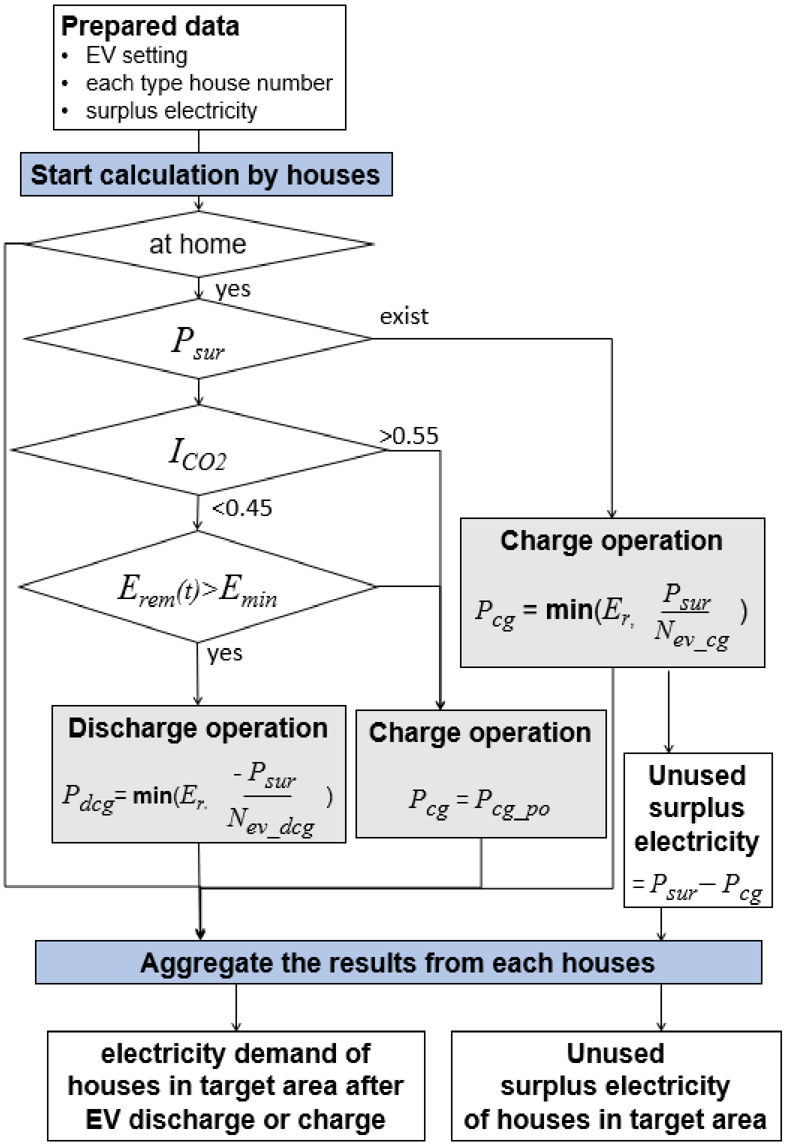

Figure 4.15 Calculation process of EV model

$$E_{min} = \frac{2d}{d_{kWh}} \tag{4-1}$$

$$P_{cg} = \min(P_{cg\_po}, \ \frac{P_{sur}}{N_{ev\_cg}}) \tag{4-2}$$

$$P_{cg\_po} = \min((E_{str} - E_{rem}(t), E_r) \tag{4-3}$$

$$P_{dcg} = \min(P_{dcg\_po}, \ \frac{P_{sur}}{N_{ev\_dcg}}) \tag{4-4}$$

$$P_{dcg\_po} = \min(P_{dcg\_po}, E_r) \tag{4-5}$$

$$E_{rem}(t+1) = E_{rem}(t) + E_{cg}(t)pcs_{cg}(t) - \frac{E_{dcg}(t)}{pcs_{dcg}(t)} - P_{d\_dcg} - P_{n\_dcg} \tag{4-6}$$

$$Lcg(t) = \frac{P_{cg\_po}}{E_r} \tag{4-7}$$

$$L_{dcg}(t) = \frac{P_{dcg\_po}}{E_r} \tag{4-8}$$

$$pcs_{cg} =- 1.3Lcg(t)^4 + 3.6Lcg(t)^3 - 3.5Lcg(t)^2 + 1.5Lcg(t) + 0.7 \tag{4-9}$$

$$pcs_{dcg} =- 0.6L_{dcg}(t)^4 + 2.1L_{dcg}(t)^3 - 2.5L_{dcg}(t)^2 + 1.3L_{dcg}(t) + 0.7 \tag{4-10}$$

$$P_{d\_dcg} = \frac{V}{d_{kWh}} \tag{4-11}$$

$$P_{n\_dcg} = \frac{E_{rem}(t)}{F_{loss}} \tag{4-12}$$

4.3.3 Simulation results of example street-level area

In chapter 2, the surplus electricity simulation was conducted of each street level area of target city. Utilizing the proposed EV model in this research, the simulation was conducted to analyze the charging/discharging patterns of EVs for houses in this example street level area. The results were obtained under different scenarios of EV introduction rates, as depicted in Figure 4.16 a), b), c). In this series of Figures, surplus electricity (PVs generation minus demand of houses), is positive or negative according to time, EVs charging is negative, and EVs discharging is positive. The electricity balance is the total value of the above types of electricity. Figure 4.16 a) shows that when the EVs introduction rate is low (3%), the electricity balance has the cases greater than 0, indicating that surplus electricity cannot be fully utilized to charge EVs. Figure 4.16 b) shows that as the introduction rate has increased to 5%, unused surplus electricity decreases but still exists. In Figure 4.16 c), when the introduction rate has increased to 8%, the electricity balance consistently remains smaller than 0, indicating that surplus electricity has been fully utilized to charge EVs. Therefore, it can be concluded that there is a minimum EVs introduction rate (critical value) to fully utilize surplus electricity of houses in each street-level area.

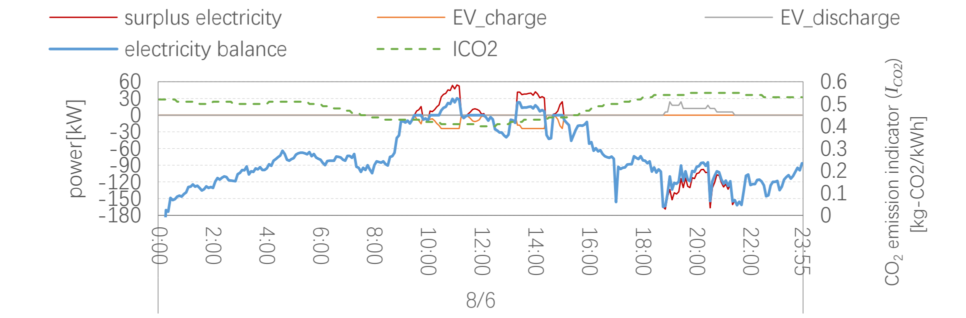

a) EVs introduction rate 3%

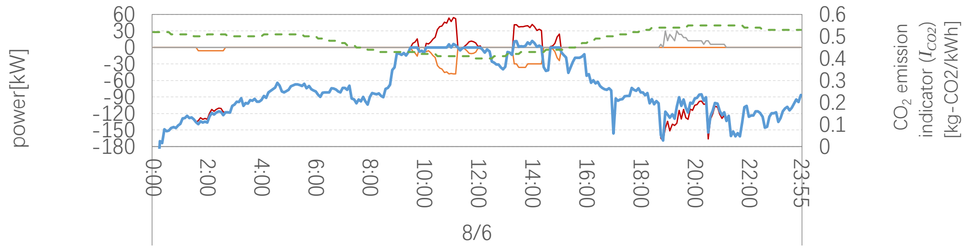

b) EVs introduction rate 5%

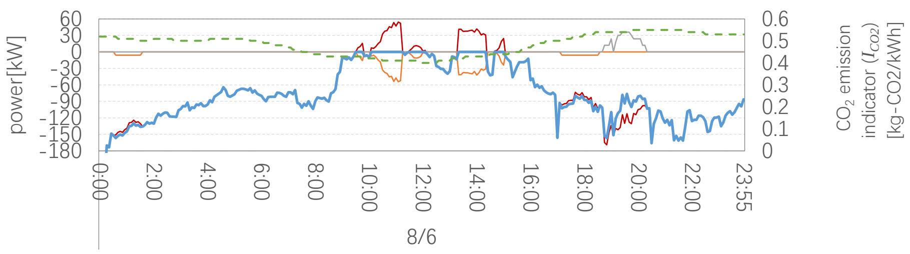

c) EVs introduction rate 8%

Figure 4.16 Simulation results of EVs charging/discharging and surplus electricity of houses in example street-level area

4.3.4 Minimum EVs introduction rate of each street-level area in target city

Through the above calculation process, the minimum EVs introduction rate of each street-level area in target city are shown in Figure 4.17 a), b), c) with three cases. In case_2020 and case_2025, the results show that the minimum EVs introduction rates of several areas have increased from 2020 to 2025, while those of other areas have decreased. This contrasting outcome is due to the expected differences in population migration between areas, resulting in either an increase or decrease in surplus electricity. Comparing the results of case_2025 and case_2025_retrofit, it is evident that houses retrofitting has increased the number of areas generating surplus electricity. The minimum EV introduction rates of these newly added areas are around 0-20%, while the minimum EV import rates of other surplus electricity regions have also increased relatively.

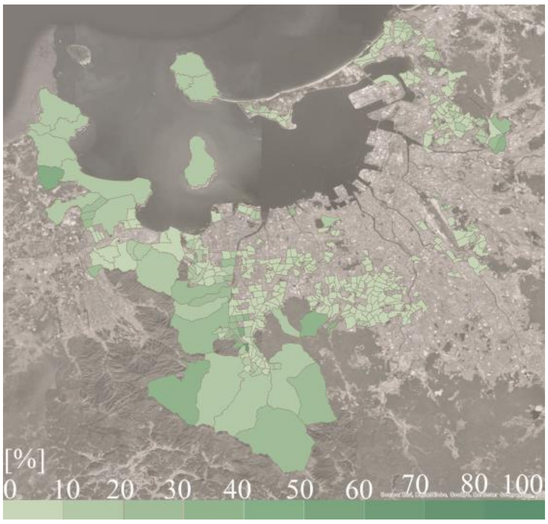

a) case_2020

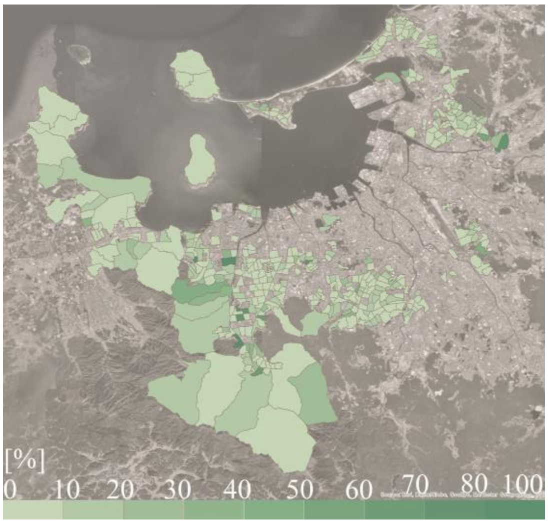

b) case_2025

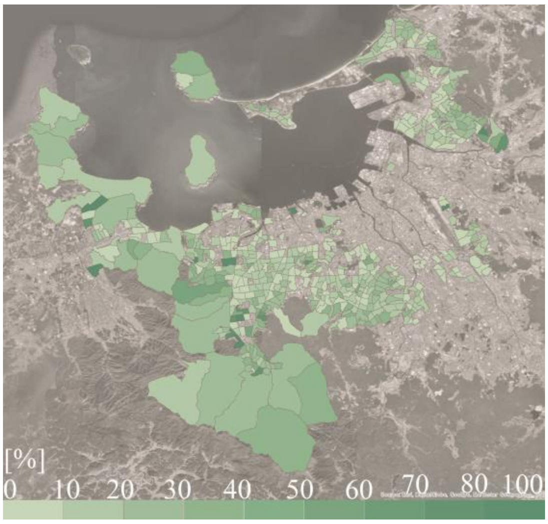

c) case_2025_retrofit

Figure 4.17 Minimum EV introduction rate to fully utilize surplus electricity of houses for all street-level areas in target city [%]

In order to analyze the relationship between the houses characteristics of the target area and the minimum EVs introduction rate, characteristics include house type (proportion of detached houses to all houses), houses construction year (average construction year) and household composition (average household size) are examined in conjunction with minimum EVs introduction rate. Figure 4.18 a) shows the results of proportion of detached houses with three cases. b) illustrates the differences between case_2025 and case_2020, while c) depicts the differences case_2025_retrofit and case_2025. The results of b) suggest that in the period between 2020 to 2025, areas with a higher proportion of detached houses may experience larger variation in the minimum EVs introduction rates. c) shows that compared to case_2025 without retrofitting, areas with a higher proportion of detached houses (especially greater than 0.2) may experience larger increases in the minimum EVs introduction rates under retrofitting.

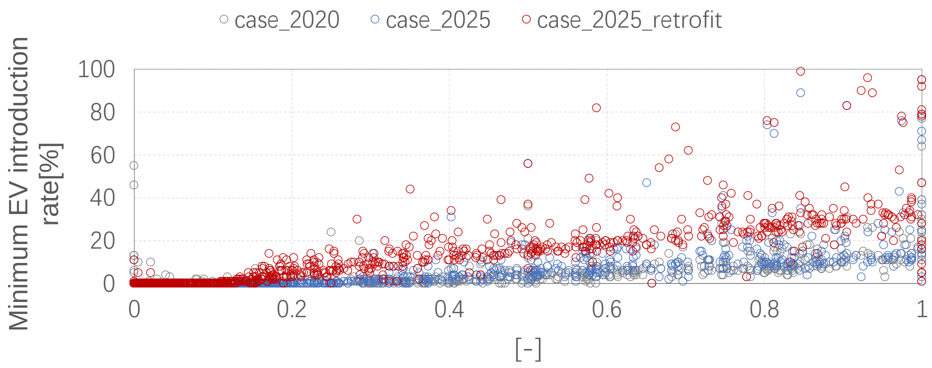

a) Minimum EVs introduction rate and proportion of detached housed to all houses

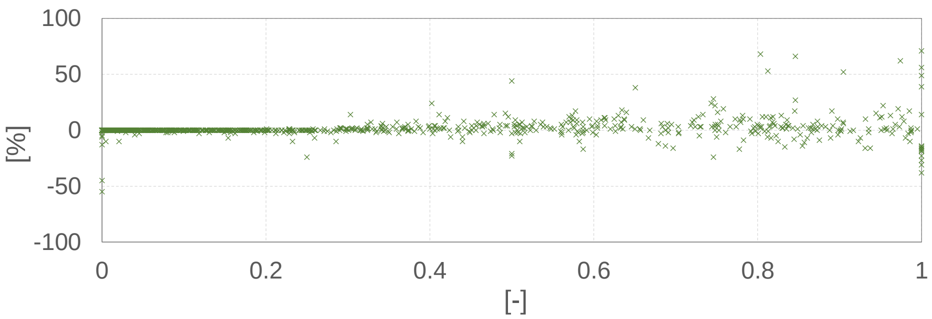

b) Difference of case_2025 to case_2020

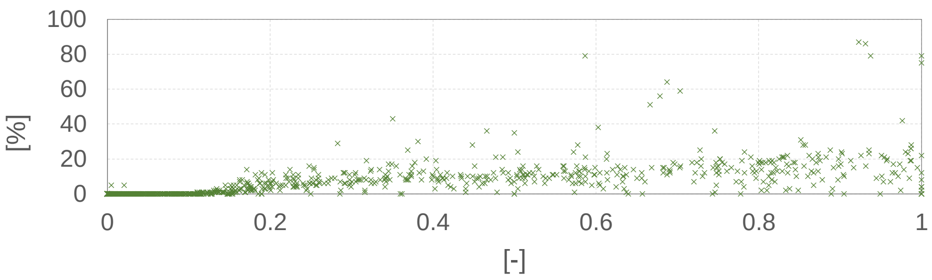

c) Difference of case_2025_retrofit to case_2025

Figure 4.18 Relationship between minimum EVs introduction rate and houses type of each street level area with three cases

Figure 4.19 a) shows the results of average construction year of houses with three cases. The results of b) suggest that in the period between 2020 to 2025, areas with an average houses construction year between 1995 and 2000 tend to have approximately equal numbers of increases and decreases in the minimum EV introduction rate. However, in areas where the average houses construction year is after 2000, there is a high likelihood of an increase in the minimum EV introduction rates. c) shows that compared to case_2025 without retrofitting, the minimum EV introduction rates have increased across all areas. Among them, areas with earlier average houses construction years are more likely to experience larger increases in the minimum EVs introduction rates.

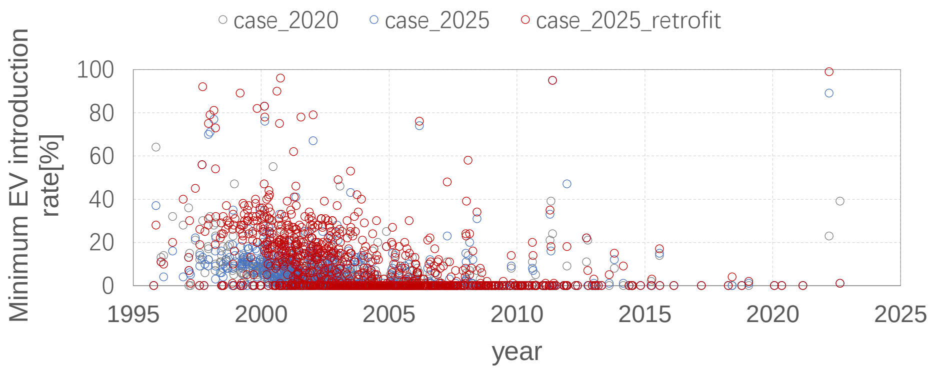

a) Minimum EVs introduction rate and average construction year of houses

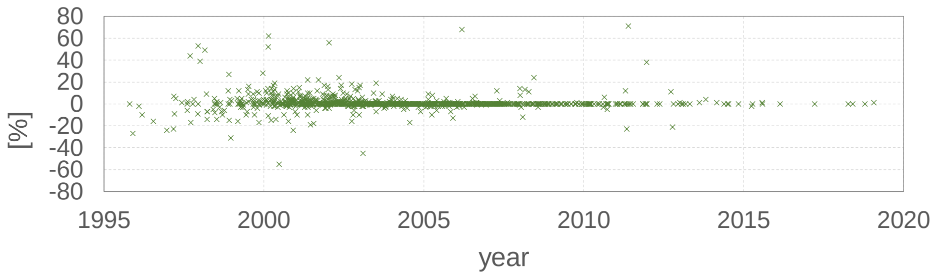

b) Difference of case_2025 to case_2020

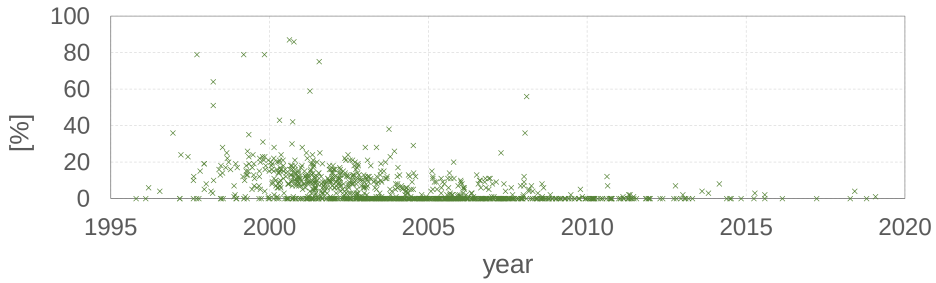

c) Difference of case_2025_retrofit to case_2025

Figure 4.19 Relationship between minimum EVs introduction rate and houses construction year of each street level area with three cases

Figure 4.20 a) shows the results of average household size of houses with three cases. The results of b) suggest that in the period between 2020 to 2025, in areas where the average household size is less than 1.5 or greater than 2 but less than 3, there are significant fluctuations (increases or decreases exceeding 40%) in the minimum EV introduction rates. c) shows that compared to case_2025 without retrofitting, apart from a few areas, the increase in the minimum EV introduction rates due to houses retrofitting is within 20%, and it is not directly related to the average household size.

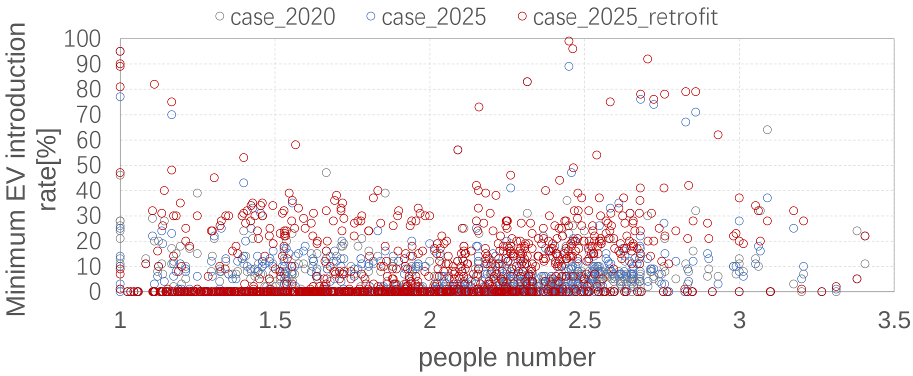

a) Minimum EVs introduction rate and average construction year of houses

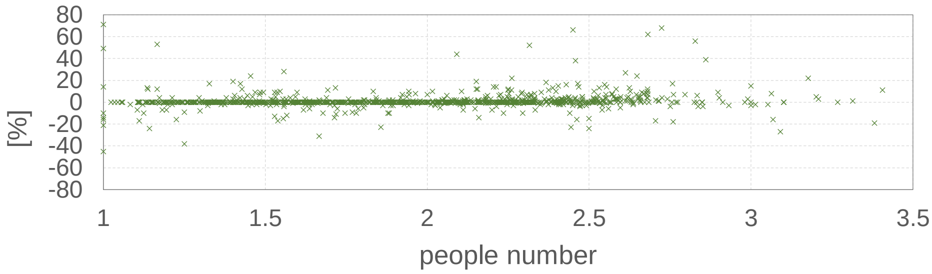

b) Difference of case_2025 to case_2020

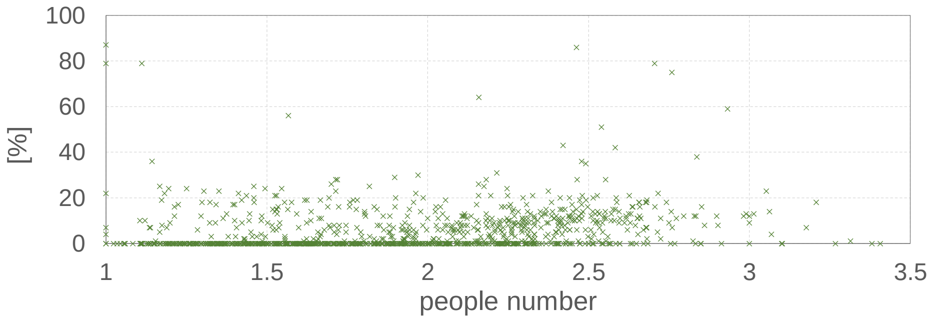

c) Difference of case_2025_retrofit to case_2025

Figure 4.20 Relationship between minimum EVs introduction rate and average household size of each street level area with three cases

4.4 Conclusions

In this chapter, based on the results of urban-scale residential electricity demand from Chapter 3, simulations were conducted for PV generation and surplus electricity with case_2020, case_2025 and case_2025_retrofit. The relationships between the maximum power, duration of surplus electricity and residential characteristics of the target area (proportion of detached houses, average house construction year, and average household size) are analyzed. There are several conclusions about surplus electricity as follow:

- Residential areas in the city center (District-2,3) generate almost no surplus electricity.
- Houses retrofitting is unlikely to generate surplus electricity in areas where surplus electricity does not occur.
- Areas with higher maximum surplus power experience a more significant increase in the duration of surplus electricity occurrence due to houses retrofitting.
- In terms of occurrence duration, the peripheral areas of the city have longer durations compared to the internal regions, while there is no apparent geographical difference in terms of maximum power.

To fully utilize this surplus electricity by electric vehicle (EV) charging, a model of EV driving, charging/discharging has been developed. By the proposed model, the minimum EVs introduction rate for each street-level area has been calculated with three cases. The relationships between the minimum EV introduction rate and residential characteristics of the area considering retrofitting or not are also analyzed separately. There are several conclusions about minimum EVs introduction rate as follow:

- Minimum EVs introduction rates of several areas have increased from 2020 to 2025, while those of other areas have decreased.
- Houses retrofitting has increased the number of areas generating surplus electricity. The minimum EVs introduction rates of these newly added areas are around 0-20%.
- From 2020 to 2025, areas with higher proportion of detached houses may experience larger variation in the minimum EVs introduction rates. Considering houses retrofitting, these areas may experience larger increase in the minimum EVs introduction rates too.
- From 2020 to 2025, areas with average houses' construction year between 1995 and 2000 tend to have approximately equal numbers of increases and decreases in the minimum EVs introduction rate. Considering houses retrofitting, minimum EVs introduction rates have increased across all areas especially areas with earlier average houses' construction year.
- From 2020 to 2025, there are significant fluctuations (increases or decreases exceeding 40%) in the minimum EVs introduction rates in areas with average household size in (1 ~ 1.5) or (2 ~ 3). Considering houses retrofitting, the increases in minimum EVs introduction rates have no connection with average household size.

Reference

[1] Ministry of the Environment, Government of Japan. 6th Basic Energy Plan. Oct. 2021. (in Japanese) https://www.meti.go.jp/press/2021/10/20211022005/20211022005.html

[2] George Alex Thopil, Christiaan Eddie Sachse, Jörg Lalk, Miriam Sara Thopil, Techno-economic performance comparison of crystalline and thin film PV panels under varying meteorological conditions: A high solar resource southern hemisphere case. Applied Energy, Vol.275, 115041, Oct. 2020.

[3] Jonas Allegrini, Kristina Orehounig, Georgios Mavromatidis, Florian Ruesch, Viktor Dorer, Ralph Evins, A review of modelling approaches and tools for the simulation of district-scale energy systems, Renewable and Sustainable Energy Reviews, Vol.52, pp.1391-1404, Dec. 2015.

[4] Liang Cheng, Fangli Zhang, Shuyi Li, Junya Mao, Hao Xu, Weimin Ju, Xiaoqiang Liu, Jie Wu, Kaifu Min, Xuedong Zhang, Manchun Li, Solar energy potential of urban buildings in 10 cities of China, Vol.196, No.1, 117038, Apr. 2020.

[5] Marco Massano, Enrico Macii, Andrea Lanzini, Edoardo Patti, Lorenzo Bottaccioli, A GIS Open-Data Co-Simulation Platform for Photovoltaic Integration in Residential Urban Areas, Vol.26, pp.198-213, July 2023.

[6] L.K. Wiginton, H.T. Nguyen, J.M. Pearce, Quantifying rooftop solar photovoltaic potential for regional renewable energy policy, Computers, Environment and Urban Systems, Vol.34, Issue 4, pp.345-357, July 2020.

[7] Luca Bergamasco, Pietro Asinari, Scalable methodology for the photovoltaic solar energy potential assessment based on available roof surface area: Application to Piedmont Region (Italy), Solar Energy, Vol.85, Issue 5, pp.1041-1055, May 2011.

[8] Marcel Šúri, Thomas A. Huld, Ewan D. Dunlop, PV-GIS: a web-based solar radiation database for the calculation of PV potential in Europe, International Journal of Sustainable Energy, Vol.24, Issue 2, 2005.

[9] Luyao Liu, Yi Zhao, Dongliang Chang, Jiyang Xie, Zhanyu Ma, Qie Sun, Hongyi Yin, Ronald Wennersten, Prediction of short-term PV power output and uncertainty analysis, Applied Energy, Vol.228, No.15, pp.700-711, Oct. 2018.

[10] Wei Liao, Chulho Kim, Yiqiang Xiao, Hanjoo Kim, Tageui Hong, Shi Yin, Yeonsook Heo, Quantifying Photovoltaic surplus at an urban scale: A case study in Seoul, Energy and Buildings, Vol.298, No.1, 113523, Nov. 2023.

[11] Antonio Gomez-Exposito, Angel Arcos-Vargas, Francisco Gutierrez-Garcia, On the potential contribution of rooftop PV to a sustainable electricity mix: The case of Spain, Renewable and Sustainable Energy Reviews, Vol.132, 110074, Oct. 2020.

[12] Building Energy Conservation Law, Agency for Natural Resources and Energy in Japan. (in Japanese) https://www.enecho.meti.go.jp/category/saving_and_new/saving/general/housing/index.html

[13] Mohamed A. Eltawil, Zhengming Zhao, Grid-connected photovoltaic power systems: Technical

and potential problems—A review, Renewable and Sustainable Energy Reviews, Vol.14, Issue 1, pp.112-129, Jan. 2010.

[14] Gabino Jiménez-Castillo, Francisco José Muñoz-Rodríguez, Antonio Javier Martinez-Calahorro, Giuseppe Marco Tina, Catalina Rus-Casas, Impacts of Array Orientation and Tilt Angles for Photovoltaic Self-Sufficiency and Self-Consumption Indices in Olive Mills in Spain, Electronics, 9(2), 348, 2020.

[15] M. Castillo-Cagigal, E. Caamaño-Martín, E. Matallanas, D. Masa-Bote, A. Gutiérrez, F. Monasterio-Huelin, J. Jiménez-Leube, PV self-consumption optimization with storage and Active DSM for the residential sector, Solar Energy, Vol.85, Issue 9, pp.2338-2348, Sep. 2011.

[16] Paul Denholm, Robert M. Margolis, Evaluating the limits of solar photovoltaics (PV) in electric power systems utilizing energy storage and other enabling technologies, Energy Policy, Vol.35, Issue 9, pp.4424-4433, Sep. 2007.

[17] N. Kawasaki and Y. Muromachi, "Building zero-emission cities with EV, PV, and stationary storage battery system in Tokyo metropolitan area," Journal of the City Planning Institute of Japan, vol.56, no.3, pp.1366-1373, October 2021

[18] T. Nishioeda, M. Suzuki, K. Morino, T. Oka and Y. Takebayashi, "Load leveling by using electric vehicle batteries to store surplus energy generated by photovoltaic systems on single-family houses in Japan," Journal of environmental engineering: transactions of AIJ, vol.80, no2yue.708, pp.149-158, February 2015

[19] K. Ichii, I. Takahara and M. Taniguchi, "Verifying DC smart grid effects based on residential area characteristics," Japanese Journal of JSCE, vol.75, no.6, pp.231-238, 2020

[20] Ministry of Economy, Trade and Industry, Japan, Solar power generation status
- Continuing to develop new projects necessary to become a main power source -
Procurement price calculation committee materials, Oct. 29, 2019. (in Japanese).
https://www.meti.go.jp/shingikai/santeii/pdf/062_01_00.pdf

[21] Fukuoka City Transportation Planning Division, "Movement of people in Fukuoka City - Based on the 4th Northern Kyushu Person Trip Survey," May 2007

[22] N. Tadokoro, et al, "Current usage status and user awareness of electric vehicles and plug-in hybrid vehicles," Central Research Institute of Electric Power Industry Report, April 2013 (in Japanese)

[23] T. Ikeda, et al. "Development of optimal placement and operation planning method for urban energy supply facilities based on time-series data - Part10 Impact of area power load leveling effect due to the spread of electric vehicles," AIJ Kyushu chapter architectural research meeting, March, 2021. (in Japanese)

Chapter-5
Summary and Discussion

5.1 Summary

This study focused on the electricity issues of urban area. Specifically, this study developed an urban-scale residential electricity demand model considering occupants' lifestyles and residential thermal insulation performance. Using this model, the residential electricity demand in various areas of Fukuoka was simulated and the relationship between electricity demand differences and regional characteristics was explored. Additionally, the impact of houses retrofitting and the widespread introduction of electric vehicles on the electricity supply and demand in different areas was evaluated, along with their relationship to regional characteristics.

The following summarizes the conclusions of each chapter:

In Chapter 1,

The background, the related issues, the purpose and structure of this research was described.

In Chapter 2,

A occupants’ behavior model was developed to generate occupants’ behavior schedules for electricity demand simulation of residential buildings. To ensure that the statistical values of the generated schedules matched those of public data (NHK National Life Survey), Particle Swarm Optimization (PSO) algorithm was utilized to make the generated results close to public data. By the proposed model, 1000 behavior schedules for five types of occupants (working-male, working-female, housewife, child, teenager and elder) were generated. Furthermore, based on the correlations between household members' behaviors (eating at the same time and shower at different times), these schedules were combined to create behavior schedules combnations of household members.

In Chapter 3

Based on the results of Chapter 2, a simulation model for urban-scale residential electricity demand was developed, which could be utilized in any region of Japan. The accuracy of model was verfied with measured electricity data of 93 houses in Ozase residential area. By this model, 5-minutes interval electricity demand of entire target city and street-level areas with three scenarios (2020, 2025 and 2025 with houses retrofitting) were simulated separately. The following aspects of residential electricity demand were identified by simulation results: At the urban level, the houses retrofitting scenario would reduce the urban's residential electricity consumption from 2319 GWh to 2141 GWh in 2025. Specifically, electricity of summer air conditioning would decrease from 180 GWh to 125 GWh, and those of winter would decrease from 359 GWh to 252 GWh. At the street-area level, electricity demand in the city center area has been reduced by approximately 10% or less, while in suburban areas, the reduction ranges from 15% to 40%.

In Chapter-4

Based on the current residential PV adoption rate, the urban-scale PV generation was calculated.

Compared with the electricity demand results in Chapter 3, the surplus electricity for all street-level areas was determined. The results revealed that during spring noon, the target city experienced the highest surplus electricity generation in most areas. Additionally, the relationship between the maximum power and duration of surplus electricity and the characteristics of houses group (proportion of detached houses, the age of houses, and the number of household members) was analyzed. Among the three characteristics, the proportion of detached houses is the most significant characteristic influencing both the peak power and duration of surplus electricity in a region. Also, the results that houses retrofitting would increase in surplus electricity power and duration was demonstrated. To fully utilize this surplus electricity, the developed electric vehicles (EV) charging/discharging model was utilized to explore the minimum EV introduction rate (proportion of houses owning EV) in all areas experiencing surplus electricity. Additionally, the relationship between the minimum EVs introduction rate and characteristics of houses group, as well as the impact of houses retrofitting, was analyzed. The results show that areas with higher proportion of detached houses, earlier houses' construction year may experience larger variation in the minimum EVs introduction rates by houses retrofitting. On the onter hand, there is no obvious connection with household size and minimum EVs introduction rates change by houses retrofitting.

5.2 Discussion

This study developed a model for simulating electricity demand of residential buildings in urban scale, which could be utilized to explore different effects of energy policies implementation in different urban area. However, there are some issues that need to be point out.

- Due to a lack of data, the model relied on several assumptions (probability of air conditioning usage based on temperature solely, uniform ownership rates of appliances, air conditioning, and PV across all urban areas, etc.) for simulation. As a result, there are disparities between the simulated results and real-world situation. Furthermore, due to the absence of measured data for large-scale urban residential buildings, it is challenging to validate the simulation results at an urban scale. This study validated the model using measured electricity data from 93 apartment houses and compared the validation results with other studies. However, considering the differences among urban areas, this validation is still insufficient. In the future, the assumptions used in the model will be supplemented and adjusted through field surveys or other means. Additionally, more residential electricity data will be obtained to validate the simulation results more comprehensively.
- In this study, surplus electricity of area is obtained by subtracting the total electricity demand of houses in that area from the total PV generation at that time. This necessitates the deployment of regional smart microgrids to manage the supply and demand of PV energy across different houses, which imposes significant requirements on the electricity infrastructure. Additionally, the simulation results significantly underestimated the occurrence of surplus electricity when compared to the similar study that involves one PV system per house.

- The prediction of urban residential quantity for the year 2025 in this study was based on regression forecasting using past data, which overly simplifies urban evolution. Future research will integrate demographic, geographical, economic, and other data to simulate urban evolution. Additionally, forecasts will be extended to more distant years such as 2035 and 2050 to align with decarbonization plans for 2050.
- This study focused on simulating residential sector. In the future, it will be expanded to include non-residential sectors for comprehensive simulation.

謝辞

本論文作成にあたり、修士研究生から現在までの５年半間において多くの方々のご支援、ご指導を頂きました。この場を借りて心よりお礼申しあげます。

九州大学大学院人間環境学研究院 住吉大輔教授には、私が研究室に配属されてからの５年半間において、日々の研究、都市エネルギーの知識、論文の方向性、研究に対する姿勢、研究発表のロジックなど、研究者生活のありとあらゆる面でご指導いただき、度々の相談、質問にも親身に応じていただきました。心より感謝申し上げます。

九州大学大学院人間環境学研究院 尾崎明仁教授には、建築環境学の基本概念や研究者のあり方、研究に対する考え方など様々なことを学ばせていただきました、心より感謝申し上げます。

副査として本論文の審査を引き受けていただきました九州大学大学院人間環境学研究院趙世晨教授には、本論文をまとめるに際し、論文としての表現方法や内容に関して貴重なご意見、ご助言を頂きました。心より感謝申し上げます。

尾崎・住吉研究室事務補佐の相原桂子さんには、出張手続きなどで研究活動を支えていただき 大変お世話になりました。また日々の研究時においても暖かい励ましの言葉を頂きました。心より感謝申し上げます。

住吉研究室の博士先輩たち金惠美さん、吳濟元さんには、独立研究者として、多くの貴重な経験を頂きました。心より感謝申し上げます。

修士課程時から都市チームで共に研究を進める機会のあった松山諒太郎君、松宗君、阿波廉君、朝倉洸樹君には、指導を通じて私自身が教わることも多く、互いに励まし合いながら研究を進 めることができ、大きな心の支えとなりました。深く御礼を申し上げます。

尾崎・住吉研究室の中国人の友人たちには、異国の地で互いに支え合い、一緒に学んできたことに深く感謝します。

最後に、九州大学への入学の機会を与えて頂き、温かく見守ってくれた両親に、そして何よりも、私と人生を共にすることを誓ってくださり、日々の生活を献身的に支えてくれている妻の屈陽さんに心より感謝いたします。

２０２４年5月

王 恒煊